ธรณีวิทยาและลักษณะเฉพาะการเกิดแร่

ของแหล่งแร่ทองคำคำเกิดแสนอุดม

แขวงบริคำไชย สาธารณรัฐประชาธิปไตยประชาชนลาว

นางสาวกมลลักษณ์ ฉนัดกิจ

วิทยานิพนธ์นี้เป็นส่วนหนึ่งของการศึกษาตามหลักสูตรปริญญาวิทยาศาสตรมหาบัณฑิต
สาขาวิชาธรณีวิทยา ภาควิชาธรณีวิทยา
คณะวิทยาศาสตร์ จุฬาลงกรณ์มหาวิทยาลัย
ปีการศึกษา 2559

GEOLOGY AND MINERALIZATION CHARACTERISTICS OF KHAMKEUT SAEN OUDOM GOLD DEPOSIT, BOLIKHAMXAI, LAO PDR

Miss Kamonluk Tanutkit

A Thesis Submitted in Partial Fulfillment of the Requirements
for the Degree of Master of Science Program in Geology
Department of Geology
Faculty of Science
Chulalongkorn University
Academic Year 2016

Thesis Title	GEOLOGY AND MINERALIZATION CHARACTERISTICS OF KHAMKEUT SAEN OUDOM GOLD DEPOSIT, BOLIKHAMXAI, LAO PDR
By	Miss Kamonluk Tanutkit
Field of Study	Geology
Thesis Advisor	Abhisit Salam, Ph.D.
Thesis Co-Advisor	Associate Professor Chakkaphan Sutthirat, Ph.D.

Accepted by the Faculty of Science, Chulalongkorn University in Partial Fulfillment of the Requirements for the Master's Degree

.....Dean of the Faculty of Science
(Associate Professor Polkit Sangvanich, Ph.D.)

THESIS COMMITTEE

.....Chairman
(Professor Montri Choowong, Ph.D.)

.....Thesis Advisor
(Abhisit Salam, Ph.D.)

.....Thesis Co-Advisor
(Associate Professor Chakkaphan Sutthirat, Ph.D.)

.....Examiner
(Associate Professor Pitsanupong Kanjanapayont, Dr.rer.nat.)

.....External Examiner
(Somboon Khositanont, Ph.D.)

กมลลักษณ์ ถนัดกิจ : ธรณีวิทยาและลักษณะเฉพาะการเกิดแร่ของแหล่งแร่ทองคำคำเกิดแสนอุดม แขวงบริคำไชย สาธารณรัฐประชาธิปไตยประชาชนลาว (GEOLOGY AND MINERALIZATION CHARACTERISTICS OF KHAMKEUT SAEN OUDOM GOLD DEPOSIT, BOLIKHAMXAI, LAO PDR) อ.ที่ปรึกษาวิทยานิพนธ์หลัก: ดร. อภิสิทธิ์ ซาลำ, อ.ที่ปรึกษาวิทยานิพนธ์ร่วม: รศ. ดร. จักรพันธ์ สุทธิรัตน์, หน้า.

แหล่งทองคำคำเกิดแสนอุดม ตั้งอยู่แขวงบริคำไชย ทางตอนกลางของสาธารณรัฐประชาธิปไตย ประชาชนลาว วางตัวอยู่ในแนวชั้นหินคดโค้งทุ่งสง ที่ซึ่งมีความหลากหลายของแหล่งแร่ที่สำคัญ โดยเฉพาะอย่างยิ่งทองคำและทองแดง แหล่งคำเกิดแสนอุดม มีลักษณะสายแร่เป็นแบบ สายแร่ควอร์ต-คาร์บอเนต, สายแร่ร่างแห และสายแร่หินเหลี่ยมเล็กน้อย สายแร่ขนาดใหญ่วางตัวในแนวตะวันออก-ตะวันตก ที่ซึ่งมันเป็นสายแร่เดี่ยวขนาดใหญ่ทางด้านตะวันออกแล้วมีการแตกออกสามสายแร่ทางด้านตะวันออกของพื้นที่ ความหลากหลายของการเกิดแร่ในแนวโครงสร้างของตะวันออก-ตะวันตก (ตัวอย่างเช่น ห้วยแก, น้ำพานทางตะวันออก, น้ำพานทางตะวันตก) การเกิดแร่มีการสะสมตัวในหินกึ่งแปรสภาพ (ตัวอย่างเช่น หินทรายกึ่งแปรสภาพ, หินทรายแป้งกึ่งแปรสภาพ, หินชนวน) ซึ่งมีอายุออร์โดวิเชียนถึงอายุไซลูเรียน การเกิดสายแร่มีการพบอย่างน้อย 3 ครั้ง ซึ่งถูกตั้งชื่อตามนี้ ครั้งที่ 1 ควอร์ต-อาร์ซีโนไพไรต์-ไพไรต์, ครั้งที่ 2 ควอร์ต-แคลไซต์-ซัลไฟต์ (อาร์ซีโนไพไรต์-ไพไรต์-สฟาเลอไรต์-ชาร์โคไพไรต์-กาลีนา-พิโรไทต์)-ทอง และครั้งที่ 3 ควอร์ต-คลอไรต์-คาร์บอเนต การแปรเปลี่ยนของหินท้องที่บริเวณแหล่งคำเกิดแสนอุดมมีการกระจายตัวและแผ่ออกน้อยมาก และมีการแปรเปลี่ยนของหินท้องที่แบบควอร์ต-แคลไซต์-เซอริไซต์ และแบบคลอไรต์-เซอริไซต์-แคลไซต์ ของทั้ง 2 บ่อ ซึ่งแบบควอร์ต-แคลไซต์-เซอริไซต์ มีลักษณะเด่นของควอร์ต แคลไซต์ และเซอริไซต์ จากการวิเคราะห์อีพีเอมเอของทองบริเวณบ่อน้ำพานเกิดเป็นแบบอิเลคตรัม อยู่ในช่วง 637 ถึง 715 ในทางตรงกันข้ามบ่อห้วยแกเกิดเป็นแบบทองคำ อยู่ในช่วง 827 ถึง 866 จากการวิเคราะห์แร่สฟาเลอไรต์สีอ่อนของบ่อน้ำพานมีค่าเหล็กออกไซด์ 8.49 ถึง 16.08 โมลเปอร์เซ็นต์ ในทางกลับกันแร่สฟาเลอไรต์สีเข้มของบ่อห้วยแกมีค่า 8.49 ถึง 16.08 โมลเปอร์เซ็นต์ จากการใช้ค่าเหล็กออกไซด์ของแร่สฟาเลอไรต์ อุณหภูมิและความดันของการเกิดทองที่แหล่งคำเกิดแสนอุดมคำนวณได้ประมาณ 320 ถึง 450 เซลเซียส และ 7.17 ถึง 15.08 กิโลบาร์ตามลำดับ จากหลักฐานทั้งหมดที่กล่าวมา (ตัวอย่างเช่น หินท้องที่แปรสภาพ การแปรเปลี่ยนน้อย กลุ่มแร่ความบริสุทธิ์ของทองคำ และค่าเหล็กออกไซด์ของแร่สฟาเลอไรต์) ทำให้ทราบว่าแหล่งทองคำคำเกิดแสนอุดมมีแนวโน้มที่จะเป็นแหล่งแร่แบบออโรจินิค

ภาควิชา ธรณีวิทยา ลายมือชื่อนิสิต .....

สาขาวิชา ธรณีวิทยา ลายมือชื่อ อ.ที่ปรึกษาหลัก .....

ปีการศึกษา 2559 ลายมือชื่อ อ.ที่ปรึกษาร่วม .....

5771908623 : MAJOR GEOLOGY
KEYWORDS: GOLD / FINENESS / MINERALIZATION / KSO

KAMONLUK TANUTKIT: GEOLOGY AND MINERALIZATION CHARACTERISTICS OF KHAMKEUT SAEN OUDOM GOLD DEPOSIT, BOLIKHAMXAI, LAO PDR. ADVISOR: ABHISIT SALAM, Ph.D., CO-ADVISOR: ASSOC. PROF. CHAKKAPHAN SUTTHIRAT, Ph.D., pp.

The Khamkeut Saen Oudom (KSO) gold deposit is located at Bolikhamxai district, central Lao PDR. It lies within the Truong Son Fold Belt where there are several significant mineral deposits particularly gold and copper. At KSO deposit, the mineralization occurs as quartz-carbonate-sulfides veins, minor stockworks and breccias. Major veins are trending almost E-W where it forms as single ore zone in the west and splays to three narrow veins at the eastern part of area. Several ore lenses are present along this E-W structure (e.g. Houay Keh, Nam Pan-east, Nam Pan-west). The gold mineralized veins are mainly hosted by meta-sedimentary rocks (e.g. meta-sandstone, meta-siltstone and slate). At least three stages of mineralization have been identified namely; Stage 1, microcrystalline quartz - arsenopyrite - pyrite; Stage 2, quartz ± calcite - sulfides (arsenopyrite - pyrite - sphalerite - chalcopyrite - galena-pyrrhotite) - gold and Stage 3, quartz - chlorite - calcite. Gold is closely associated with sulfide minerals (e.g., pyrite, arsenopyrite, chalcopyrite, sphalerite and galena), quartz and calcite. Alteration associated with gold mineralization is less pervasive and extensive and mainly characterized by 1) quartz - calcite - sericite - chlorite and 2) chlorite - sericite - calcite assemblages. EPMA analyzes of gold reveals that at Nam Pan ore lens it occurs as electrum with gold fineness range from 637 to 715 whereas, at Houay Keh ore lens it occurs native gold with gold fineness ranges from 827 to 866. EPMA analyzes of light-color sphalerite from Nam Pan has FeS content of 5.00 to 8.05 mole %. In contrast, dark-color sphalerite from Houay Keh ore lens has values of 8.49 to 16.08 mole %. Using FeS content of sphalerite, T and P of gold mineralization at KSO were calculated to be 320 to 450°C and 7.17 to 15.08 kbar respectively. Based on the above evidences (e.g., metamorphic host rocks, weak alteration, mineral assemblages, gold fineness and FeS content of sphalerite), the KSO gold deposit is likely to be orogenic deposit.

Department:	Geology	Student's Signature	.....
Field of Study:	Geology	Advisor's Signature	.....
Academic Year:	2016	Co-Advisor's Signature	.....

ACKNOWLEDGEMENTS

The author would like to express her special gratitude to her advisor and co-advisor, Dr. Abhisit Salam and Assoc. Prof. Dr. Chakkaphan Sutthirat, Department of Geology, Faculty of Science, Chulalongkorn University, for her invaluable supervision, suggestion, encouragement and contribution, especially to make this research well achieved. Thank you for Dr. Takayuki Manaka to suggestion and make corrections. Thanks to Weerasak Luangwongsa and his colleague at KSO mine who have assisted in this research. Special thank is given to Akita University for training. Sample preparation and laboratory were supported by Sopit Poompuang and Prajin Thongchum.

My MSc. Study is financially supported by Development and Promotion of Science and Technology talents (DPST) fund Graduate school, Chulalongkorn University. Field investigation in Laos was supported by Khamkeut Saen Oudom Gold Mine, Lao PDR.

This research program has been carried out at Department of Geology, Faculty of Science, Chulalongkorn University.

Finally, the author is indebted to my parents for their stimulation and encouragement.

CONTENTS

Page

LIST OF TABLES

LIST OF FIGURES

CHAPTER I

INTRODUCTION

1.1 General Statement

Laos's mining industry has been expanded in recent years (last two decades) due the government policy of opening exploration and mining in the country. Mining industry has driven economic growth. Among the earlier company explored and mined in the country are Oxiana Limited and Pan Aust Ltd. which have successfully explored and have been mining for the last 15 years. Major metals produced in Laos are copper, gold, copper and silver. Copper and gold are mainly produced from Phu Kham and Sepon deposit whereas silver produced from Ban Houayxai. Gold, silver and copper are also explored and mining in adjacent countries (e.g. Thailand and Vietnam). Chatree deposit in Thailand was mined by Kingsgate Consolidate NL for gold and silver more than 15 years and recently has been terminated by Thailand Government. Phu Thap Fah deposit was produced for gold in northeastern Thailand and has been terminated by Thai Government in the year 2015. Phouc Son and Bong Mieu deposits in Vietnam are producing gold for more than 10 years (Fig. 1.1).

Khamkeut Saen Oudom (KSO) gold deposit is located in Bolikhamxai district in central eastern Laos (Fig. 1.1). The KSO gold deposit is undertaken by SRK Exploration Services Ltd. and associated approximately 1,802 km^2 exploration concession. The mine is operated by the Phonesack Group as open pit mining method (Fig. 1.3). KSO gold mine has been mined in six small pits, namely HKC, HKS, HKW, NPE, NPW and VK. Gold grade ranging from 0.5 g/t Au through to 1.4 g/t Au for a potential total of ounces ranging from 32,417 Oz Au through to 291,752 Oz Au (SRK, 2011).

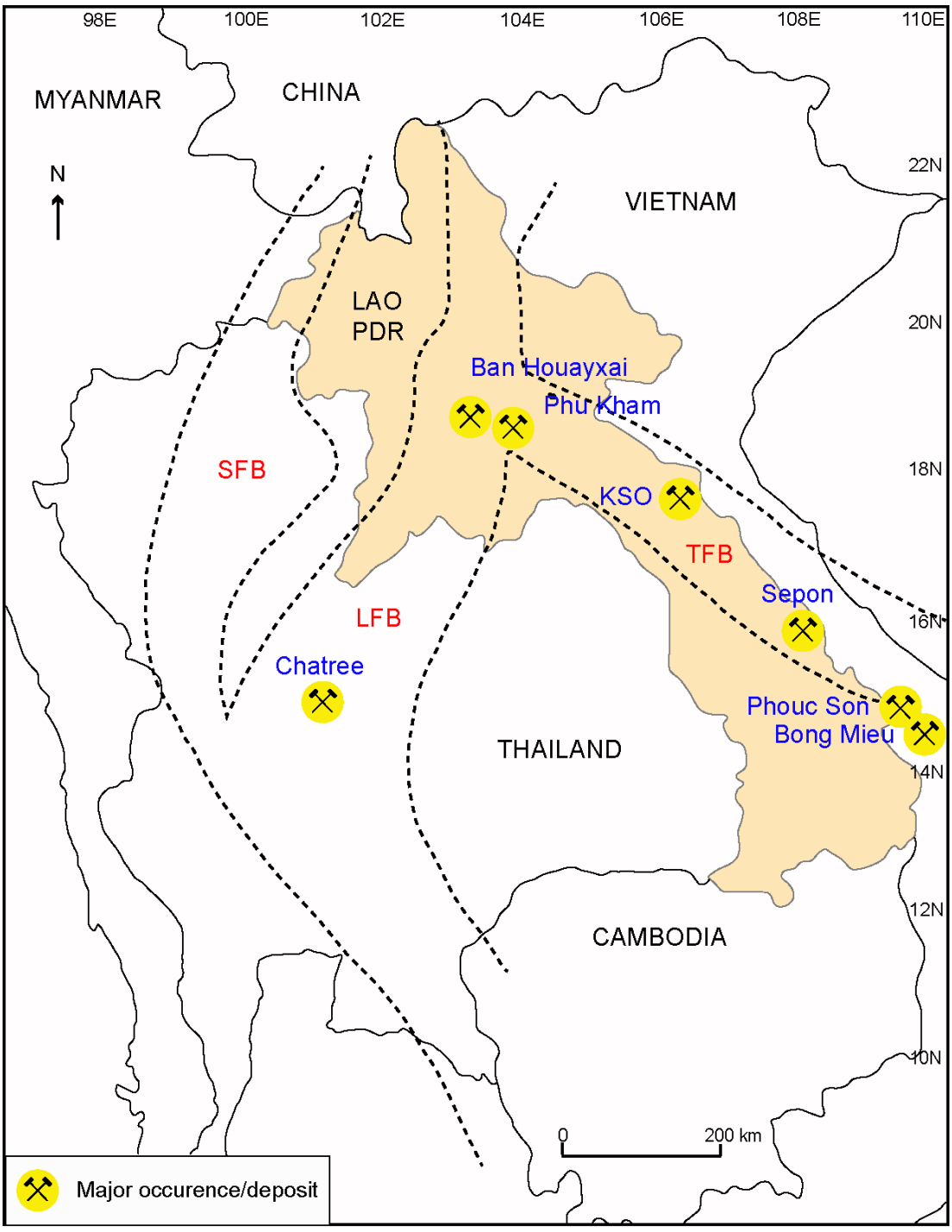

Fig. 1. 1 The map shows position of Khamkeut Saen Oudom mine in Bolikhamxai district, Central Laos (from Nakhon Panom). The yellow circle indicates Khamkeut Saen Oudom mine, the study area (Tate, 2005).

1.2 Location and Accessibility

The Khamkeut Saen Oudom (KSO) gold deposit is located within the Bolikhamxai district in central eastern Laos at latitude of 2,012,000 mN and longitude of 509,570 mE (Fig. 1.2). Nam Pan and Houay Keh pits located in the northern part of KSO mine are the focus for this study (Fig. 1.2)

The KSO mine is located about 400 km from Nakhon Panom (Thailand; Fig. 1.2). This area can be accessed by using boat across Mekong river to Thakhek (Laos side). From Thakheh take the road number H131 or Route 12 to road number 1E. From E1 continue driving about 14 km to Khamkeut Saen Oudom gold mine.

Fig. 1. 2 Map showing accessibility to the study area in a Khamkeut Saen Oudom mine, Laos (United Nations, 2004).

1.3 Land use and climate

Laos is characterized by steep terrain and narrow river valleys. The topography is largely mountainous in the northern part of the country with elevations typically ranging several hundreds of meters excluding the plain of Vientiane and the Plain of Jars in Xiangkhoang Province.

The country has a tropical monsoon climate. The rainy season begins in May and continues until October, a dry and cool season is from November through February, and a hot, dry season prevailing in March and April temperatures range from highs around 40 ◦C along the Mekong river valley in March and April to lows of 5 ◦C or less in the highlands. The country's average humidity varies between 87% in rainy season and 69% in hot dry season.

Fig. 1. 3 Khamkeut Saen Oudom mine area, central Laos. **A.** View of Nam Pan-west pit (looking east). **B.** View of processing plant. **C.** View of campsite.

1.4 Objectives

- To classify the mineralization styles in terms of mineral paragenesis, mineral assemblages, alteration and fluid chemistry.
- To construct a robust model linking between ore formation and geologic-tectonic development of the region.

1.5 Methodology

Methodology of this study is given in a flow chart (Fig. 1.5) which consists of five steps as described below.

1.4.1 Literature review

The study begins with reviewing several previous works on tectonic setting, regional geology, and magmatism especially intrusive rocks in the region. In addition, possible styles of KSO mineralization were also reviewed to better data and samples collections.

1.4.2 Fieldwork and sample collection

The fieldwork investigation; example, surface data, geologic map, geological structures, landforms, rock units, two cross-sections (508700E and 509570E) of two pits (Nam Pan and Houay Keh pits), core logging of three drill hole and sampling of Diamond drilling and Reverse Circulation (RC) drilling around 300 meters of depth. These were logged and sampled with emphasis on the relationships between lithology, wall rock alteration patterns, and distribution of the mineralization. Sixty-four samples were taken into laboratory works.

1.4.3 Laboratory study

Sixty rock samples were slab-cut and sample preparation has twelve polished thin sections, thirty-four polished mounts and eighteen thin sections which were made for petrographic and ore microscopy analysis using transmitted and reflected light microscopy to identify and petrography description for mineral textural relationships and paragenesis of ore minerals. Almost all of the laboratory work, for example

Energy Dispersive X-ray Scanning Electron Microscope (EDS-SEM) at Akita University in Japan, Electron Probe Micro-Analysis (EPMA, model JXA-810) at Department of Geology, Faculty of Science, Chulalongkorn University by polished mounts and polished thin sections were coated carbon before analysis. EPMA equipment operates in conditions setting of 15 kV with 24 nA current of focused beam. Alteration minerals were identified by an ore microscope from thin sections that are closely vein zones to indicate the alteration characteristics and zonation of the KSO deposit and confirm by using X-Ray Diffraction (XRD) analysis.

1.4.4 Interpretation, Discussion and Conclusion

Results of Field work and laboratory work in this study were collected for discussion and after that conclusion such as geology, tectonic setting, paragenesis, alteration, gold fineness and sphalerite chemistry. This information was carried out and conclusion in next step.

1.4.5 Report writing

Thesis writing and prepares presentation about all this research and also defense. Moreover, draft publication for international journals.

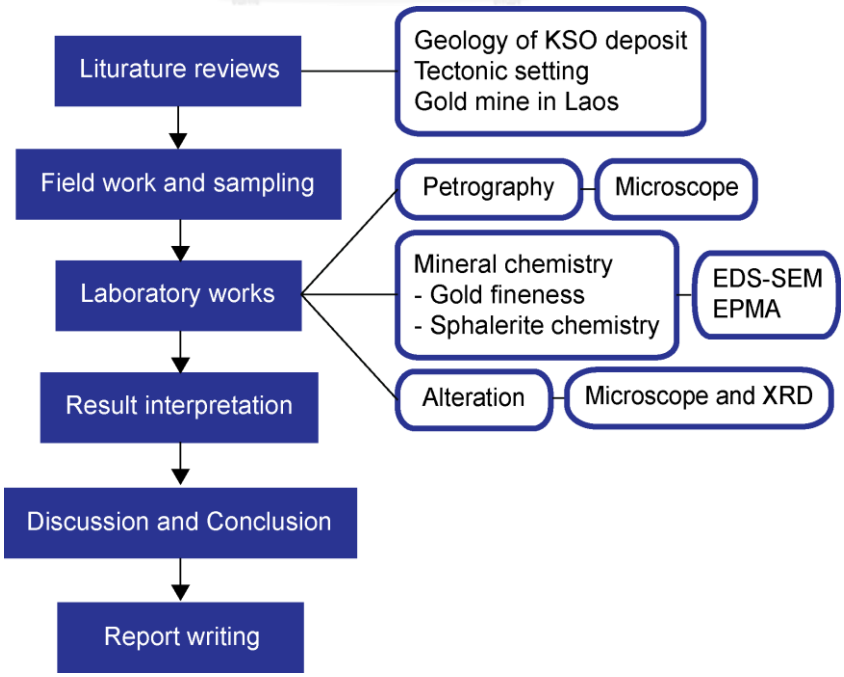

Fig. 1. 4 Schematic diagram shows sequences in this research.

1.6 Thesis organization

This thesis is divided into six chapters and organized as follows:

- **Chapter 1** (Introduction) provides the general background of the Khamkeut Saen Oudom (KSO) deposit, including the location and transportation to the area. The objectives and an overview of the analytical methods are outlined and the contents of each Chapter are summarized.
- **Chapter 2** (Regional geology) provides an overview of the tectonic setting of mainland SE Asia and the regional setting of Laos, including the brief summaries of each Terrane involved with the tectonic evolution. Moreover, the stratigraphic and tectonic framework of the Khamkeut Saen Oudom (KSO) deposit is also discussed. It is mainly based on previous studies and published literature.
- **Chapter 3** (Geology of deposit) presents the nature of mineralization for the Khamkeut Saen Oudom (KSO) deposit. It also describes unit rocks and cross sections in this study area.
- **Chapter 4** (Mineralization and Alteration) presents the nature of mineralization and paragenesis for the Khamkeut Saen Oudom (KSO) gold deposit. And it also describes alteration assemblages for evaluation in only stage 2 (main gold stage).
- **Chapter 5** (Mineral chemistry) covers results of Energy Dispersive X-ray Scanning Electron Microscope (EDS-SEM), Electron Probe Micro-Analysis (EPMA) and X-Ray Diffraction (XRD) analysis which have previously never been studied in this deposit.
- **Chapter 6** (Discussion and Conclusions) involves discussion and conclusion of all investigations in this study, and introduces the interpretation, genesis and exploration implications of the Khamkeut Saen Oudom (KSO) deposit. This Chapter also compares the most important geological characteristics of the Khamkeut Saen Oudom (KSO) deposit to the other gold deposits worldwide. Some suggestions for future work are stated in the last section of this thesis.

CHAPTER II

TECTONIC SETTING AND REGIONAL GEOLOGY

2.1 Introduction

This chapter presents a literature review of regional geological setting of Laos and provides a geological framework for the KSO deposit in chapter 3. There are 2 principal aims of the chapter 2: (1) review tectonic setting of mainland Southeast Asia with emphasize on the Indochina Terrane and Truong Son Fold Belt (TFB), and (2) the regional geology and major mineral deposits in Laos and adjacent countries.

2.2 Tectonic setting

The KSO deposit is located within the Truong Son Fold Belt (TFB) on the northeastern edge of the Indochina Terrane in central Laos (Fig. 2.1). The tectonic setting of mainland Southeast Asia consists of three major terranes including the South China, Indochina and Shan-Thai Terranes (Lepvrier et al., 2004; Metcalfe, 1995; Metcalfe, 2006) (Fig. 2.1). Laos and its adjacent area are confined to two major tectonic terranes namely, South China Terrane in the east and Indochina Terrane on the west (Fig. 2.1). These two terranes were separated by TFB. The TFB was formed as a result of the closure of Laos - North Vietnam Strait of Paleo-Tethys (Intasopa et al., 1995).

The Indochina Terrane is the biggest tectonic unit in mainland SE Asia (Fig. 2.1). This Terrane borders the South China Terrane along Song Ma Suture to north and northwest (Khin Zaw et al., 2014). The Indochina terrane can be divided by geologically distinct terranes, as the followings.

(1) The Kontum Massif, an high grade metamorphic rocks exposed in southern Laos and Vietnam, which is mainly characterized by high grade gneiss and schist of Middle Permian metamorphic core complex (Lepvrier et al., 2008). The Kontum Massif comprises chiefly metamorphic rock including low grade schist amphibolite to

granulite facie which referred to the biggest core complex of Indochina terrane (Osanai et al., 2004).

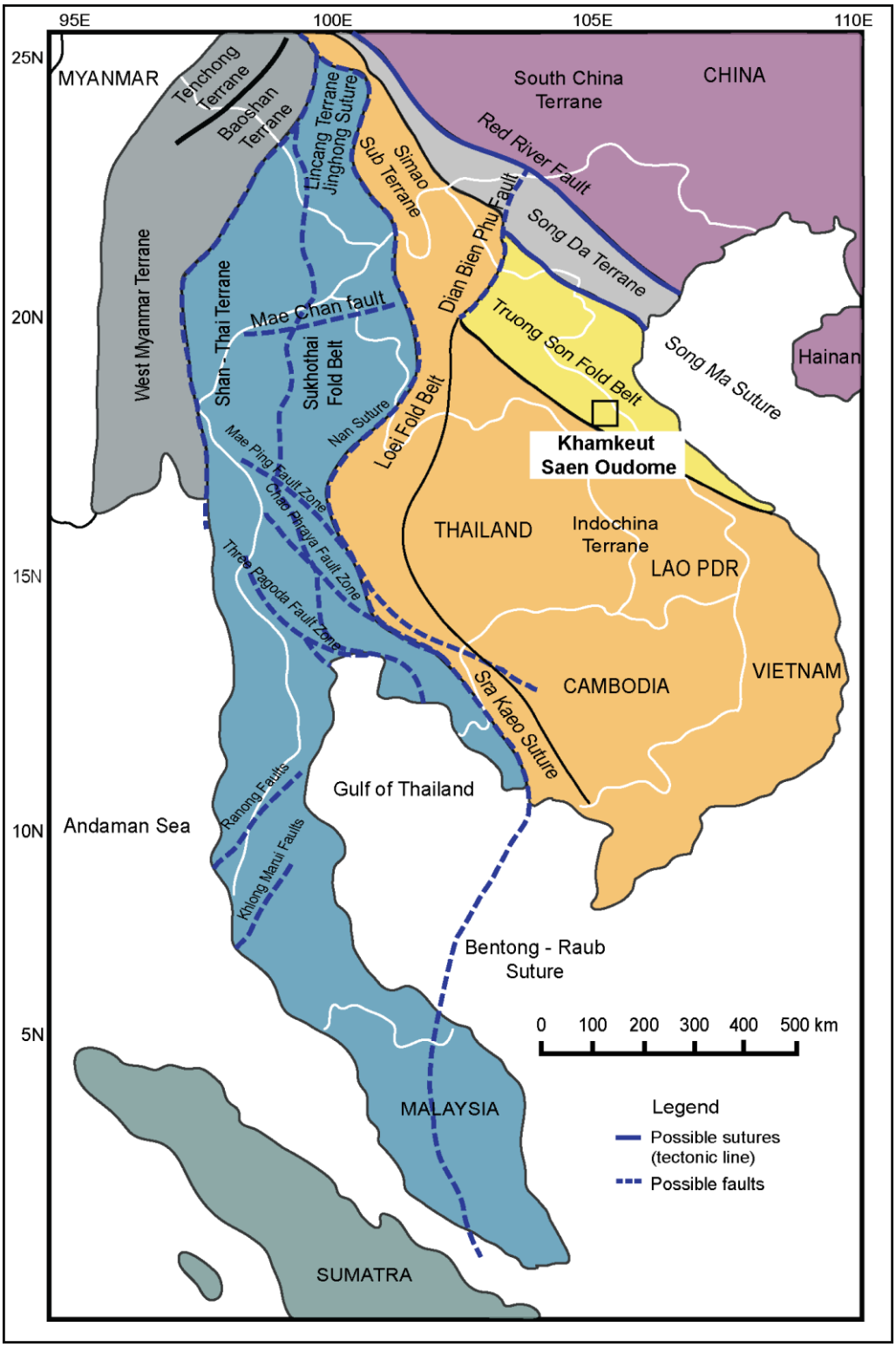

Fig. 2. 1 Map showing major tectonic terranes and suture zones of mainland SE Asia (Salam et al., 2007; Sone and Metcalfe, 2008)

(2) The TFB covers an area eastern part of Indochina Terrane in Laos, Vietnam and northeast of Cambodia, is a Paleozoic volcano-sedimentary sequence. It is previously known as the Annamitic Cordillera forming as elongated mountain system covering central Vietnam and central eastern Laos (Fig. 2.1). This fold belt is widely covered by Paleozoic sedimentary and volcanic rocks, and Late Paleozoic to Early Mesozoic volcano-plutonic rocks (Lepvrier et al., 1997; Lepvrier et al., 2008). In this region, the Paleozoic sedimentary rocks consist of conglomerate, arkosic and feldspathic sandstone, tuffaceous sandstone, shale, carbonaceous siltstone and limestone.

Igneous rocks in the TFB consist mainly of plutonic rocks (e.g., granite and granodiorite) and volcanic rocks (e.g., rhyodacite and andesite porphyry). Hutchison (1989) suggested that the TFB is developed by Paleozoic volcano-sedimentary arc in the Paleo-Tethys Ocean (Fig. 2.2). Ordovician to Devonian volcanic rocks which include andesite and tuffs occurs in association with sedimentary rocks. The volcanic rocks in this area were intruded by Early Permian plutonic rocks of I-type and S-type affinities.

In Permian, the TFB was dominated by deposition of limestone. Hutchison (1989) suggested that the andesitic volcanic rocks were overlain by shallow marine clastic rocks of Early Triassic age. According to (Lepvrier et al., 2004; Lepvrier et al., 1997) the high grade metamorphic rocks up to amphibolite facies were formed during 240 to 250 Ma as a result of dextral strike slip faults and shear zones in the TFB. It should be noted that this is a major period for mineralization in the LFB particularly for Cu-Au (±Ag) deposits (Fig. 2.3, Salam et al., 2014).

The S-type granitoid formed along the TFB has ages of 240 Ma to 270 Ma (Hoa et al., 2008; Lepvrier et al., 1997; Lepvrier et al., 2008). These granitic rocks might have responsible for tin mineralization in this region (Sanematsu et al. 20xx). DGM (2000a) reported that the Permo – Triassic volcano – plutonic rocks emplacing in the Ordovician – Carboniferous sedimentary rocks in southwestern of TFB (Fig. 2.3). These volcano-plutonic rocks are divided into 1) the Phou Thoun Complex (PTC) and 2) Say Phou Ngou Complex (SNC). The PTC consists of medium- to fine-

grained biotite ± hornblende granite and granodiorite which intrude into the Devonian sandstone and limestone. The SNC emplaces on sandstone during Triassic period comprising dacite, trachyte and rhyolite (DGM, 2000a). For the intrusive rocks, they consist of Permo – Triassic Nape Complex (NPC) and Cretaceous Poung Kuak Complex (PKC; DGM, 2000a). The NPC comprises of medium – grained biotite granite, granodiorite, porphyritic granite, aplite and pegmatite (DGM, 2000a) whereas, the PKC consists medium – grained leucocratic granite and mica granite. These granitic rocks are reported to associate with Cu – Au mineralization (Fig. 2.2; DGM, 2000a).

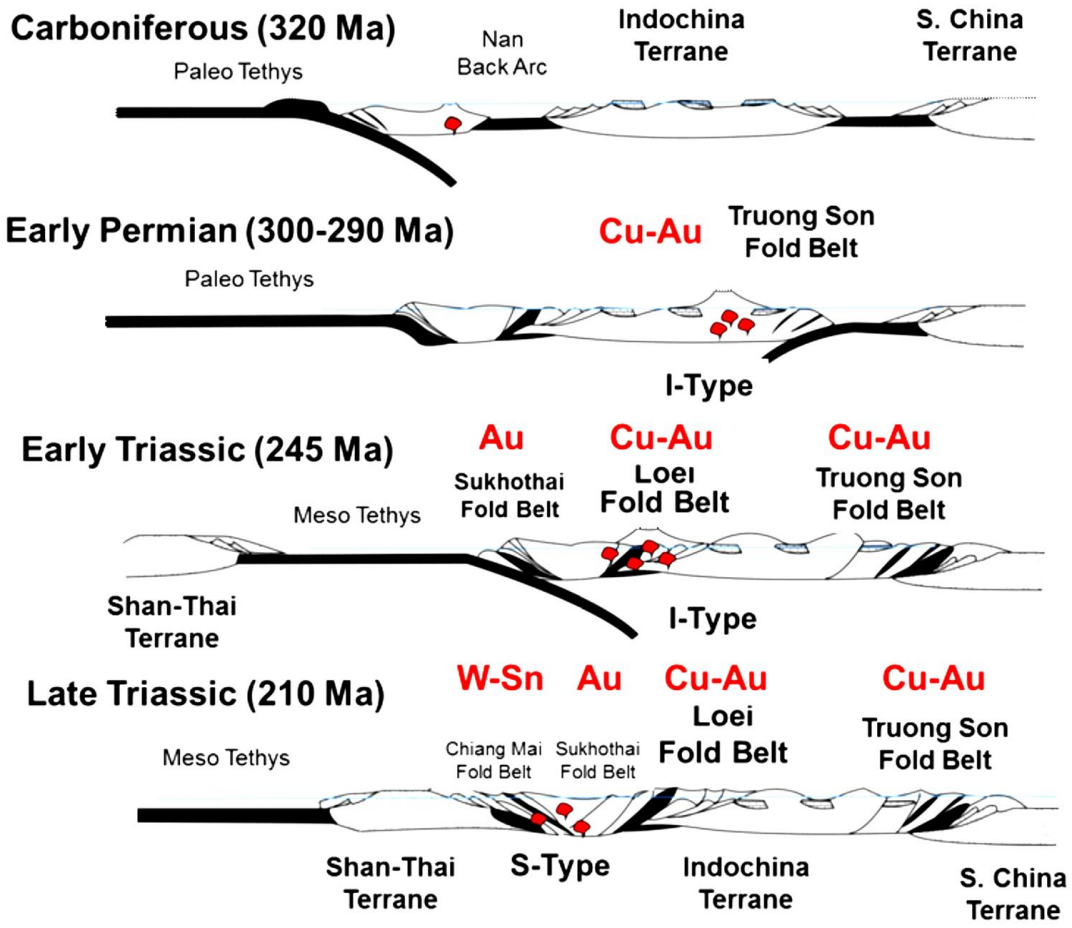

Fig. 2. 2 Carboniferous to Triassic (330-210 Ma) tectonic and metallogenic evolution of mainland SE Asia (Khin Zaw et al., 1999; Khin Zaw et al., 2007a; Khin Zaw et al., 2014).

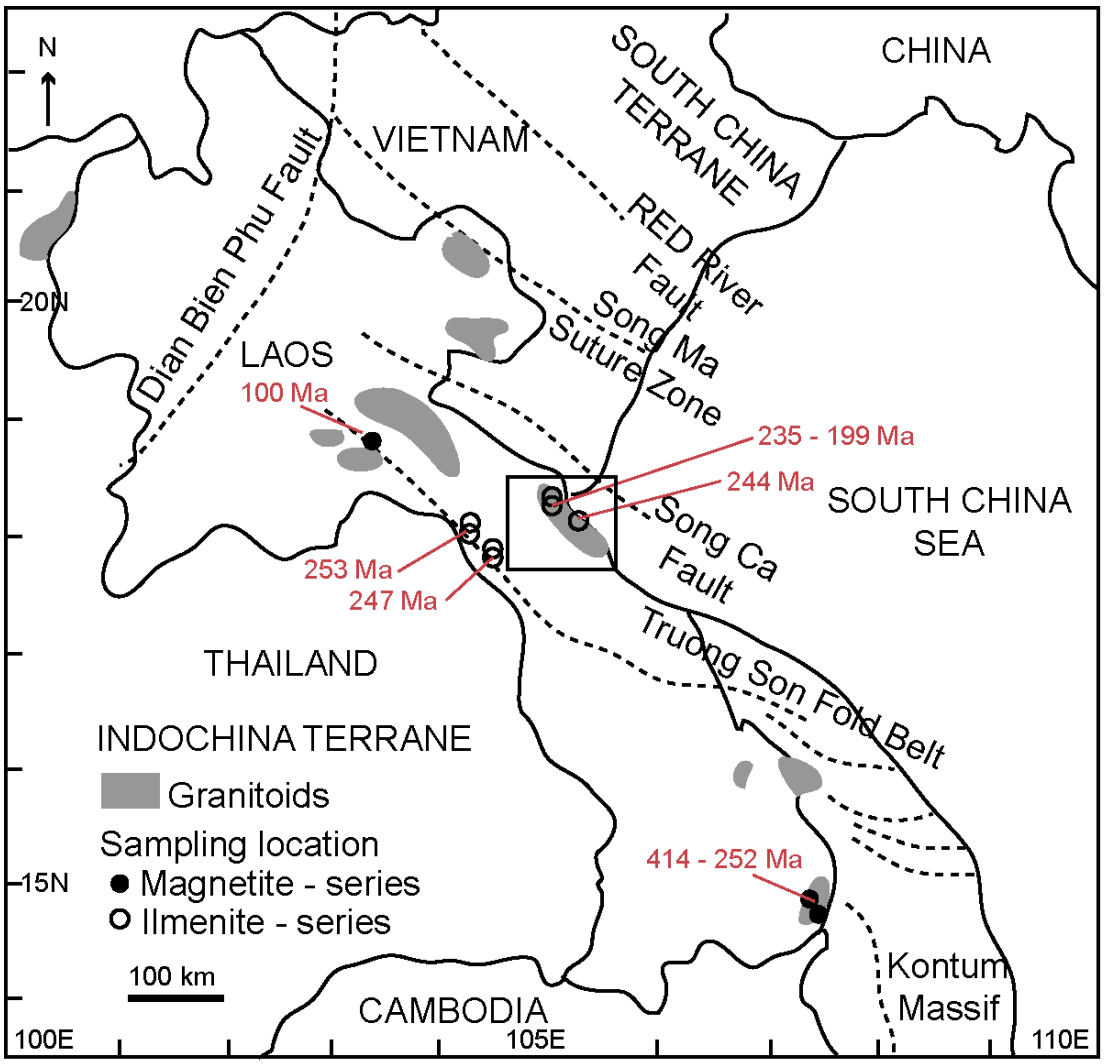

Fig. 2. 3 Map showing distribution of granite of various ages in Truong Son fold belt and Kontum massif in Laos and Vietnam (Nakano et al., 2008; Sanematsu et al., 2011).

(3) Loei Fold Belt (LFB) is located in the western edge of the Indochina terrane. Sukhothai Fold Belt (SFB) is located on the eastern edge of Shan-Thai or east of Indochina terranes (LFB). Nan-Uttaradit- Sra Kaeo forms as suture zone between LFB and SFB (Fig. 2.1; (Hutchison, 1989; Stokes et al., 1996). The LFB comprises of Devonian volcano sedimentary sequence and covered by deep water chert that overlain by Carboniferous to Permian fossiliferous limestone (Bunopas and Vella, 1983). Late Permian (258 to 250 Ma) arc related volcanic rocks are widely distributed in LFB particularly in central Thailand (e.g. Phetchabun and Nakhon Sawan area),

and were intruded by Early to Middle Triassic (249 to 241 Ma) granite, granodiorite and diorite (Hutchison, 1989). These volcanic rocks are closely associated with Au-Ag mineralization (e.g. Chatree epithermal gold-silver deposit; Salam et al., 2014) whereas, the Middle Triassic granitic rocks often associated with Cu-Mo mineralization (e.g. N-prospect, south of Chatree mine; Fig. 2.2).

SFB consists predominantly of Cambrian to Triassic sedimentary and volcanic rocks. The Cambrian to Ordovician rocks include conglomerate, metasandstone and shale then covered by Ordovician limestone, dolomite and calcareous shale (Bunopas and Vella, 1983). Late Permian to Early Triassic arc related volcanic rocks ranging in composition from basaltic andesite to rhyolite are also widely distributed (Srichan et al., 2008) Singharajwarapan (1994) reported that the intrusive rocks in SFB are of Triassic age including granite, granodiorite, and diorite. In SFB, the mineralization is less developed. However, where it presents it tend to characterized by antimony-gold (Bo Thong, eastern Thailand; (Paipana, 2014))

2.3 Regional geology of Laos

The regional geology of Laos is given in Figure 2.4. The oldest in Laos is Precambrian rocks second older rocks Phanerozoic in age. Their distribution and nature are summarized below in order from older to the younger units.

2.3.1 Precambrian and Phanerozoic metamorphic rocks

Precambrian metamorphic rocks in Laos consist of two basement complexes namely (1) the Song Ma Massif and (2) the Pak Lay Massif (Chiang Saen). The Song Ma Massif is in northeastern Laos; the zone is NW-trending. The age of Song Ma Massif is Late Proterozoic identified as low-grade metamorphic rocks consisting mica schist, quartz-chlorite-sericite schist intercalated with marble and quartzite. The Pak Lay Massif is in northwest Laos which is comprised of non-foliated leucocratic granite, gneiss and minor biotite amphibolite schist (Fig. 2.4; (Stokes et al., 1996; Vilaihongs and Areesiri, 1997).

2.3.2 Paleozoic sedimentary rocks

Cambrian

The Cambrian rocks in Laos can be divided into two Formations namely 1) Middle Cambrian Song Ma Formation and Late Cambrian Samneua Formation (Fig. 2.4). The former one is about 1,300 meters thick consisting of conglomerate, micaceous quartzose schist, amphibolite schist, quartzite and limestone. The later one is Late Cambrian Samneua Formation which is about 1100 meters thick and it composes of mudstone, shale and limestone (Stokes et al., 1996; Workman, 1975).

Ordovician

Ordovician rocks in Laos are composed of shale, sandstone and limestone, which have thickness up to 3000 meters and overlying Cambrian rocks (Fontaine and Workman, 1978). The Ordovician stratigraphy in the Nape district and Nam Nhuong in eastern Laos can be divided into three sequences such as (1) early: non-fossiliferous black shales; (2) middle: fossiliferous shales which consisting echinoderms and trilobites, and; (3) late: sandstone consisting large trilobites (Fromaget, 1927).

Silurian

Silurian sequences are located the northern and eastern margins of the Indochina Terrane which consisted of shales and thickness of this sequence in eastern Laos and central Vietnam up to 5000 meters. The Silurian stratigraphy is generally consisted of shale, sandstone, and greywacke containing crinoids, trilobites and brachiopods *(Spirifer sulcatus)* which indicating deposition in Llandovery to Wendlockian age (Fontaine and Workman, 1978; Stokes et al., 1996).

Devonian

Devonian stratigraphy is in the north, east and south of Laos and thickness of fossiliferous marine sequences 4000 meters (Fontaine and Workman, 1978). Shallow brackish-water marine facies in Early Devonian of eastern Laos preserved along Truong Son Fold Belt which consisted sandstone, shale, calcareous shale, marl and

limestone consisting brachiopod and coral fossils. The Middle Devonian stratigraphy in a NE-SW trending belt at Pak Lay northwards consist sandy shale, shale, calcareous shale, chert and minor limestone containing stromatoporoids, corals and brachiopods (Fontaine and Workman, 1978; Stokes et al., 1996).

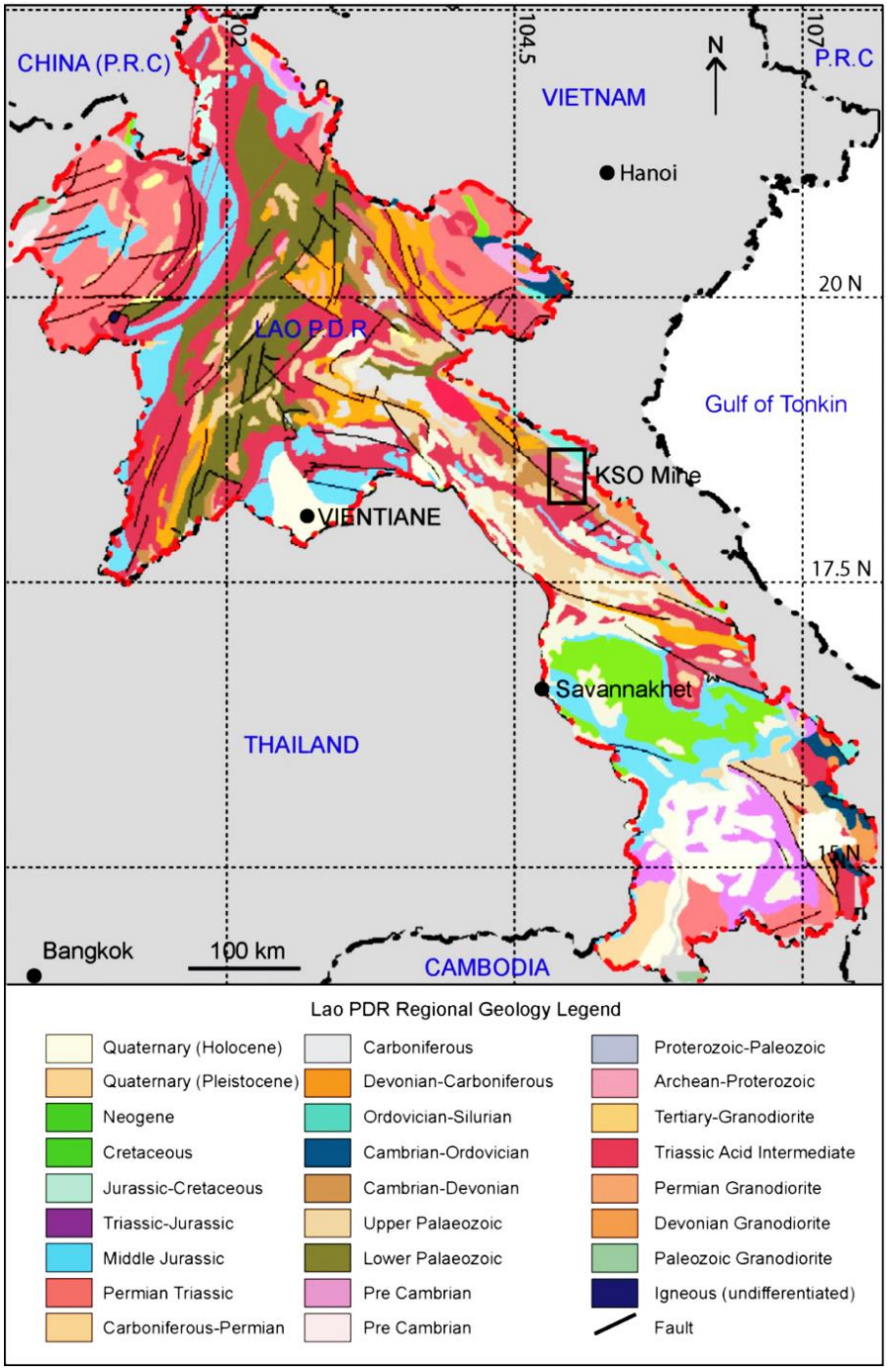

Fig. 2. 4 Regional geology map of Laos shows the location of KSO mine (black rectangle) (Cromie et al., 2010).

Carboniferous

Carboniferous rocks generally occur in northern and eastern of Laos and are importantly discordant with Devonian marine facies rocks, where the boundary is presented that terrestrial facies deposited during a marine regression period in the Carboniferous age (Fontaine and Workman, 1978; Stokes et al., 1996). The Kontum Massif in Carboniferous age is interpreted to forming the Proto-Indosinia continental fragment which consisted of sandstone, shale, chert, coal and limestone (Stokes et al., 1996). Carboniferous stratigraphy in eastern Laos contains foraminifers' fossils which are deposited between 1000 and 2000 meters of thickness (Fontaine and Workman, 1978).

Permian

Early to Middle Permian sedimentary rocks comprise limestone, chert, shale, sandstone, conglomerate, coal and tuffs. Thickness of Permian sequences up to 2,500 meters. Permian coal beds occur in the north at Phong Saly and limestone karsts are deposited in the west of Laos and clastic rocks generally occur in the south of Laos (Fig. 2.4). Fossils in the Permian limestone sequences compose corals, algae, brachiopods and foraminifera. The Late Permian sequences are during marine regressive environment which have bauxite occurrences in Laos (Fontaine and Workman, 1978; Stokes et al., 1996; Workman, 1975).

2.3.3 Mesozoic sedimentary rocks

Mesozoic rocks in Indochina comprises two major facies such as (1) Middle Triassic to Early Jurassic which is non-oxidized marine facies developed in sedimentary basins and (2) Triassic to Cretaceous which continental facies as red bed facies (Hutchison, 1989; Stokes et al., 1996; Workman, 1975). In the Mesozoic sequences found vertical transition from marine to continental facies which have dominantly characteristic of interfingering of the two facies types. The Mesozoic sequences which overlying the Kontum Massif are known as the Khorat Group depositing in eastern Thailand and southern Laos (Fig. 2.4; (Workman, 1975). There

are discontinuities of sequences between Permian and Middle to Late Triassic sequences (Stokes et al., 1996).

Triassic

The Middle to Late Triassic marine sequence composes mainly of limestone, sandstone and siltstone and it occurs mainly in northern Laos (Fig. 2.4; (Workman, 1975). However, the younger rocks (Late Triassic) observed in the northern part of Indochina Terrane is folded. The rocks of Late Triassic to Cretaceous age in the southern Laos is identified as continental red bed consisting of sandstone and conglomerate (Fig. 2.4; (Fontaine and Workman, 1978; Workman, 1975).

Jurassic - Cretaceous

Early Jurassic rocks in the central and southern Laos are part of continental red bed known as “Terrane Rouge” composing dominantly of purplish-red sandy shales, sandstone, and conglomerate (Fig. 2.4; (Fontaine and Workman, 1978; Stokes et al., 1996). Moreover, the red-beds of the Early Jurassic age in Laos are reported to have interbedded with calcareous shale containing significant of Plesiosaur fossils (Stokes et al., 1996).

Cretaceous

In Laos, the Early Cretaceous red bed sequences has thickness up to 2000 meters (Stokes et al., 1996). However, the Cretaceous red beds in northern and central Laos consist of mudstone, siltstone and fine-grained sandstone with evaporates units (Fig. 2.4; Workman, 1990). The Cretaceous sedimentary rocks in southern Laos are reported to have interbedded with gypsum and rock salt and this sequence is about 100 to 300 meters thick. In Southern Laos, this sequence contains fossils such as *Mandchurosaurus, Titanosaurus* and *Hadrosaurus* of dinosaur and theropods, turtles and crocodiles (Stokes et al., 1996).

2.3.4 Cenozoic

The Early Tertiary rocks have not been reported in Laos whereas, Late Tertiary sequences was identified in northern Laos and is interpreted to have derived

from terrestrial freshwater deposits consisting of conglomerate, sandstone, shale, carbonaceous mudstone, marl and lignite. For the Late Tertiary rocks in western Laos were deposited from fluvial sands and gravels. The Quaternary sediments in the northern Laos particularly along Mekong River are fluvial terraces consisting of gravels, sands and silts, and may also include loess and ash deposits (Stokes et al., 1996; Workman, 1975).

2.3.5 Igneous Intrusions

In Laos, at least four generations of magmatic rock cycles occur during Late Proterozoic to Mesozoic periods (Stokes et al., 1996; Workman, 1975). The earliest igneous rocks forms during Early to Late Proterozoic which mainly distributed in southern Laos (Kontum Massif) and northern Laos in Samneua and Xieng Khouang Provinces consisting of gneiss, granodiorite, granite, migmatite and pegmatite intrusions/dyke (Fig. 2.4; (Stokes et al., 1996). In Laos, the Proterozoic igneous rocks are mainly gneissic rocks (Kontum Massif) age 1400 Ma (U-Pb zircon ages; (Nam et al., 2001)).

The second cycle forms during Early to Middle Paleozoic occur along deep-seated faults in Northeast and Northwest fold belts. This magmatic cycle consists of granodiorite, granite and ultramafic rocks (dunite and serpentine) (Stokes et al., 1996). The Paleozoic rocks in northern Laos are represented by granite intrusion of 434 Ma (Silurian; (Metcalfe, 2006)). In south and central Laos, the intrusive rocks are rhyodacite porphyry age of 290 Ma (Loader, 1990). In the northern Laos especially Pak Lay to Luang Prabung provinces represented by granodiorite (264 ± 10 Ma) and monzonite (255 ± 10 Ma) by K/Ar method (Fontaine and Workman, 1978).

Late Paleozoic to Early Mesozoic cycle in northern to central Laos consists of (a) Carboniferous monzonite, diorite, granodiorite, granite and aplite and (b) Triassic quartz-diorite, and granite porphyry. In Laos the ultramafic rocks of Triassic age consists dunite, peridotite and serpentinite (Fig. 2.4; (Stokes et al., 1996; Workman, 1975). The fourth cycle consisted of (a) Cretaceous age granite, porphyry and biotite muscovite granite, (b) Paleogene age granosyenite porphyry and (3) Pliocene to Pleistocene age gabbro-dolerite (Stokes et al., 1996; Workman, 1975).

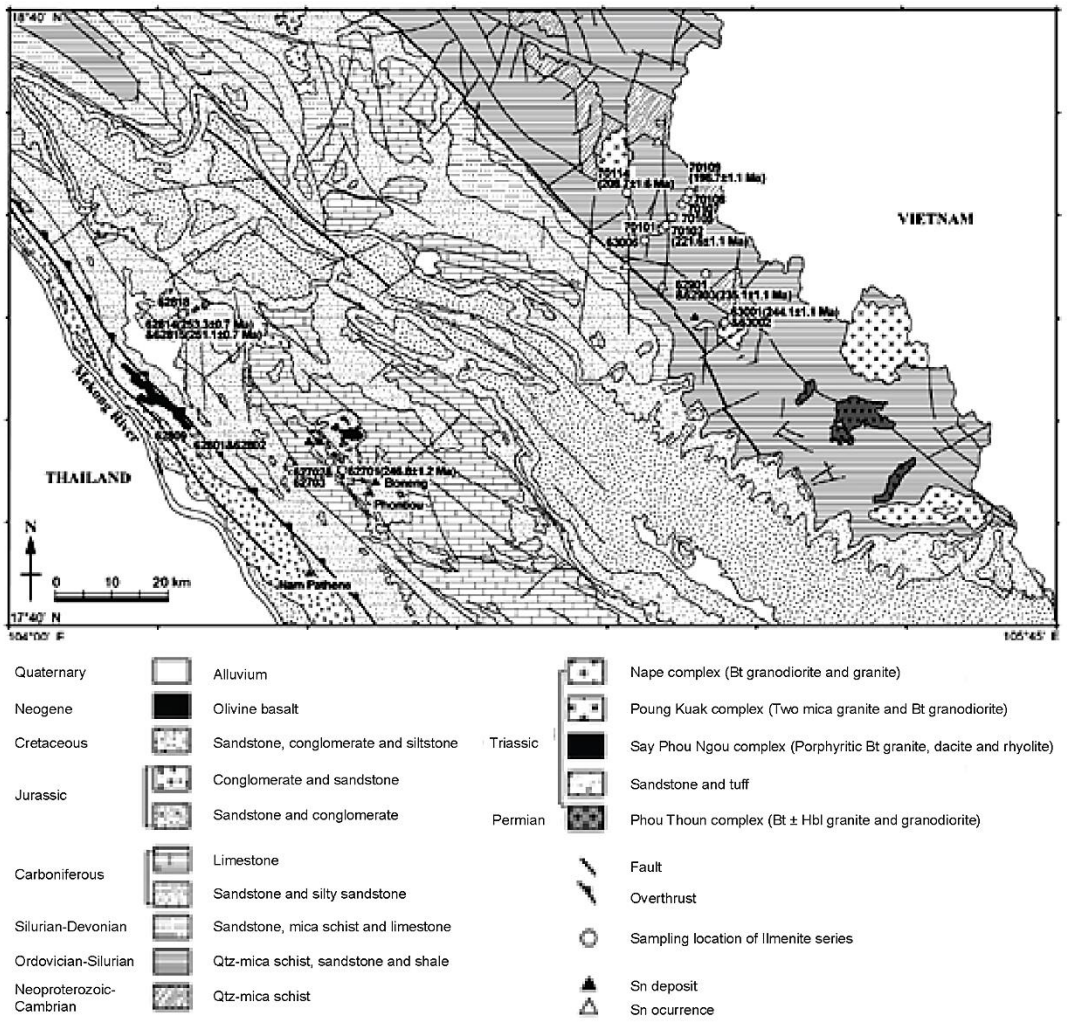

Fig. 2. 5 Geologic map showing the distribution of granite in the Truong Son fold belt from central Laos to central Vietnam. $^{40}Ar/^{39}Ar$ ages determined in this area shown in the map (Sanematsu et al., 2011).

2.4 Major mineral deposits

Mineral deposits in Truong Son Fold Belt

(1) Phu Kham deposit is located in the area where TFB and LFB jointed (Fig. 2.6). This deposit has been assigned to locate in TFB by some authors. However, it is possible to be part of LFB. The Phu Kham deposit is porphyry-related skarn copper-gold deposits with grade 0.8% Cu and 0.3 g/t Au (Backhouse, 2004; Kamvong et al., 2014; Tate, 2005). It is hosted in volcaniclastic rocks and bedded limestone of Late Carboniferous (306 - 304 Ma) and Middle Triassic (244 - 241 Ma) ages which were

intruded by diorite porphyry of Early Permian age (Kamvong et al., 2014). At Phu Kham, gold associates with chalcopyrite, bornite and tetrahedrite (Kamvong et al., 2014; Tate, 2005).

(2) Sepon deposit is of the important gold deposit in mainland Southeast Asia which has been identified as sediment–hosted gold deposits with gold grade about 1.8 g/t (Cromie et al., 2006; Smith et al., 1996). However, due to several similarities with the Carlin-type deposit, the Sepon deposit has been identified as Carlin-like gold deposit. Hence, gold is associated with disseminated pyrite in Ordovician to Carboniferous calcareous sedimentary rock units that occurs with jasperoid (silica replacement) zone at the contact with Permian to Carboniferous rhyodacite porphyry stocks (Cromie et al., 2006; Cromie et al., 2010; Smith et al., 2005).

(3) Phouc Son deposit is located in Vietnam. It consists of two gold orebodies namely, Bai Dat and Bai Go (Banks et al., 2004; Manaka et al., 2010). The Phouc Son gold deposit has gold grade >12 g/t Au. The deposit consists several mineralization styles; for example, intrusion-hosted (e.g., Round Hill), skarn (e.g., Khe Rin), and low-angle shear-hosted (e.g. Bai Dat and Bai Go) (Banks et al., 2004; Manaka et al., 2010). Based on data such as geology, geochemistry and geophysics the deposit is classified as intrusion related gold system (Banks et al., 2004).

(4) Bong Mieu deposit is situated in Bong Mieu area in the southeast of Quang Nam Province, central Vietnam (Fig. 2.6). It consists two styles of mineral deposits in which Ho Gan represent intrusion-related gold deposit and Ho Ray represent skarn deposit. The gold grade is > 10 g/t (Quynh et al., 2004). Gold mineralization is characterized by assemblage of pyrite, chalcopyrite, pyrrhotite, sphalerite, galena, hematite, magnetite and bismuth (Lee et al., 2010; Quynh et al., 2004). Both skarn and intrusion related gold deposits are hosted in metamorphic rocks consisting of sericite-biotite schist, biotite-silimanite gneiss, quartz-feldspar-biotite schist which intruded by granite and pegmatite (Lee et al., 2010; Quynh et al., 2004).

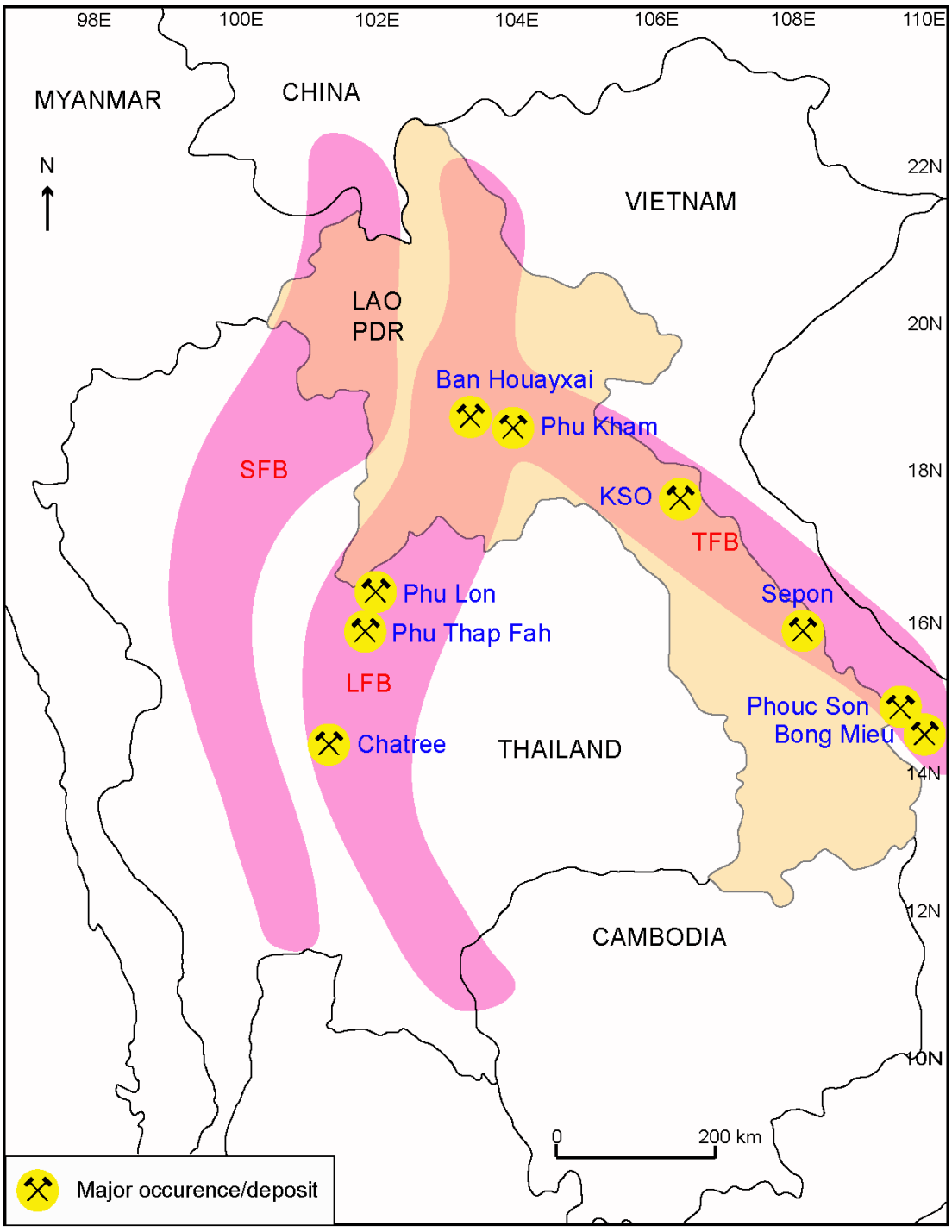

Fig. 2. 6 Map showing major mineral deposits surrounding KSO deposit that confine TFB and LFB (Kamvong et al., 2006; Salam et al., 2014).

(5) Ban Houayxai deposit is the third largest gold resource (76 Mt at 0.82 g/t Au and 7.0 g/t Ag) in the mainland southeast Asia (Fig. 2.6). The deposit is located in Bokeo province, Laos. This deposit is identified as low - sulfidation epithermal gold - silver deposit similar to Chatree deposit which is hosted by Early Permian volcano-sedimentary sequence including volcanic breccia, siltstone, tuffaceous sandstone, red bed siltstone and sedimentary breccia (Manaka, 2008; Manaka et al., 2014). U-Pb zircon dating of andesite and volcanic breccia obtained Early Permian (280 Ma) age (Manaka, 2008; Manaka et al., 2014). Here, gold occurs as electrum which associates with chalcopyrite, tetrahedrite, sphalerite and galena.

Mineral deposits in Loei Fold Belt

(6) Chatree deposit has been defined as low - sulfidation epithermal gold-silver deposit Salam, 2013). The deposit is located between Phichit and Phetchabun province in central Thailand (Fig. 2.6). Total mineral reserve is 81 million tons at 1.2 g/t Au and 10 g/t Ag (Salam et al., 2014). At Chatree, the mineralization occurs as veins/veinlets, stockworks and minor breccia and hosted by volcaniclastics and volcanogenic-sedimentary rocks of Late Permian to Early Triassic (Dedenczuk, 1998; Kromkhun, 2005; Salam et al., 2014; Salam et al., 2013). Gold occurs as electrum in association with quartz and calcite and commonly associates with sulfide minerals particularly pyrite, sphalerite, galena, chalcopyrite and argentite (Salam et al., 2008; Salam et al., 2007).

(7) Phu Thap Fah deposit is copper-gold skarn deposit located in Loei province, Northeastern Thailand (Fig. 2.6). Total reserve of 407,000 tons at 3.54 g/t Au (Khin Zaw et al., 2007b). The mineralization is hosted by Permian sedimentary sequences including crystalline limestone, muddy sandstone, carbonaceous siltstone and shale. Triassic granodiorite and microdiorite shallow intrusive bodies responsible for skarn mineralization (Khin Zaw et al., 2007a). Gold occurs as electrum, native gold, gold-bismuth and gold-bismuth-telluride. It associates with chalcopyrite, pyrrhotite, bismuth and telluride. A characteristic of vein is gold ± bismuth ±

tellurium mineralization which related to retrograde reduced pyrrhotite-rich massive sulfide and quartz veins (Khin Zaw et al., 2007a).

(8) Phu Lon deposit has been classified as copper-gold skarn deposit with ore reserve of 5.4 million tons at 2.4 % Cu and 0.64 g/t Au (Meinert et al., 2005). The deposit is located in Sang Khom province, Northeastern Thailand (Fig. 2.6). Skarn alteration occurs as result of Triassic quartz monzodiorite intrudes the Early Carboniferous volcaniclastics and limestone (Kamvong et al., 2006; Khin Zaw et al., 2007a; Sitthithaworn et al., 1993). This deposit is identified as calcic skarn with the present of both endoskarn and exoskarn. In skarn facies, andradite and diopside represent main prograde skarn minerals, whereas epidote, chlorite, tremolite, actinolite and calcite are retrograde skarn minerals (Kamvong and Zaw, 2009). Gold mineralization is characterized by chalcopyrite, bornite and magnetite assemblage.

Table 2. 1 Geological characteristics of important mineral deposits along Indochina Terrane

Deposit	Location	Host rocks/(age)	Intrusions/(age)	Alteration types	Ore type/Mineralogy	Resource/Reserve	Reference
Phu Kham	Laos: 18° 55' N, 102° 55' E	Volcaniclastics and interbedded limestone (Carboniferous - Early Permian)	Diorite porphyry (Early Permian)	Potassic, phyllic, skarn (prograde and retrograde)	Porphyry-related skarn (oxidised): chalcopyrite, bornite, tetrahedrite, gold	108 Mt @ 0.8% Cu, 0.3 g/t Au	(1); (12);
Sepon	Laos: 16° 58' N, 105° 59' E	Sandstone, mudstone, calcareous shale, limestone, dolomite (Ordovician - Carboniferous)	Rhyodacite Porphyry (Permian - Carboniferous)	(A) Sedimentary rocks: decalcification, silicification, dolomitisation, skarn, (B) Intrusions: potassic, propylittic, phyllic, skarn	(A) SHGD: pyrite, gold, sphalerite, galena (B) Skarn: chalcocite, chalcopyrite, bornite	4.75 Moz Au for 83 Mt @ 1.8 g/t Au; 2 Mt Cu metal	(4); (8); (11); (13)
Phouc Son	Vietnam (central), Quang Nam Province	Greenschist facies metasediments and intercalated metavolcanics (Precambrian-Cambrian)	Granites (Devonian, Permian, Triassic); Gabbro and diorite (Phaneorozoic)	(A) Metapelite rocks: sericite-biotite-albite; (B) Metabasites: chloritealbite-actinolite-epidote	Intrusion-associated: pyrrhotite, pyrite, bismuth, sphalerite, galena, tellurium, silver, gold	0.21 Moz Au for 0.5 Mt @ >12 g/t Au	(2);
Bong Mieu	Vietnam (central), Quang Nam Province	Metamorphosed facies: sericite-biotite schist, biotite-silimanite gneiss, quartz-feldspar-biotite schist.	Ganite and pegmatite (Undifferentiated)	Potassic, phyllic, skarn (prograde and retrograde)	Intrusion-associated skarn: pyrite, chalcopyrite, pyrrhotite, sphalerite, galena, hematite, magnetite, bismuth	0.61 Moz Au for 5 Mt @ >10 g/t Au	(15);
Ban Houayxai	Laos: 18° 56' N, 102° 50' E	Siltstone and volcaniclastics (Early Permian)	Feldspar porphyry (Early Permian)	Quartz, sericite, chlorite, pyrite, clacite, adularia	Epithermal: electrum, chalcopyrite, tetrahedrite sphalerite, galena	No Data	(14);
Chatree	Thailand: 16o 17' N, 100o 39' E	Volcaniclastics (Permian - Early Triassic)	Hornblende diorite dyke (Early Triassic)	Quartz, pyrite, calacite, adularia chlorite, sericite	Epithermal: electrum, minor chalcopyrite	1.8 Moz Au (1.8 g/t Au)	(3); (7) (9);(5)
Phu Thap Fah	Thailand: 17° 56' N, 101° 40' E	Siliciclastics and Limestone (Permian)	Granodiorite (Triassic)	Prograde and retrograde skarn assemblages	Skarn (reduced): electrum, Au, bismuth, telluride, chalcopyrite, pyrrhotite	0.7 Mt @ 7.97 g/t Au,	(7); (16)

Reference to numbers (Refs) shown in Table 2.1: (1) Backhouse (2004); (2) Banks et al. (2004); (3) Cumming et al. (2008); (4) Cromie et al. (2010) ; (5) ; (6) Kamvong et al. (2006); (7) Khin Zaw et al. (2007a); (8) Manini et al. (2001); (9) Salam et al. (2007); (10) Sitthithaworn et al. (1993); (11) Smith et al. (2005); (12) Tate (2005); (13) Olberg and Manini (2005); (14) Manaka (2008); (15) Quynh et al. (2004); (16) Rodmanee (2000).

Table 2. 2 Geological characteristics of important mineral deposits along Indochina Terrane

Deposit	Location	Host rocks/(age)	Intrusions/(age)	Alteration types	Ore type/Mineralogy	Resource/Reserve	Reference
Phu Lon	Thailand: 18° 12' N, 102° 08' E	Limestone and Volcaniclastics (Late Devonian)	Diorite and quartz monzonite porphyry (Triassic)	Potassic, propylitic, phyllic, skarn (prograde and retrograde)	Porphyry-related skarn (oxidised): chalcopyrite, bornite, magnetite, gold	5.4 Mt @ 2.4% Cu, 0.64 g/t Au	(10); (17);
Long Chieng Track	Laos: 18° 56' N, 102° 53' E	Volcaniclastics and interbedded limestone (Carboniferous - Permian)	Monzonite porphyry (Early Permian)	Quartz, sericite, chlorite, pyrite, clacite, adularia	Epithermal: electrum, chalcopyrite, tetrahedrite sphalerite, galena	0.62 Mt @ 0.96 g/t Au	(14);
Puthep 1	Thailand: 17° 28' N, 101° 52' E	Siliciclastics and Limestone (Carboniferous)	Diorite and quartz monzonite porphyry (Triassic)	Potassic, propylitic, phyllic, skarn (prograde and retrograde)	Porphyry-related skarn (oxidised): chalcopyrite, pyrite, magnetite	85 Mt @ 0.4 % Cu,	(6);
Puthep 2	Thailand: 17o 28' N, 101o 52' E	Siliciclastics and Limestone (Carboniferous)	Diorite and quartz monzonite porphyry (Triassic)	Potassic, propylitic, phyllic, skarn (prograde and retrograde)	Porphyry-related skarn (oxidised): chalcopyrite, pyrite, magnetite	36 Mt @ 0.43 % Cu,	(6);
Wang Yai	Thailand: 16° 22' N, 100° 38' E	Volcaniclastics, rhyolite (Early Triassic)	Diorite (Early Triassic)	Quartz, pyrite, calacite, adularia chlorite, sericite	Epithermal: electrum, argentite, chalcopyrite	No Data	(18);
Frenchmen	Thailand: 13° 57' N, 101° 49' E	Volcanoclastics and interbedded limestone (Lower Permian)	Granodiorite (Late Triassic)	Prograde and retrograde skarn assemblages	Porphyry-related skarn (oxidised): chalcopyrite, pyrite, molybdenite	No Data	(19);
Khao Phanom Pha	Thailand: 16° 18' N, 100° 33' E	Volcaniclastics (Late Permian)	No known intrusion	Pyrrhotite, pyrite, chalcopyrite, galena, native	Chlorite, muscovite	No data	(20); (21);
Khao Lek	Thailand: 15° 56' N, 100° 46' E	Volcaniclastics and limestone	Biotite-hornblende granodiorite (Late Permian to Early Triassic)	Magnetite, pyrite, chalcopyrite, gold	Skarn (prograde and retrogrde)	No data	(7); (20);

Reference to numbers (Refs) shown in Table 2.2: (17) Kamvong and Zaw (2009); (18) De Little (2005); (19) Muller (1999); (20) Khositanont (2008); (21) Crossing (2004).

2.5 Regional Geology

The KSO license area (Fig. 2.7) comprises Middle to Upper Paleozoic rocks and granitic rocks of the Late Paleozoic. The Lower Paleozoic (Upper Ordovician to Lower Silurian) includes Nam Houay Formations and Koduk Formations. The Nam Houay Formation occurs in the eastern part of area (Fig. 2.7). It is believed to have evolved in a deep marine basin formed in response to large regional northwest-southeast trending structures. It is characterized by low grade metamorphism.

The Phon Keo Formation of Upper Silurian-Devonian comprises schists, siltstone, and some sandstone. The Carboniferous and Permian is characterized largely by the Boulapha Formation consists of terrigeno-cherty sediments in lower part and pure limestone forming large karst topography area in the upper part.

Mesozoic (Triassic, Jurassic and Cretaceous) rocks in central Loas are represented by sedimentary and volcanogenic-sedimentary formations, including the Triassic Lingkho Formation; the Jurassic and Cretaceous Ban Lao Formation, the Nam Theun Group, the Nam Phouan, Nam Xot, Nam Noy and Nong Boua Formations.

The Cenozoic sedimentary and volcanogenic formations in Mid Central Laos have thin and limited distribution and comprise of unconsolidated Quaternary (<5.3 Ma) alluvial sediments. It covers in the intermountain plains and in valleys of large rivers.

The granitoid in TFB occurs along NW – trending from Vietnam to central Laos has age of 240 Ma to 270 Ma, and is classified as S-type granite (Hoa et al., 2008; Lepvrier et al., 2004). The closest intrusive rocks to KSO area are Permo – Triassic Nape Complex (NPC) and Cretaceous Poung Kuak Complex (PKC) (DGM, 2000a). The distance between these granitic bodies and KSO mine approximately 1 km (Fig. 2.7). The Nape complex (NPC) consists of medium – grained biotite granite, granodiorite, porphyritic granite, aplite and pegmatite (DGM, 2000a). The Poung Kuak Complex (PKC) composes of medium – grained leucocratic porphyritic two – mica granite and its age is Triassic (198 to 244 Ma; (Sanematsu et al., 2011). This complex is reported to associate with W – Au mineralization (DGM, 2000a).

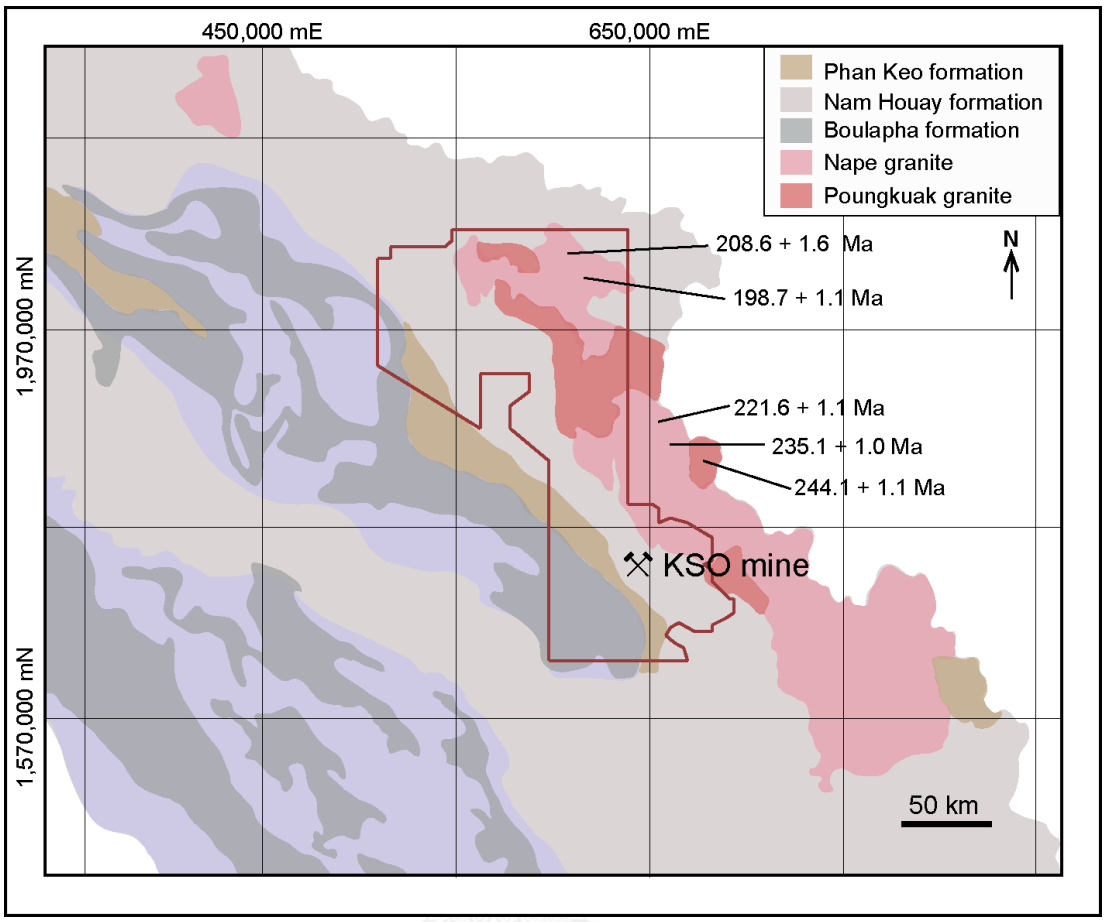

Fig. 2. 7 Geologic map showing distribution of granites and their ages in Truong Son fold belt and Kontum massif of Laos and Vietnam (Nakano et al., 2008; Sanematsu et al., 2011).

CHAPTER III

GEOLOGY OF DEPOSIT

3.1 Introduction

This chapter documents detailed deposit-scale geology of the Khamkeut Saen Oudom deposit (Fig. 3.1). This follows by a description of rock types (Appendix A) and nature of ore lenses. This study base on pits investigation and drill core logging focusing on selected cross sections (Section 508700mE and 509570mE) and others individual drill holes that are not shown in cross sections.

The geology of the deposit area has been rechecked based on the company pre-existing geologic map scale 1: 30000 (SRK, 2011). Field checking and drill core logging has been undertaken to identified rock units and structural features. Intensive petrographic study has been followed up to confirm field observations and drill core logging. Two cross sections are including A-A' and B-B' are shown in Figure 3.3 and 3.4 which located in major ore zone of east – west trend.

3.2 Lithology

The KSO mine area is underlain mainly by sedimentary rocks of Nam Houay Formation (Figs. 2.1 and 3.1) inferred Ordovician to Silurian ages (Hoa et al., 2008; Thassanapak et al., 2012). Based on field investigation during this study, the Nam Houay Formation in the mine area is divided into two units namely, 1) Unit 1: Sandstone dominated Unit and 2) Unit 2: Siltstone dominated unit.

Stratigraphically, the sandstone dominated unit is older. The thickness of this unit is not known as it extends beyond the pit area and no information available to estimate its thickness. Both Units generally strike northwest-southeast with moderate to steep westerly dipping (Fig. 3.1).

3.2.1 Unit 1: Sandstone dominated

This unit is characterized by fine-grained sandstone interbedded with thinly bedded laminated siltstone (Fig. 3.1). This unit is mainly observed at Houay Keh and Nam Pan-east ore lenses (Fig. 3.1) in the eastern part of the mine area, in which the rocks are dominated by sandstone interbedded with thin to medium beds of siltstone. The contact between fine-grained sandstone, the thinly bedded siltstone and/or laminated siltstone is gradational (Figs. 3.4 and 3.5). The unit strikes approximately northwest-southeast with dip of approximately 40° to 70° to the southwest (Figs. 3.1 and 3.2). Based on field observation, the thickness of this unit is approximately 40 to 60 meters (Figs. 3.2 and 3.4). This unit is characterized by thinly bedded siltstone and shale. Its thickness is about 20 to 30 meters (Figs. 3.2 and 3.4). The sandstone dominated unit mainly consists of fine-grained sandstone and siltstone (Fig. 3.2). This unit is commonly fine-grained sandstone interbedded with siltstone which show well interbedded in the field (Fig. 3.6).

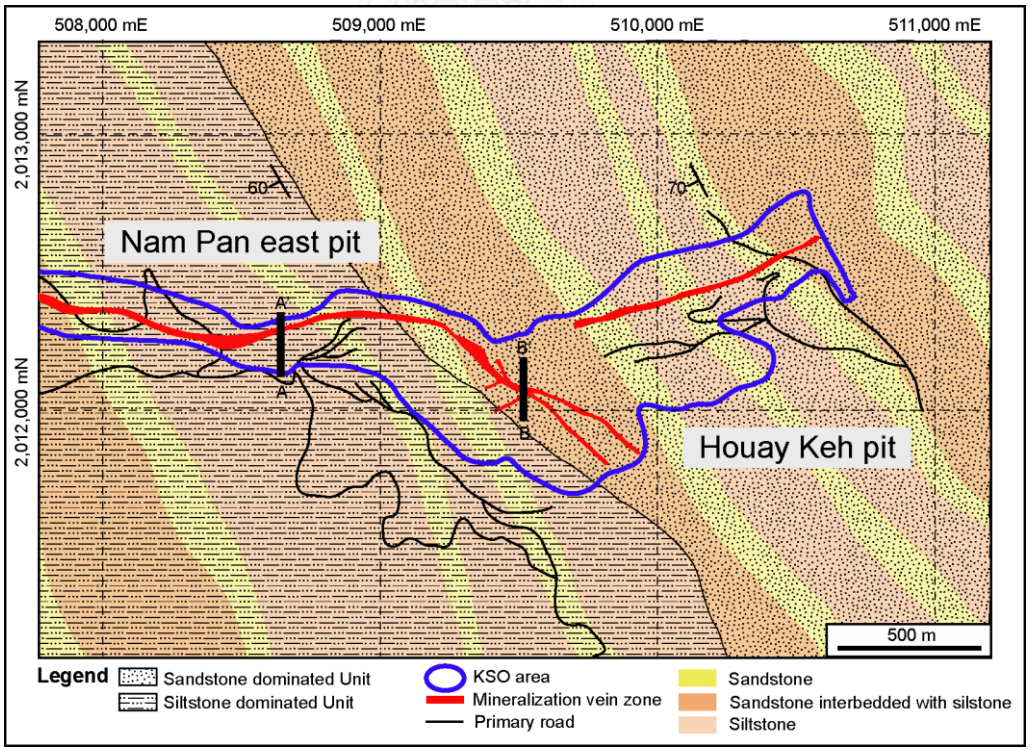

Fig. 3. 1 Interpreted geological map of the KSO deposit shows lithology and structural relationships and two geological cross-sections (A-A' and B-B'). Note that at least two rock units can be classified namely, (1) Sandstone dominated unit (2) Siltstone dominated unit. Blue line (KSO area) is pit outline.

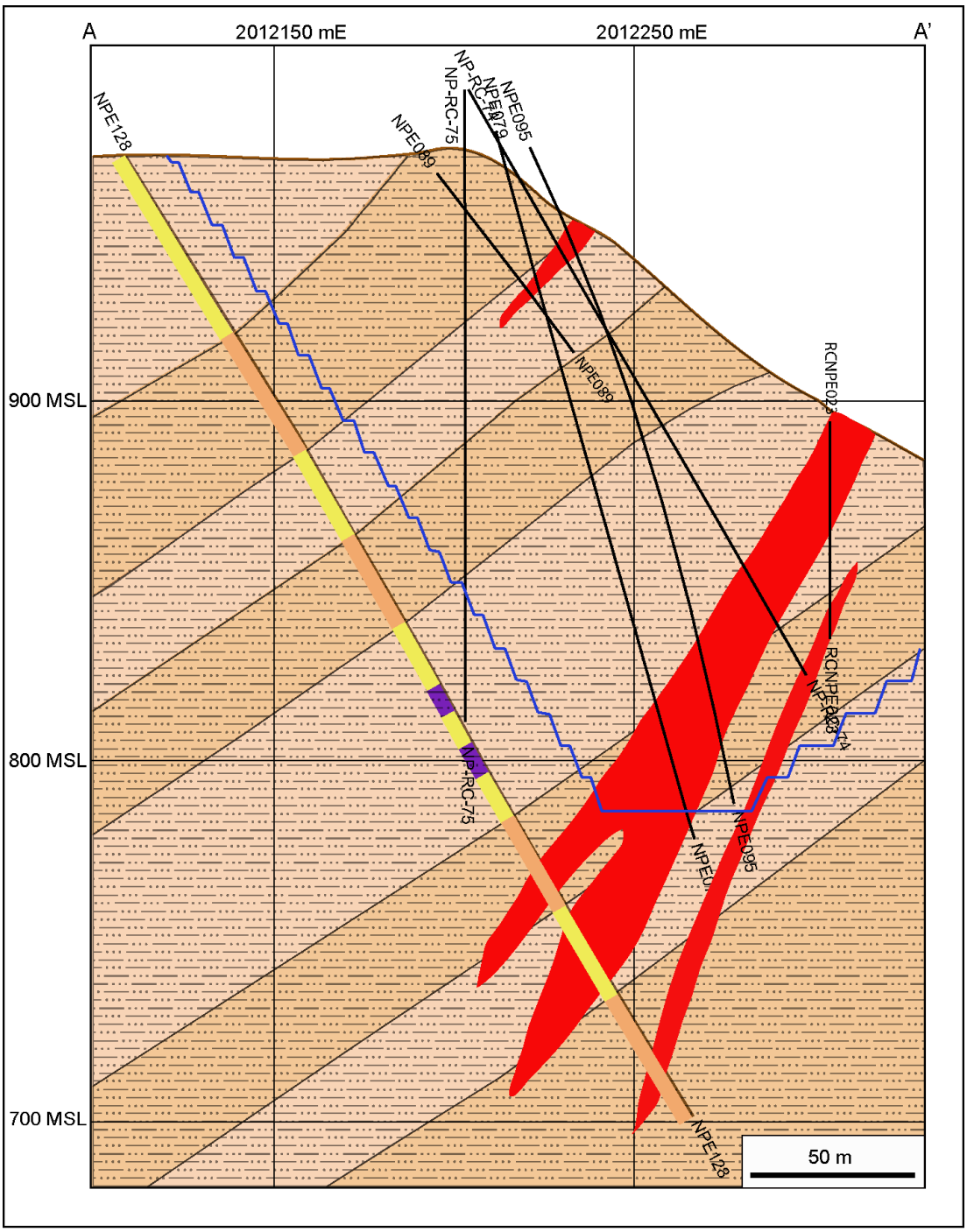

Fig. 3. 2 Interpreted geological cross-section along 508700mE (SRK, 2011). Mineralization zone is represented in red.

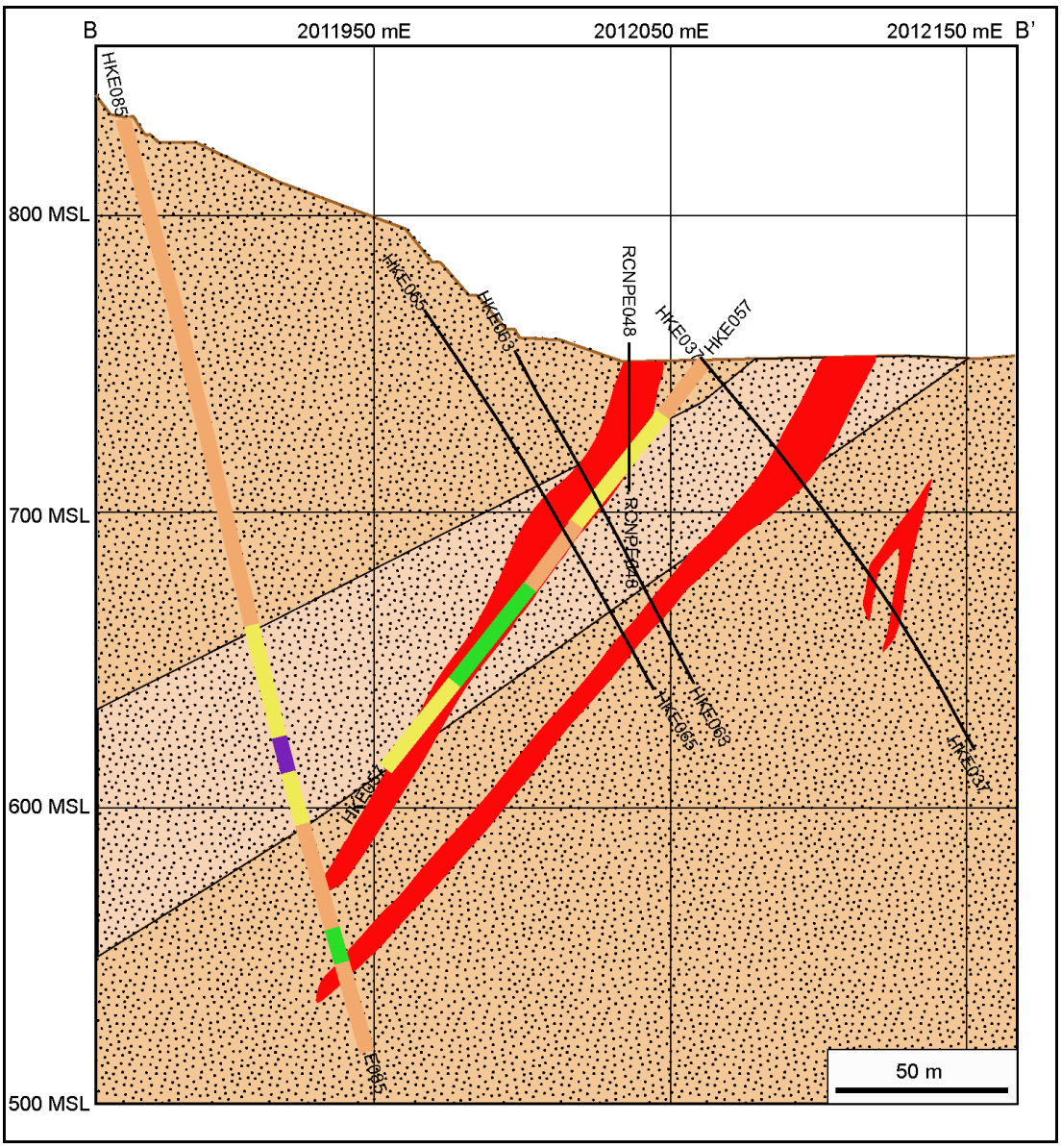

Fig. 3. 3 Interpreted geological cross-section along 509570mE (SRK, 2011). Mineralization zone is represented in red.

Sandstone

In hand specimens, the sandstone is pale grey to green grey, moderately hard and is slightly laminated and moderately sorted in general (Fig. 3.4). This sandstone is similar to sandstone in siltstone dominated unit.

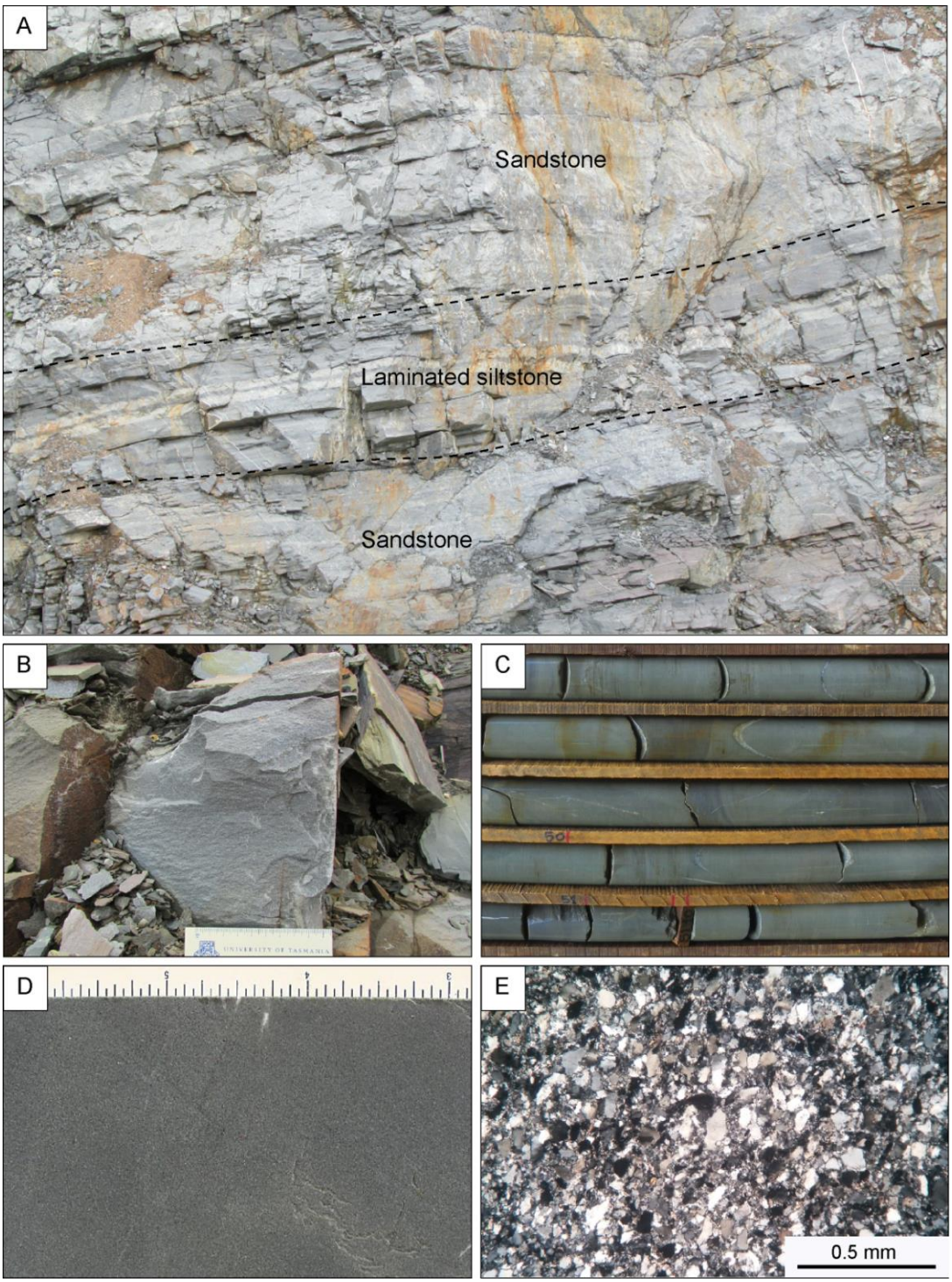

Fig. 3. 4 Characteristic features of Unit 1 in Houay Keh ore lens (Sandstone dominated unit). **A**. Outcrop of fine-grained sandstone interbedded with laminated siltstone. **B**. Hand specimen of fine-grained sandstone. **C**. Diamond drill core of fine-grained sandstone interbedded with thinly bedded laminated siltstone. **D**. Close-up of Fig. C showing fine-grained sandstone. **E**. Photomicrograph of fine-grained sandstone showing of fine-grained quartz, feldspar and clay minerals (mostly sericite) cross nicol.

Microscopically, the sandstone consists mainly of quartz and feldspar with some chlorite which could have been derived as alteration product of mafic minerals.

Opaque minerals include organic matter and pyrite. Quartz is the most predominant mineral and occurs as fine - grained crystals ranging in size from 10-30 μm in diameter (Fig. 3.4E). Quartz constitutes about 50% and feldspar about 40 %. Muscovite consists about 7%. Opaque minerals make up about 2%. It is commonly found in association with feldspar. Some amount of muscovite is also present between quartz grains (Fig. 3.4E). Feldspar is partly altered to sericite and calcite.

Siltstone

In hand specimens, the siltstone is grey to dark grey, slightly hard and generally shows moderately laminated and well sorted features (Fig. 3.5). This siltstone e is similar characteristic to siltstone in siltstone dominated unit.

Microscopically, the siltstone comprises mainly quartz and K-feldspar with some clay minerals, chlorite and opaque minerals which could have been derived from mafic minerals as alteration product. Opaque minerals include organic matter and pyrite. Quartz is the most predominant mineral and occurs as very fine-grained crystals having generally less than 70 μm in diameter (Fig. 3.5E). It is commonly found in association with feldspar. Quartz and feldspar constitute about 85%, whereas opaque minerals and clay minerals and pyrite make up about 15%. Some grains of chlorite and opaque minerals such as Fe-oxides have 70 μm in diameter and have constituted approximately 3% (Fig. 3.5E). Some amount of sericite is also present between quartz grains (Fig. 3.5E). These microcrystalline quartz, sericite, clay minerals and iron oxides which are comprehended as alteration products are occasionally present in some samples (Fig. 3.5E).

3.2.2 Unit 2: siltstone dominated

This unit is characterized by laminated siltstone interbedded with thin beds of fine-grained sandstone (Fig. 3.1). This unit is mainly observed at Nam Pan ore lens (Fig. 3.1) in the western part of the mine area in which the rocks are dominated by

siltstone interbedded with thin to medium beds of fine-grained sandstone. The contact between the thinly bedded sandstone with siltstone and/or laminated siltstone is gradational (Figs. 3.4 and 3.5). This unit strikes almost northeast with dip of approximately 40° to 60° to the southwest (Figs. 3.1 and 3.3).

This siltstone dominated unit is extensively distributed in Nam Pan-west pit or the western part of the KSO mine area. The common trend of this unit is almost North – South with moderate dipping (50° to 70°) to the west similar to the Unit 1 (Fig. 3.3). The thickness of this unit which has been estimated based on geologic map and field investigation is at least about 40 to 80 meters (Figs. 3.3 and 3.5). Sandstone beds were identified in this unit in the pits range in thickness about 20 to 40 meters (Figs. 3.3 and 3.5). Siltstone dominated unit is characterized by siltstone, partly laminated interbedded with thin-bedded to medium-bedded fine-grained sandstone (Fig. 3.5 field photo here). This unit is mainly identified at the Nam Pan pit in the western part of mine area. Here this unit from field information is dominated by siltstone dominated unit. The siltstone dominated unit occurs as multiple forms, which generally have laminated siltstone and fine-grained sandstone beds (Fig. 3.3).

Siltstone

In hand specimen, the siltstone is grey to dark grey and less hard and is generally moderately laminated and well sorted (Fig. 3.5). This siltstone shows laminated feature which is same to thinly bedded laminated siltstone interbedded with fine-grained sandstone of Unit 1.

Under microscope, the laminated siltstone consists predominantly of quartz and clay minerals such as sericite (Fig. 3.5E). The grain sizes of minerals including quartz are usually less than 70 μm in diameter. Quartz constitutes about 50 % and feldspar about 35, Opaque minerals including pyrite consists 2% and clay minerals make up about 13 %. Sizes of chlorite and opaque minerals are >70 μm in diameter (Fig. 3.5E). Ferric – oxide or opaque minerals may be very rich in some samples. They generally occur as spot, layer or lenses (Fig. 3.5E). The fissility of this rock is defined by the orientation of sericite and some clay minerals including illite (Fig. 3.5E).

Sandstone

In hand specimen, sandstone is pale grey to grey and moderately hard and generally shows slightly laminated and moderately sorted nature (Fig. 3.4). The sandstone is same with thinly bedded fine-grained sandstone interbedded with laminated siltstone of Unit 1.

Under microscope, the laminated siltstone consists predominantly of quartz and clay minerals such as sericite (Fig. 3.4E). The grain sizes of minerals including quartz usually range from 10 to 30 μm in diameter. Quartz and feldspar constitute about 95%, whereas opaque minerals and clay minerals make up about 1%. Ferric – oxide or opaque minerals may be very rich in some samples. They generally occur as spot, layer or lenses (Fig. 3.4E). The fissility of this rock is defined by the orientation of sericite and some clay minerals including illite (Fig. 3.4E).

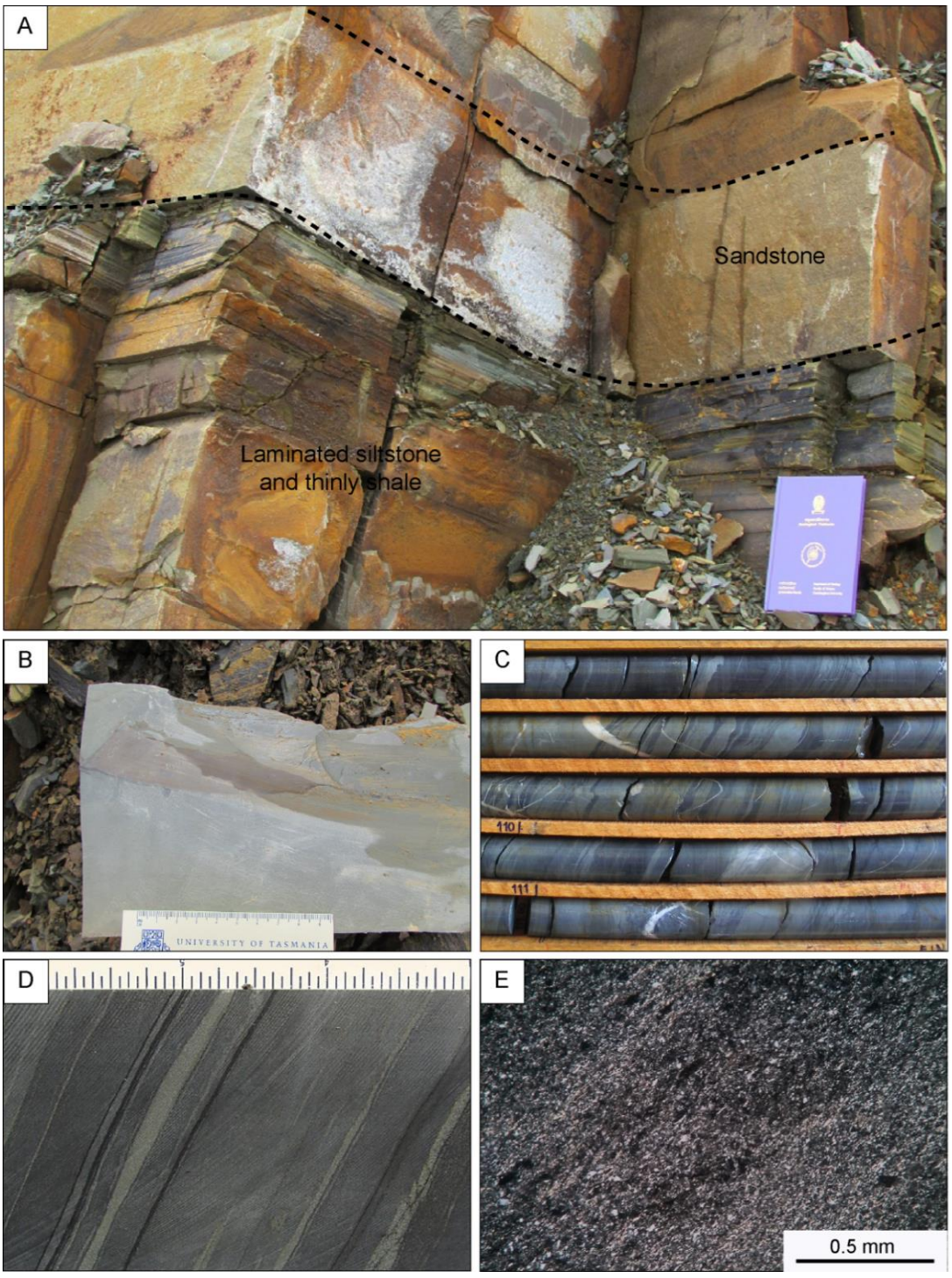

Fig. 3. 5 Characteristic features of Unit 2 in Nam Pan ore lens (Siltstone dominated unit). **A**. laminated siltstone interbedded with fine-grained sandstone. **B**. Hand specimen of laminated siltstone. **C**. Diamond drill core showing laminated siltstone interbedded with thinly bedded fine-grained sandstone. **D**. Close-up of Fig. C showing laminated layers of siltstone. **E**. Photomicrograph of laminated siltstone showing fine-grained quartz, feldspar and clay minerals (sericite), Cross nicol.

Metamorphic rocks

In sandstone dominated unit, the original shale has been metamorphosed to slate which is still retained the original bedding. Hence, it forms as thin beds interbedded with metasandstone and metasiltstone (Fig. 3.5 A). It displays lamination (Fig. 3.5C) and prefers to be interbedded with siltstone rather sandstone (Figs. 3.5C and D).

Under microscope, slate consists mainly of clay minerals (e.g. sericite) and minor quartz, feldspar and organic matter. Carbonate minerals may also present, however most likely derived from small veining. The orientation of fine-grained mica (sericite) revels this slate has undergone weak metamorphism (Fig. 3.5E). In some areas, slate is locally contained dark spots. It is preferred to name this slate as spotted slate.

In hand specimen, spotted slate is characterized by the presence of small black spots in grey to dark grey slate (Fig. 3.6A). In general, the rock is moderately developed fissility with about 1 mm in diameter of nodules-like black spots scatter through the rock (Fig. 3.6B).

Microscopically, the nodules-like portion contains mainly quartz and muscovite and opaque minerals (Fig. 3.6C). For slate in general, it consists mainly quartz, feldspar and muscovite (Fig. 3.6C). In addition, clay minerals such as sericite and illite may also present. It should be noted that the orientation of nodule-like portion tend to parallel to foliation of slate (Fig. 3.6B). Figures 3.6C and 3.6D shows moderately developed of foliation and rotation of nodule-like spot which is strongly suggested that the rock is locally moderately metamorphosed.

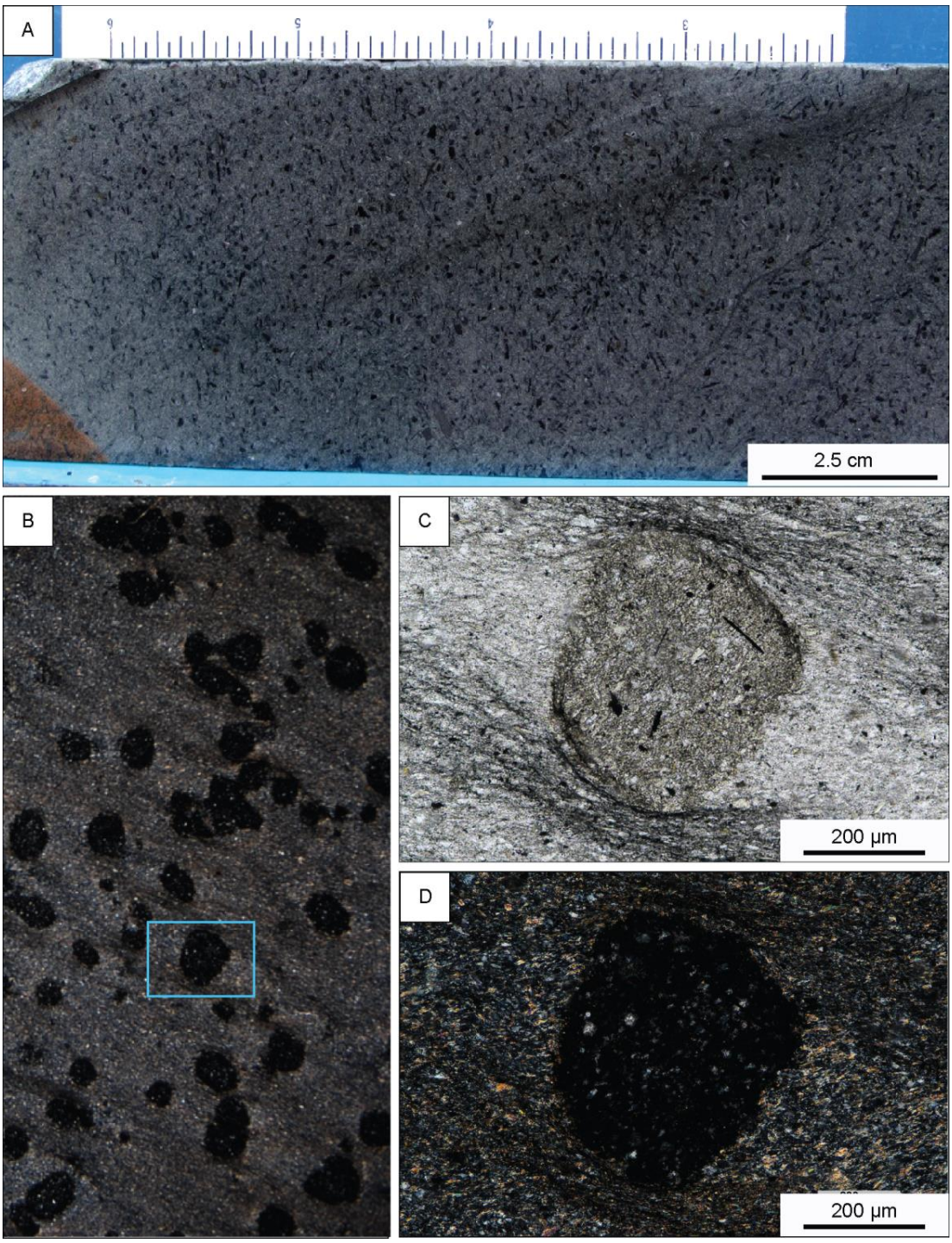

Fig. 3. 6 Petrographic characteristics of spotted slate **A**. Diamond drill core of spotted slate. **B**. Photomicrograph showing black spots in slate (cross nicol). **C**. Photomicrograph of enlarge black spots in Fig. 3.6C showing textural feature of metamorphic product (ppl). **D**. Same as Fig. 3.6C (cross nicol).

Andesitic Dyke

There is no major igneous rock exposed at open pits or intersected in drill hole in the mine area except some post-mineralization dykes (Fig. 3.7). The Nam Houay Formation in the mine area is weakly to moderately deformed. The rocks are slightly folded which are generally resulted in cylindrical folding locally in upper part of the sequence (SRK, 2011). The NE-trending andesitic dykes cut through the uppermost sedimentary sequence. This dyke is interpreted to be post-mineralization dyke (Fig. 3.7).

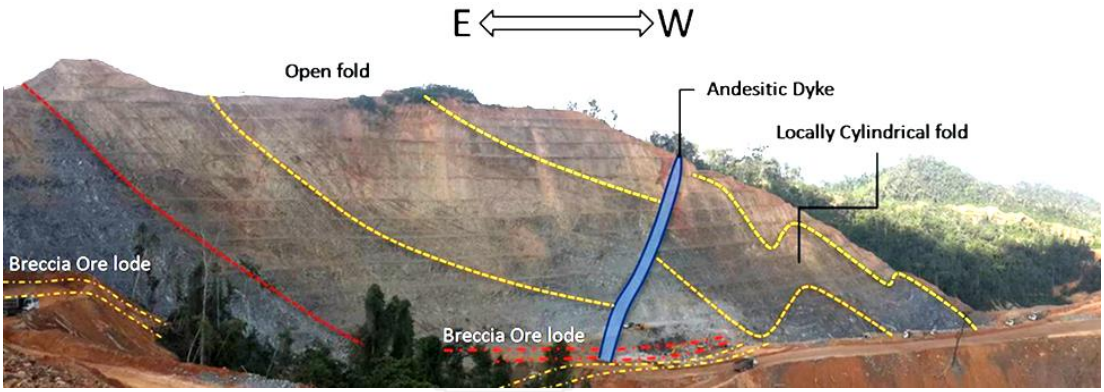

Fig. 3. 7 Andesitic dyke in the Nam Pan pit of KSO mine (SRK, 2011).

Regional Structures

This description is not intended to analyze structural features. However, it aims to provide a generally review of major structures in the area those structures that related to gold mineralization at KSO. It is based on interpreted lineaments from satellite image provided by Company.

Faults

It is clearly observed at least three major regional faults namely, 1) Northwest-southeast, 2) East-west and 3) North-south to northeast-southwest. The northwest-southeast is the most widespread and extensive including in Bolikhamxai. The second dominated structure (fault) is northeast-southwest fault which can be intensive in some areas. The north-south to northeast-southwest is apparently cross cut northwest-southeast and east-west faults.

Government of Laos (2000) has reported the above faults are identified in regional area representing by (1) the Nam Xang - Phon Kham - Nam Houay fault strikes northwest-southwest (2) the Nam Mong - Huoi Laos fault strikes east-west and (3) the Pakading fault strikes north-south to north-southwest respectively.

In KSO mine area, the east-west major fault may locally change its strike to WNW-ESE and this fault tends to be most predominant which includes the one accompanied by quartz-carbonate-sulfides veins. (1) The Nam Xang - Phon Kham - Nam Houay fault was reported to have nearly 110 kilometers in length (SRK, 2011), This fault strikes northwest - southeast and crosscuts the Nam Houay, Houay Pang and Thapachon Formations. It is a normal fault that dips 70° to the southwest.

The Pakading fault strikes northeast-southwest, crosscutting across the sedimentary rocks of the Nam Phouan, Nam Xot and Lingkho Formations. It is a normal fault that dips 70° to the northwest.

A second - order fault system is relatively well - developed in the Khamkeut Saen Oudom mine. The second - order faults are commonly 15 to 20 kilometers in length and strike northwest - southeast, northeast - southwest and less commonly

north - south and east - west. In the main mineralized areas of Nam Pan and Houay Keh a strong east - west structural fabric has emerged as is often observed in the open cut walls (Fig. 3.9).

Shear zone of at least 5 meters wide found to bound the quartz-carbonate-sulfide veins at Nam Pan ore lens. This shear zone strikes east-west with steep dipping and correspond to quartz-carbonate-sulfides veins. It appears that shear has enclosed the quartz-carbonate-sulfide veins (Fig. 3.12).

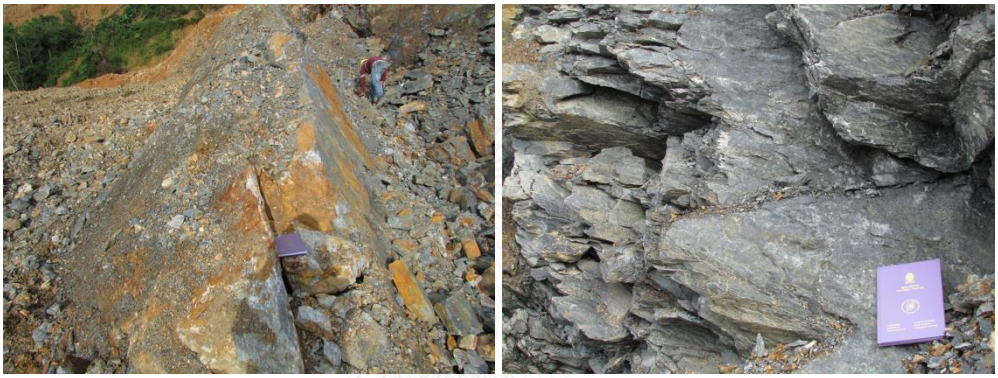

Fig. 3. 8 The Nam Pan pit showing shear along east to west.

CHAPTER IV

MINERALIZATION AND ALTERATION

4.1 Introduction

This chapter documents the characteristics of mineralization and alterations through field observation (pits) and drill cores logging. Petrographic observation of altered host rocks, veins mineralogy and textural relationships were also undertaken. Furthermore, petrographic investigation of gangue and ore minerals assemblage of Nam Pan ore lens and Houay Keh ore lenses to establish a detailed vein and mineral paragenesis of the KSO deposit. Alteration mineralogy in relationships to the gold mineralization stage has been carried out.

In this study, mineralization and hydrothermal alteration study has been on two major ore lenses (Nam Pan and Houay Keh). Field observation of vein texture, mineralogy, paragenetic relationships undertaken both pit scale, drill core were conducted which focused on major mineralization zones and rocks of Nam Pan ore lens and Houay Keh ore lens (Fig. 3.2). These are undertaken in terms of a detailed petrographic and textural relationship of ore and gangue mineral assemblages from five thin sections and thirty-one polished mounts observed in the following: Based on cross-cutting relationships, differences of mineral assemblage and textural relationships and structural orientation, the paragenetic sequences has been established. Electron Microprobe Analysis (EPMA) was used to confirmed the unidentified minerals. Those minerals such as sphalerite and gold bearing minerals then were further analyzed for their compositions using EPMA.

Three sulfide samples from KSO deposit have been analyzed using Energy Dispersive X-ray Spectrometer Scanning Electron Microscope analysis (EDS-SEM). Sulfide minerals such as galena and sphalerite associated with gold of Stage 2 used to analyse by EDS spectrum and SEM images.

For Electron Probe Micro Analyser (EPMA) approximately twenty samples of sulfides and gangue minerals (e.g. arsenopyrite, pyrite, sphalerite, chalcopyrite, galena, gold, quartz, calcite and pyrrhotite) have been analyzed.

Hydrothermal alteration investigation has been focused right from field and diamond drill core loggings. Details petrographic identification later undertaken to further confirm and finally confirmed by X-ray diffraction analyzes (XRD).

4.2 Characteristics of veins

At KSO, gold mineralization mainly occurs as veins, minor stockworks and breccia. The main ore zones are confined to north-west trending faults (Fig. 4.1). Nam Pan West, Nam Pan East, and Houay Keh ore lenses (pits) are located on the main ore zone/faults, which extend at least for 4 km. It is likely to extend further to the east and west when scale of the fault is considered. The main ore zone occurs as a single vein at Nam Pan pit striking east-west with steep dipping to south. This orebody splays into three discrete veins to east, at distance close to the Houay Keh pit (Fig. 4). Here, vein trend also changes the direction to northwest-southeast trending. At Nam Pan-west, this major vein is characterized by quartz - pyrite ± arsenopyrite-sphalerite - gold and is typically quartz-sulfide (pyrite - sphalerite ± arsenopyrite) ± gold at Nam Pan east. However, at Houay Keh it is characterized by quartz-carbonate-base metal (sphalerite, galena and chalcopyrite)-gold. At Nam Pan, the gold bearing veins locally contain some breccia clasts and tend to form as single vein, whereas at Houay Keh ore lens veins are clearly displayed as sheeted veins.

Vang Kor ore lens which consists of few small pits located further to southwest of the main orebody is confined to a parallel structure (fault). The Vang Kor ore lens consists of four small pits including Vang Kor South, Vang Kor Central, Vang Kor North and Vang Kor West. However, there is no clear gold bearing quartz veins or stockworks has been observed. The ore zone appears to confine to east-west zone that host rocks contain abundance disseminated sulfides. Gold mineralization is likely to associate with disseminated pyrite in sandstone and siltstone. Houay Bong (HBG) ore lens is the only one zone that located on northeast-southwest structure which is contrast to the rest ore lenses. HBG ore lens locates southeast of Houay Keh occupy NNE-SSW (Fig. 4.1).

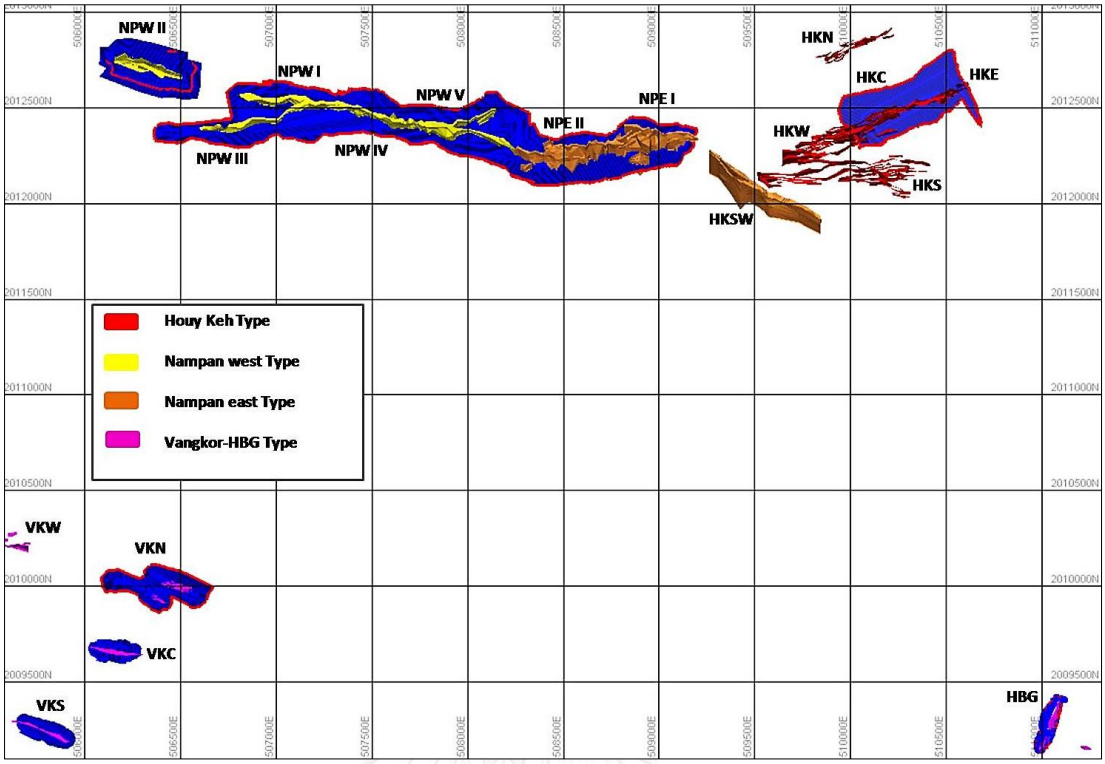

Fig. 4. 1 Mineralization vein zones of KSO area (SRK, 2011).

Major veins styles in mining area can be classified into three categories, namely 1) massive quartz sulfide vein, 2) massive quartz vein (barren vein) and 3) breccia bearing quartz veins (Fig. 4.2). At Nam Pan west and Nam Pan east ore lenses, massive quartz sulfide veins have east-west trending. However, at Houay Keh ore lens it strikes northwest – southeast (Fig. 4.2A). Massive quartz vein is barren vein (Fig. 4.2B). The massive quartz sulfide vein is widely occurred at Houay Keh ore lens and less predominant at Nam Pan west and Nam Pan east ore lens. Quartz veins contain sandstone/siltstone fragments are often observed at Nam Pan ore lens (Fig. 4.2C) whereas sheeted veins are characteristic features of Houay Keh ore lens (Fig. 4.2D).

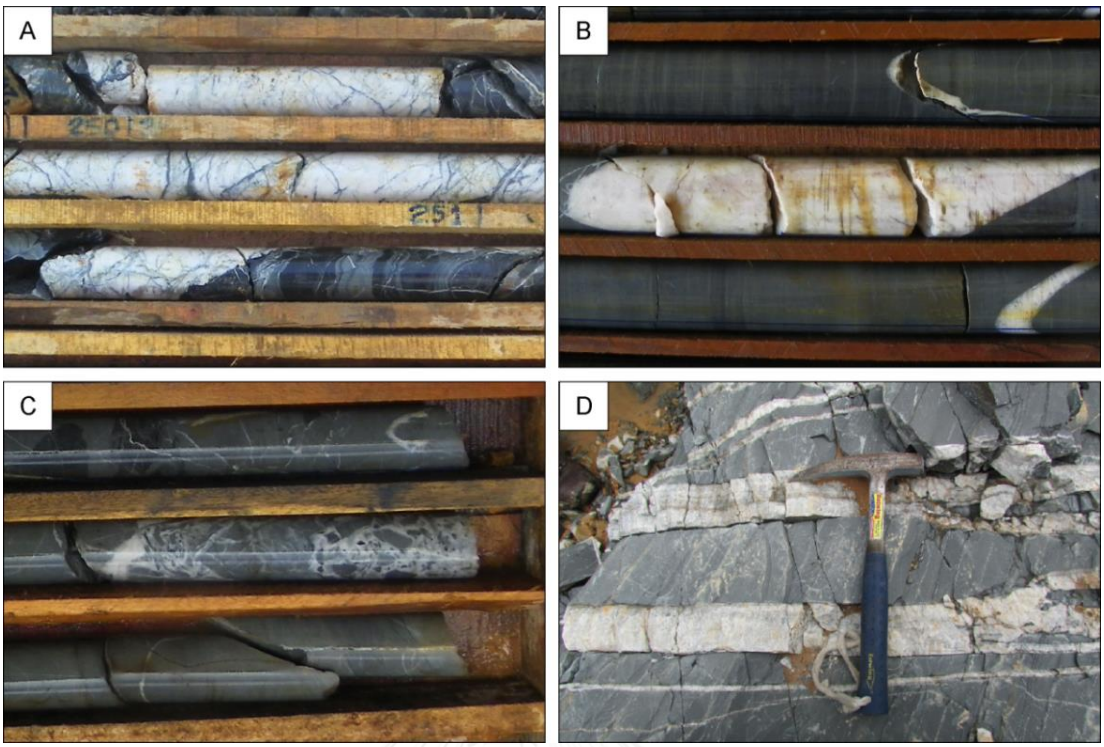

Fig. 4. 2 Characteristic features of KSO veins, **A.** Photograph of diamond drill core showing 1 to 1.5 meter wide massive quartz vein, **B.** Photograph of diamond drill core showing quartz ± carbonate vein hosted in fine-grained sandstone/siltstone, **C.** Photograph of diamond drill core showing quartz vein containing breccia fragments, **D.** Outcrop of fine-grained sandstone in Houay Keh ore lens showing sheeted veins.

4.3 Paragenesis

Based on cross cutting relationships, mineral assemblage and textural features at least three mineralization stages have been identified namely, 1) Stage 1: Microcrystalline quartz – arsenopyrite – pyrite, 2) Stage 2: Quartz ± calcite – sulfides (pyrite-chalcopyrite ± arsenopyrite – sphalerite – galena – pyrrhotite) – gold, 3) Stage 3: Quartz – calcite – chlorite (Table 4.1).

Table 4. 1 Paragenetic diagram showing order of veins formation and the relative amount of mineral abundance (e.g. ore and gangue minerals) of infill Stage at KSO deposit.

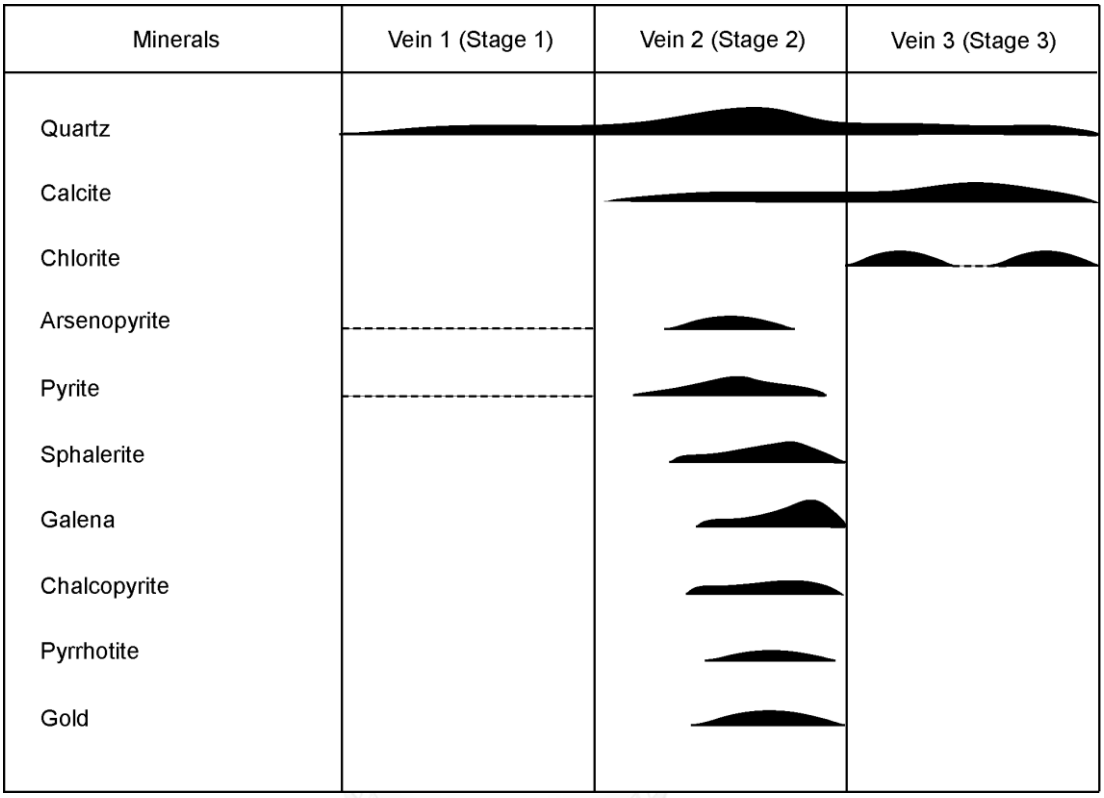

4.3.1 Vein 1 (Stage 1): Microcrystalline quartz - arsenopyrite – pyrite vein

Stage 1 occurs as small vein/veinlet, pale grey to grey color (Fig. 4.3A). The Stage 1 vein consists of mainly microcrystalline quartz and minor sulfide minerals including arsenopyrite and pyrite which is located at center of vein (Fig. 4.3B). This stage is characterized by open space infilled texture and often contains some wall-rock fragments (Figs. 4.3C and D). Stage 1 vein is widely distributed at Nam Pan and Houay Keh ore lenses. At the Nam Pan ore lens, this stage 1 vein has strike of north-south. It forms earliest in paragenetic sequence and it is considered as ground preparation for gold mineralization in KSO deposit.

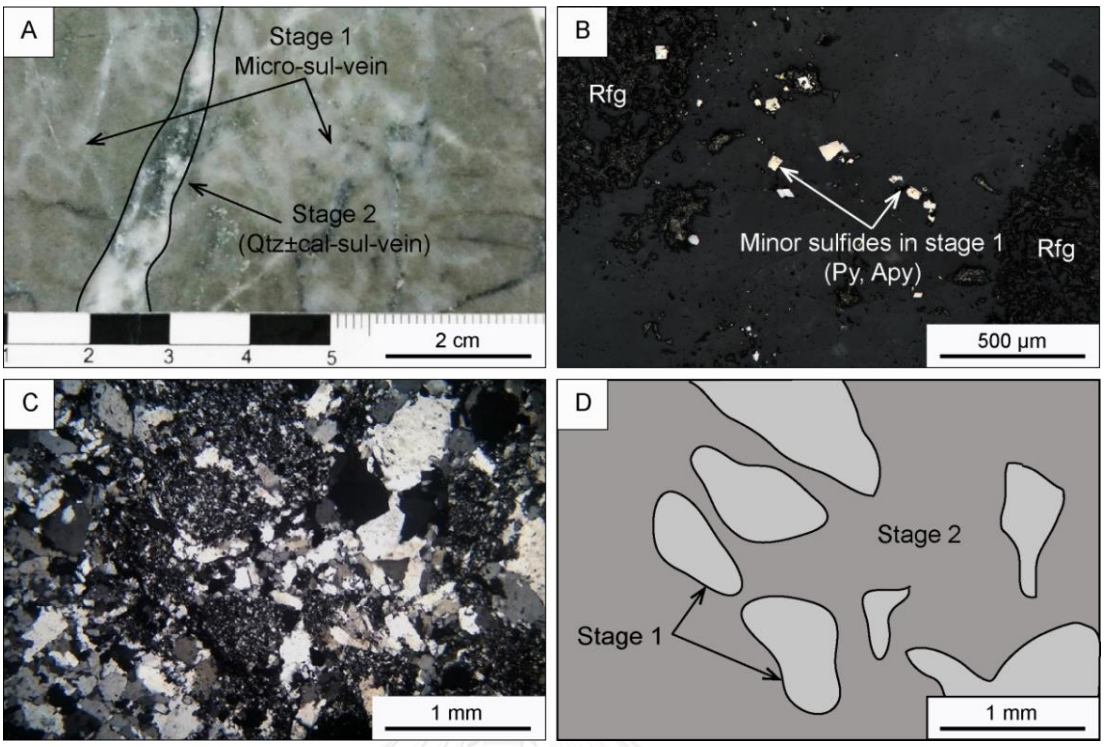

Fig. 4. 3 Characteristics of infill Stage 1 veins/veinlets **A.** Photograph of hand specimen showing cross cutting relationship of Stage 1 (microcrystalline quartz - arsenopyrite - pyrite vein) and Stage 2 (quartz ± calcite - sulfides (arsenopyrite - pyrite - sphalerite - chalcopyrite - galena) - gold vein) in siltstone, Sample No. HKE057_40.2, Houay Keh ore lens. **B.** Photomicrograph showing minerals in Stage 1 comprise microcrystalline quartz and minor pyrite and arsenopyrite (reflected light), Sample No. HKE085_266.9, Houay Keh ore lens. **C.** Photomicrograph showing microcrystalline quartz in thin section of Stage 1 (reflected light), Sample No. TS4, Nam Pan ore lens. **D.** Sketch of figure 4.1C showing clasts of Stage 1 in vein of Stage 2 introduced vein in Stage 1 occurs before Stage 2, Sample No. TS4, Nam Pan ore lens. Abbreviation: Qtz = microcrystalline quartz, Py = pyrite, Apy = arsenopyrite, Cal = calcite.

4.3.2 Vein 2 (Stage 2): Quartz ± calcite - sulfides (arsenopyrite - pyrite - sphalerite - chalcopyrite - galena - pyrrhotite) – gold vein

The Stage 2 mainly forms as veins, minor stockworks and breccia. Sheeted veins are commonly observed particularly at Houay Keh ore lens in which individual vein is approximately 6 cm to 10 cm width (Figs. 4.4A and B). Stage 2 is widely distributed of Nam Pan ore lens and Houay Keh ore lens. It has been observed at a depth approximately 750 to 550 meters above mean sea level (Figs. 3.3 and 3.4).

It should be noted that Stage 2 vein is characterized by massive texture, no crustiform and colloform banding (Fig. 4.4B). Quartz is principal silicate mineral of Stage 2 with minor calcite. Sulfide minerals of this stage include arsenopyrite, pyrite and base metal (e.g. sphalerite, chalcopyrite and galena) and often form as patches in quartz rich veins (Fig. 4.4C).

Sulfide minerals (e.g., pyrite, sphalerite, galena and chalcopyrite) prefer to situate at center of the vein (Figs. 4.4D and E). Quartz occurs as coarse - grained (0.4 cm to 1.3 mm) subhedral to euhedral aggregates (Fig. 4.4F). Pyrite is the most abundance sulfide minerals of this Stage and it is associated with sphalerite and galena (Figs. 4.4D and E). Gold forms as free grain associated with quartz and as inclusions in arsenopyrite and pyrite (Figs. 4.4E, G and H). Its size ranges from 100 to 120 microns, and associates with quartz and arsenopyrite (Fig. 4.4C).

Stage 2 is characterized by elongated shape quartz growing from vein walls similar to those found in epithermal quartz veins suggesting open space filling texture (Figs. 4.4F and 4.4D). Sphalerite is closely associated with galena and interstitially filled among quartz, arsenopyrite and pyrite (Figs. 4.4D and E). Chalcopyrite and pyrrhotite occasionally form as inclusions in sphalerite (Fig. 4.7). For chalcopyrite, it also commonly formed as chalcopyrite decease or chalcopyrite exsolution from sphalerite on the cooling of the ores after emplacement (Barton Jr and Bethke, 1987). Pyrrhotite constitutes in trace amount in some samples and often occurs at center of vein.

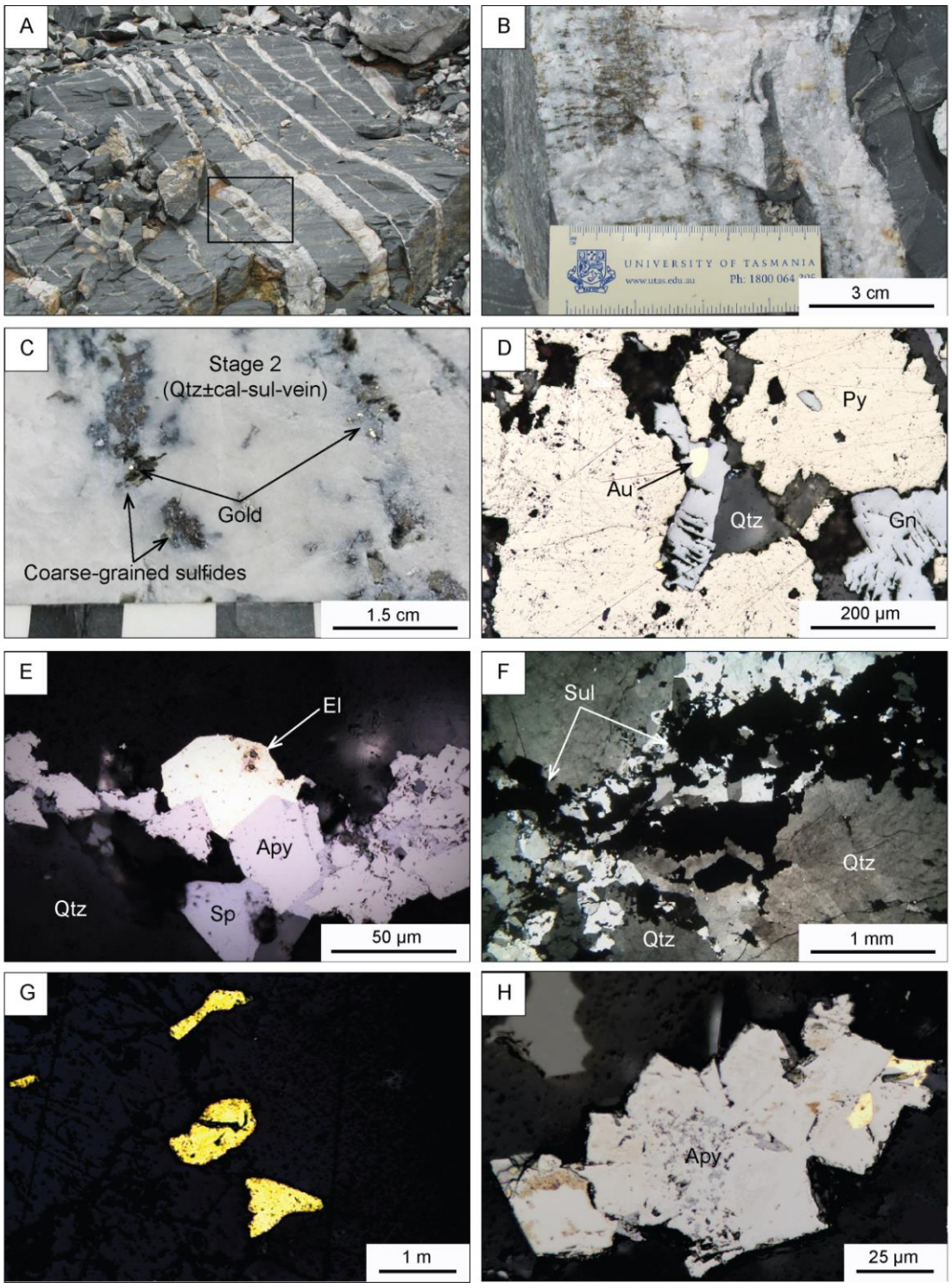

Fig. 4. 4 Characteristic features of Stage 2 **A.** Photograph of siltstone outcrop showing sheeted veins of Stage 2 at Houay Ken ore lens, **B.** Close-up area in Fig. 4.4A showing quartz ± calcite - sulfides - gold band (visible gold), Sample No. HKE-01, Houay Keh ore lens. **C.** Close-up of Stage 2 hand specimen showing abundance gold in association with sulfide minerals, Sample No. HKE-01, Houay Keh ore lens. **D.** Photomicrograph showing gold associated with galena and pyrite, Sample No. HK-

01_80, Houay Keh ore lens. **E.** Photomicrograph showing electrum intergrowth with arsenopyrite and minor sphalerite, Sample No. NPE128_282, Nam Pan ore lens. **F.** Photomicrograph showing relationship between silicate minerals (e.g., quartz and calcite) and sulfide minerals. **G.** Photomicrograph showing free gold, Sample No. HKE-01, Houay Keh ore lens. **H.** Photomicrograph showing gold inclusions in arsenopyrite, Sample No. NPE128_282, Nam Pan ore lens. Abbreviation: Qtz = quartz, Py = pyite, Apy = arsenopyrite, Sp = sphalerite, Gn = galena, Cpy = chalcopyrite, Sul = sulfides.

4.3.3 Vein 3 (Stage 3): Quartz - calcite – chlorite vein

In hand specimen or drill core, Stage 3 forms as small light to dark green vein/veinlets (Figs. 4.5A, B). The dark green patches in veins are chlorite rich. Stage 3 vein consist chiefly quartz minor calcite and chlorite (Figs. 4.5A, B, C and D). It has been observed mainly at Houay Keh ore lens in which size of the veins is approximately 1 cm in width (Figs. 4.5A and B). No sulfide mineral has been observed in this stage. The distinctive feature of stage 3 is the present of quartz-chlorite at vein wall (Figs. 4.5C and D) and quartz also closely associated with chlorite (Figs. 4.5E and F). Carbonate occurs in the innermost part of the veins and mostly fine to medium - grained calcites (Fig. 4.5B). Cross-cut relationships suggesting that Stage 3 veins cross cut Stage 2 veins.

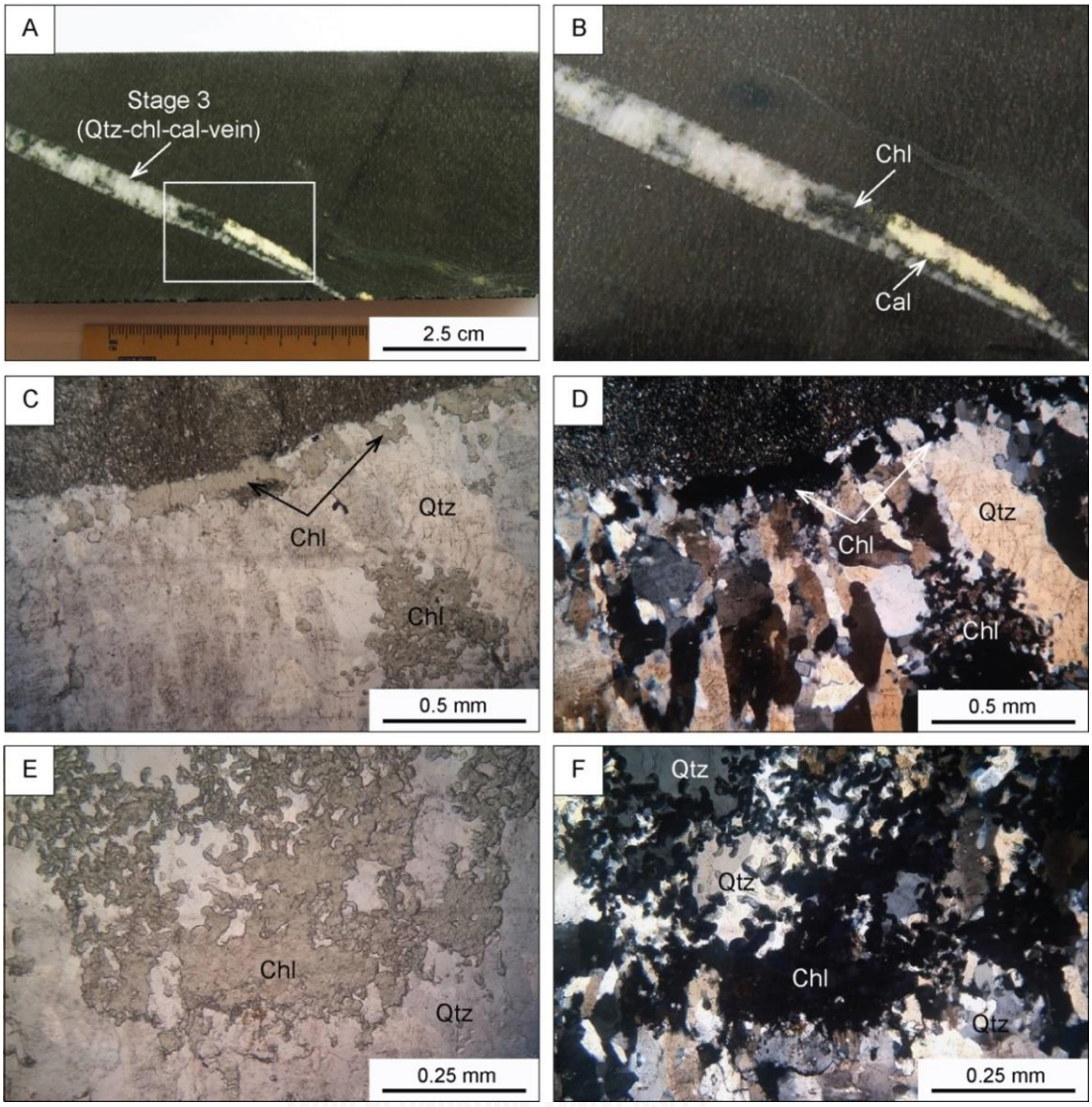

Fig. 4. 5 Characteristic features of Stage 3 vein, **A.** Diamond drill core sample of siltstone cross-cut by 0.8 mm to 1 cm wide Stage 3 (quartz-chlorite-calcite) vein, Sample No. HKE090_289, Houay Keh ore lens. **B.** Close-up of area in figure 4.5A showing a typical quartz - chlorite – calcite vein. **C.** Photomicrograph showing typical minerals assemblage of Stage 3 (PPL). **D.** Photomicrograph showing commonly minerals in Stage 3 (XPL). **E.** Photomicrograph showing chlorite in border area (PPL). **F.** Photomicrograph showing chlorite in border area (XPL). Abbreviation: Qtz = quartz, Chl = chlorite, Cal = calcite.

4.4 Mineralogy

In this section, the mineralogy and ore textures are described for each mineralization stages including Stage 1 (Microcrystalline quartz - arsenopyrite - pyrite), Stage 2 (Quartz ± calcite - sulfides (arsenopyrite - pyrite - sphalerite - chalcopyrite - galena) - gold ± pyrrhotite and Stage 3 (Quartz - chlorite - calcite). Microscopically identified and unidentified mineral will be confirmed by EDS-SEM and EPMA.

4.4.1 Ore mineralogy

Ore mineralogy in KSO deposit consisting of sulfide minerals (e.g. pyrite, arsenopyrite, sphalerite, chalcopyrite, and galena) and gold can be observed in mineralization vein zone.

Pyrite is the most abundant sulfide, which occurs in Stage 1 and Stage 2 veins. In Stage 1, it forms as fine-grained crystal (less than 50μm in diameter), anhedral to subhedral. It is commonly associated with quartz and minor arsenopyrite (Fig. 4.6A). Pyrite tends to form at vein selvage or where it contacts to the wall-rock which is likely derived from diagenetic pyrite. At Nam Pan pit, Stage 2 pyrite tends to associate with arsenopyrite (Fig. 4.6B) and sphalerite whereas, at Houay Keh ore lens, it prefers to associate with sphalerite, chalcopyrite and galena (Fig. 4.6B). Occasionally, sphalerite contains chalcopyrite and pyrrhotite (Figs. 4.6). Sulfide minerals EPMA mapping including pyrite were given in (Figs. 4.8 and 4.13).

Arsenopyrite is the second most abundant sulfide in Stages 1 and 2. In Stage 1, arsenopyrite occurs as fine-grained, subhedral to euhedral crystals. Here, it associates with quartz and minor pyrite. Arsenopyrite in this stage has size about 50 - 100 μm in diameter (Fig. 4.3B). At Nam Pan pit, Stage 2 arsenopyrite forms as the main sulfide mineral with subordinate amounts of pyrite and sphalerite (Fig. 4.4E). It should be noted that at Nam Pan ore lens, arsenopyrite is also abundance in sandstone and siltstone wall-rock which is likely derived from diagenetic arsenopyrite. Furthermore, arsenopyrite is less common at Houay Keh ore lens. Sulfide minerals EPMA mapping including arsenopyrite were given in (Fig. 4.9).

Sphalerite is present only in Stage 2 veins at Nam Pan and Houay Keh ore lens. It is mainly associated with chalcopyrite and galena, and to some extend it is also associated with arsenopyrite and pyrite (Figs. 4.6A, B and 4.7). Sphalerite identified under microscope has been confirmed using EDS-SEM analysis and the results of sphalerite and galena are shown in Figure 4.10 and 4.11. Sphalerite composition analyzed using EPMA analysis and results given in (Appendix F).

At Nam Pan pit, sphalerite forms as anhedral to subhedral, fine- to medium-grained crystals (0.1 mm to 0.5 mm). It is characterized a dark brown grey color, and appears to be fine to medium grained in core samples (Fig. 4.4E). Sphalerite of Stage 2 from Houay Keh ore lens is associated with pyrite, chalcopyrite, pyrrhotite and galena (Fig. 4.7). It forms as anhedral to subhedral, medium to coarse-grained crystals.

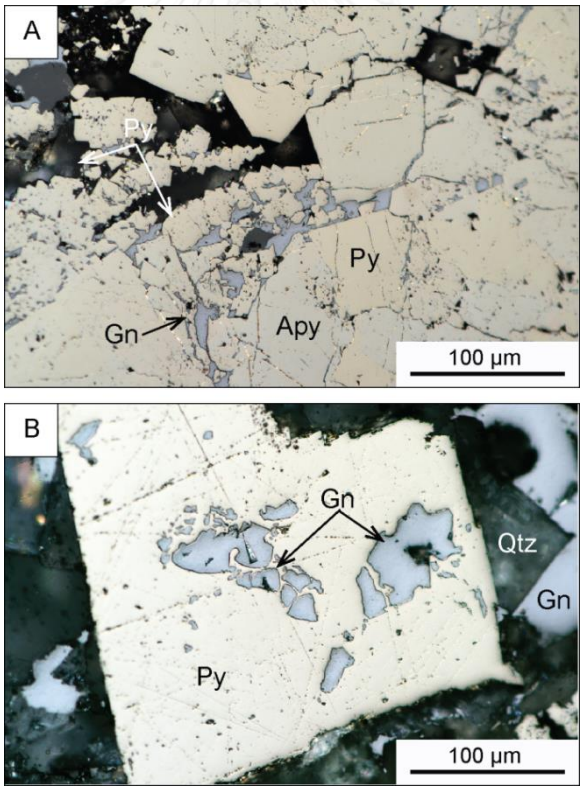

Fig. 4. 6 Characteristic features of Khamkeut Saen Oudom vein from different Stages. **A.** Stage 2 consists of arsenopyrite, subhedral to euhedral, aggregated grains intergrowth with pyrite, sphalerite, galena and chalcopyrite, Sample No. HK-01, Houay Keh ore lens. **B.** Photomicrograph showing galena intergrowth within the large pyrite, Sample No. HK-01, Houay Keh ore lens. Abbreviation: Qtz = quartz, Py = pyrite, Apy = Arsenopyrite, Gn = galena.

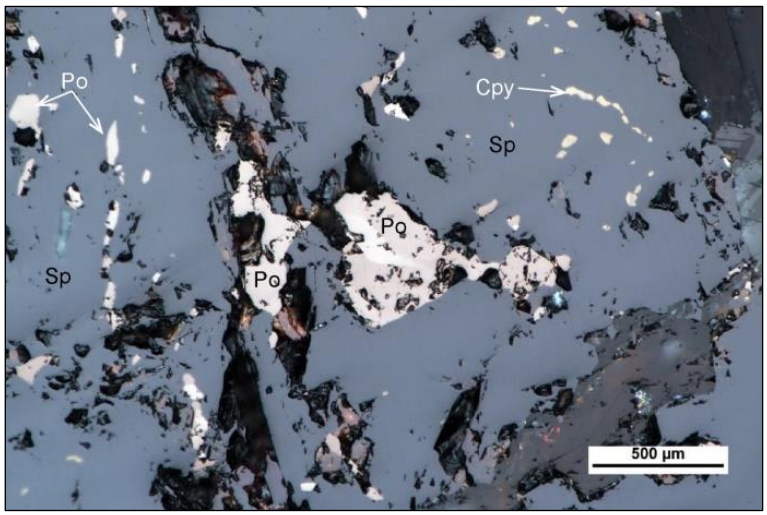

Fig. 4. 7 Photomicrograph of pyrrhotite and chalcopyrite inclusions in sphalerite Sample No. HK-01_80, Houay Keh ore lens. Abbreviation: Sp = Sphalerite, Po = Pyrrhotite, Cp = Chalcopyrite.

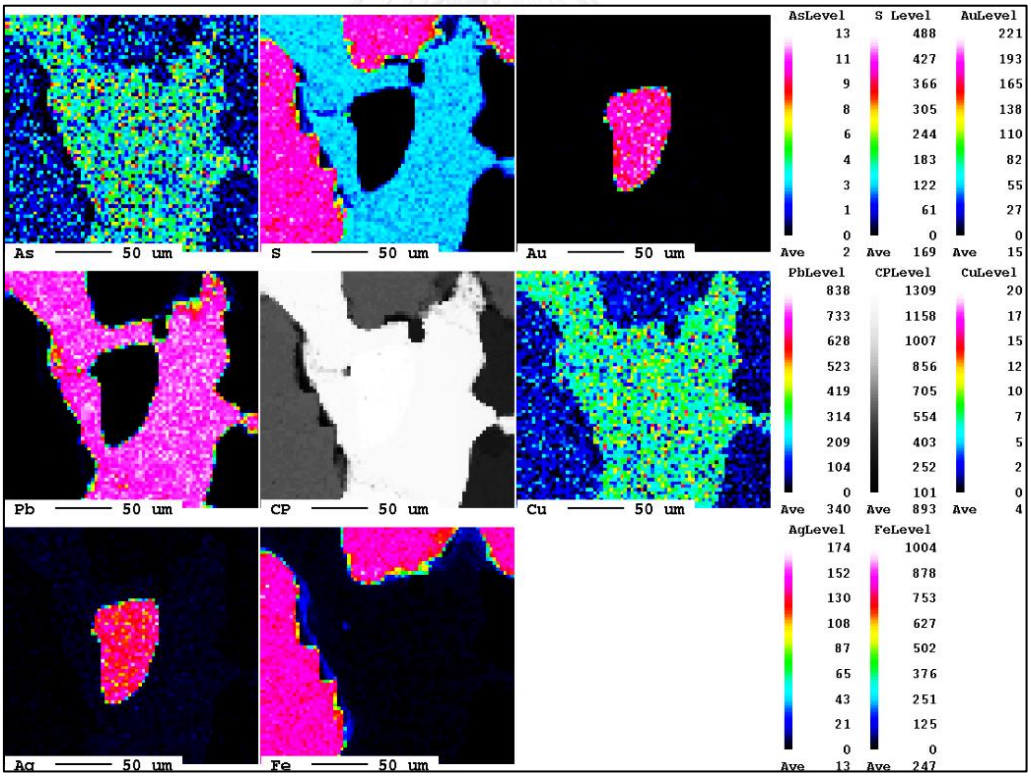

Fig. 4. 8 EPMA mapping shows galena intergrowth with pyrite and gold (electrum) from Houay Keh ore lens.

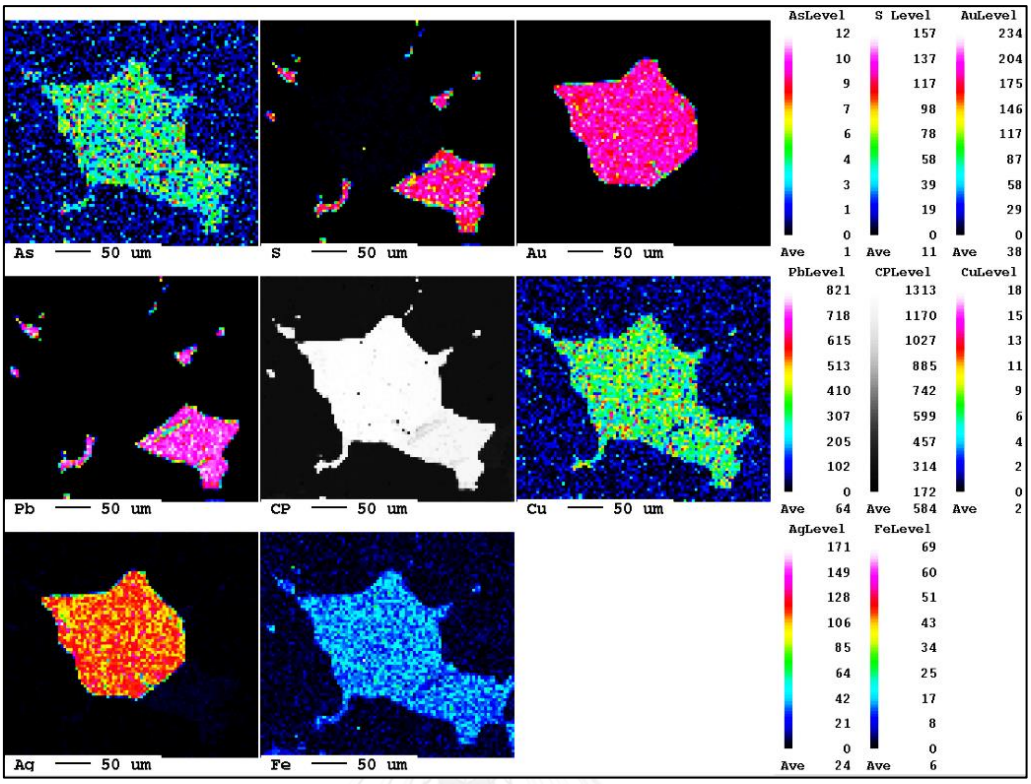

Fig. 4. 9 EPMA mapping shows gold (electrum) associated with galena from Houay Keh ore lens.

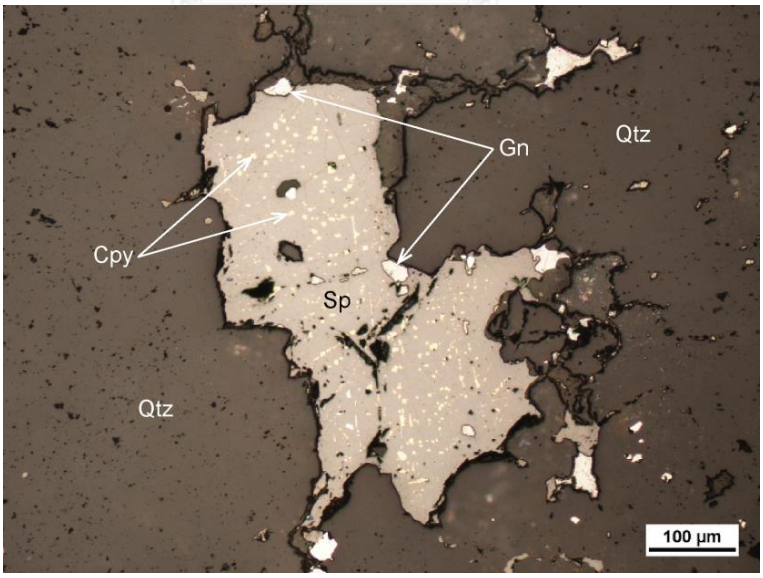

Fig. 4. 10 Photomicrograph of Stage 2 (quartz ± calcite – sulfides – gold**)** vein showing of chalcopyrite inclusions in sphalerite or chalcopyrite disease. Galena partly forms as inclusions and intergrowth with sphalerite. Sample No. HKE057, Houay Keh ore lens. Abbreviation: Qtz = quartz, Sp = sphalerite, Gn = galena, Cpy = chalcopyrite.

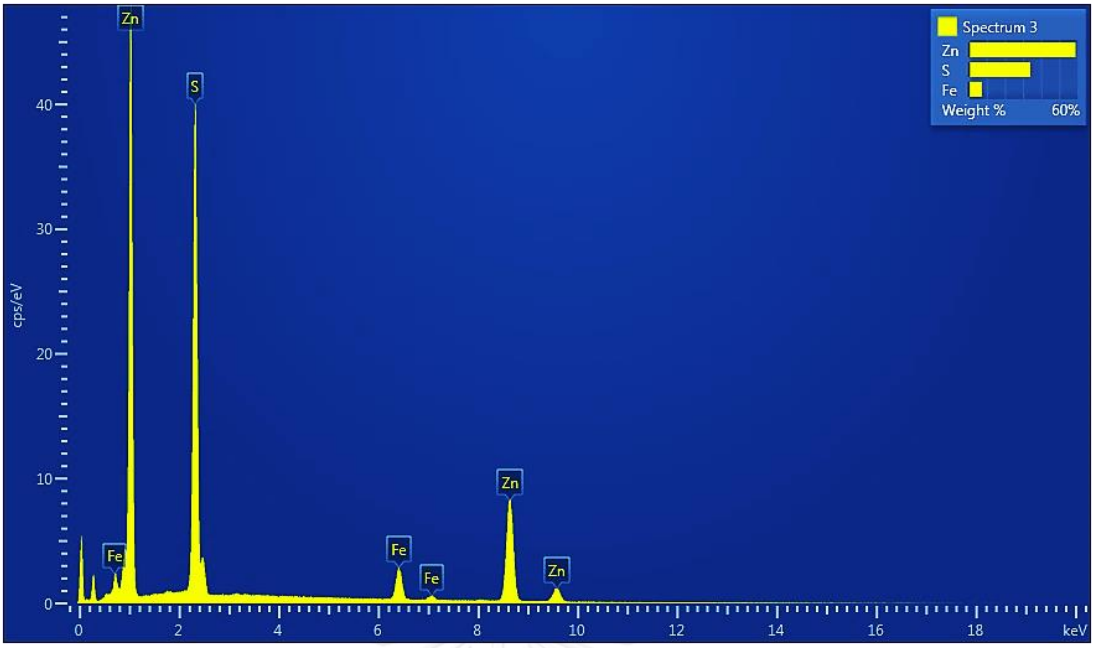

Fig. 4. 11 Result of EDS-SEM analyze shows mineral containing Fe, Zn and S indicates sphalerite, Sample No. HKE057, Houay Keh ore lens.

Chalcopyrite occurs in minor amount and only identified in Stage 2 (Figs. 4.7 and 4.10). It usually associates with sphalerite and often displays "chalcopyrite disease texture" (Figs. 4.7 and 4.10). Chalcopyrite identified under microscope has been confirmed using EDS-SEM analysis and the results of chalcopyrite are shown in Figure 4.12. Sulfide minerals EPMA mapping including chalcopyrite were given in (Fig. 4.13).

Galena is observed only in Stage 2 and relatively abundant especially at the deeper part of the Houay Keh pit. Galena is commonly associates with pyrite, sphalerite and chalcopyrite. Coarse-grained galena up to 1.5 mm in diameter has been observed in vein at the deeper level of the Houay Keh ore lens (Figs. 4.4D). Galena identified under microscope has been confirmed using EDS-SEM analysis and the results of galena are shown in Figure 4.14. Sulfide minerals EPMA mapping including pyrite were given in (Figs. 4.8, 4.9 and 4.13).

Gold identified in stage 2 veins and is often visible in hand specimen or drill core in association with quartz and calcite. Gold also forms as microscopic size associating either with quartz/calcite or sulfide minerals. Inclusions of gold in arsenopyrite and pyrite are also common (Fig. 4.4H). In the Nam Pan ore lens, gold forms as electrum associated with arsenopyrite, pyrite and minor sphalerite (Fig. 4.4E), whereas at the Houay Keh ore lens, gold tends to be coarse - grained crystal and forms as native gold. Pyrrhotite occurs only in Stage 2 in trace among as inclusions in sphalerite (Fig. 4.7).

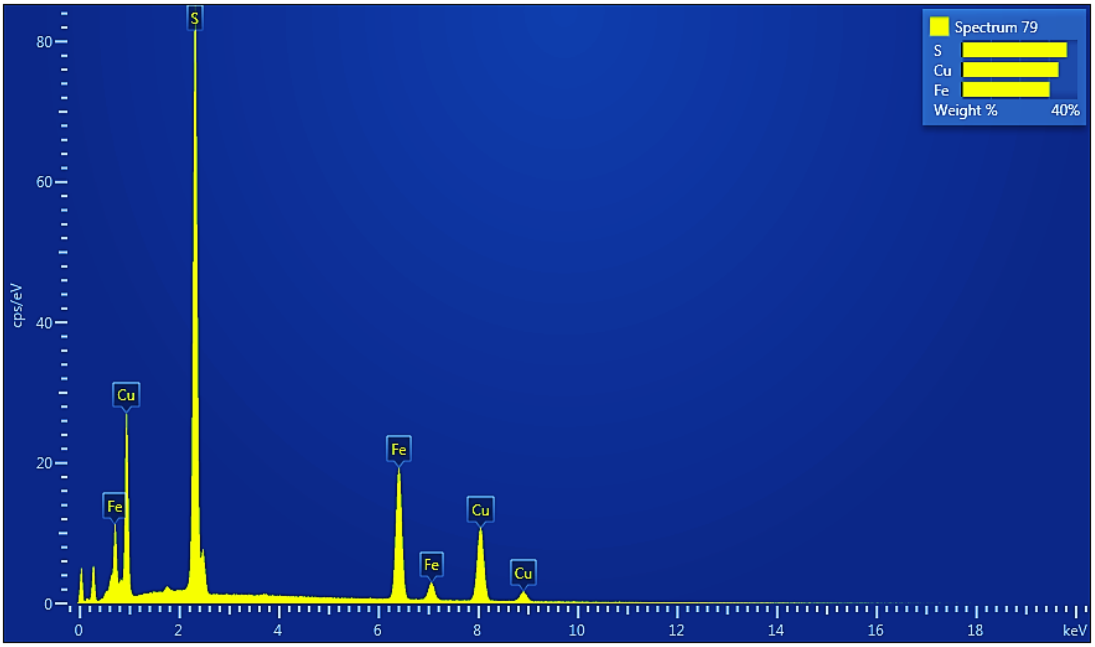

Fig. 4. 12 Result of EDS-SEM analyze shows mineral containing Fe, Cu and S reveals the presence of chalcopyrite, Sample No. HKE057, Houay Keh ore lens.

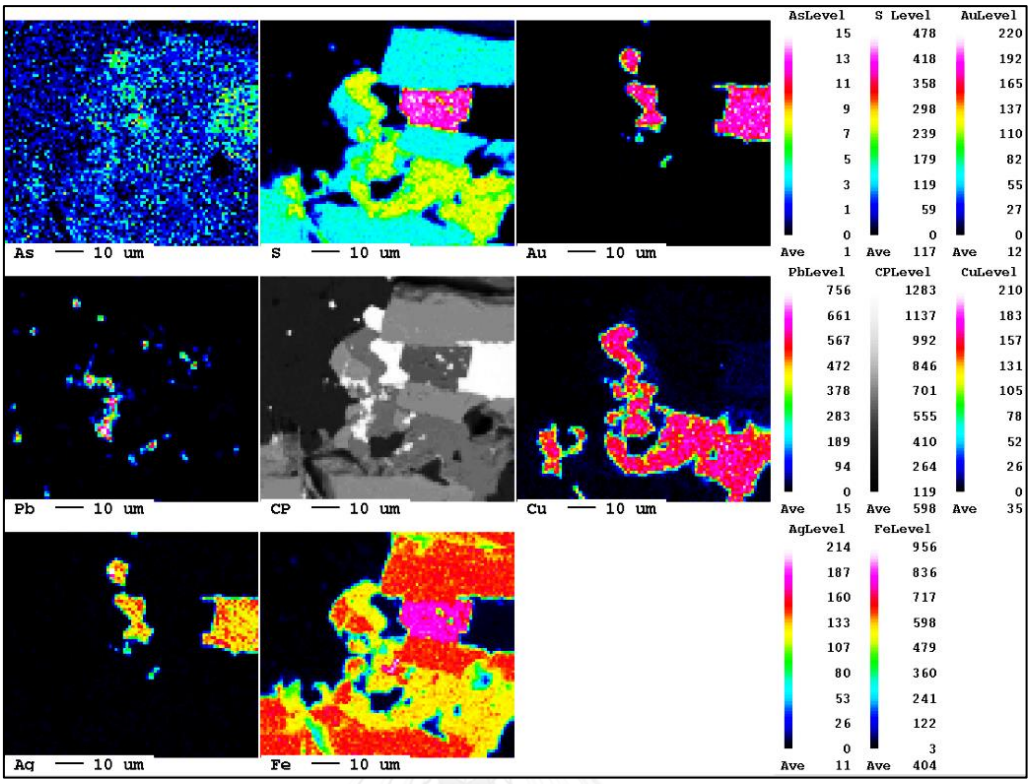

Fig. 4. 13 EPMA mapping shows native gold intergrowth with chalcopyrite, pyrite and galena from Houay Keh ore lens.

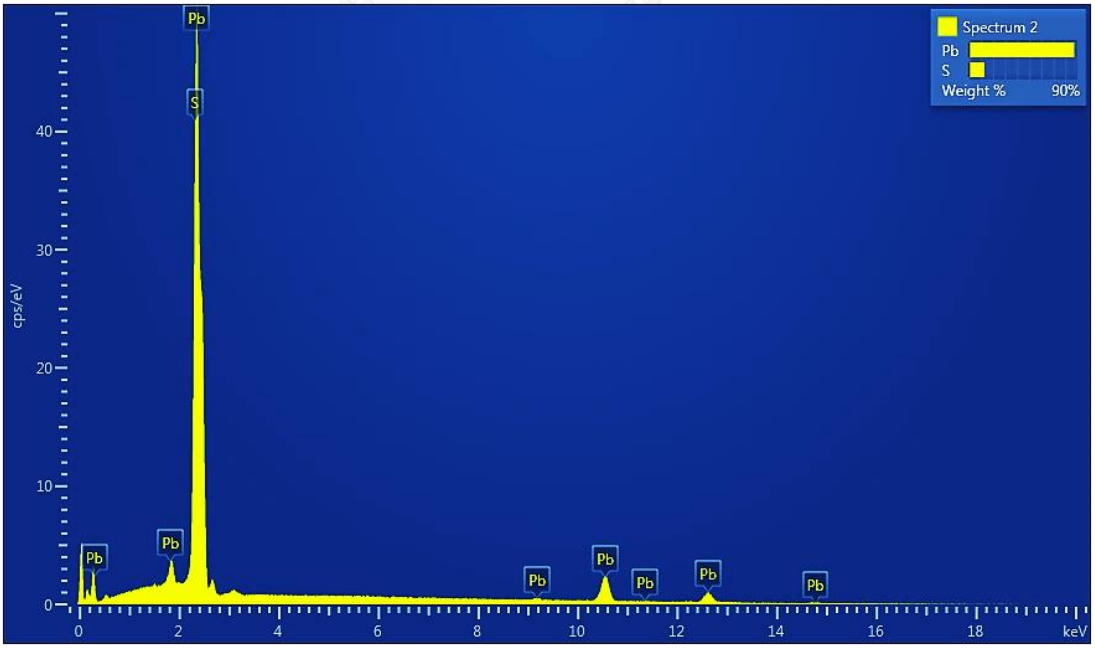

Fig. 4. 14 Result of EDS-SEM analyze shows mineral containing Pb and S indicates galena, Sample No. HKE057, Houay Keh ore lens.

4.4.2 Gangue mineralogy

Quartz is common mineral and present in all stages. In stage 1, it is characterized by microcrystalline texture, and it forms along the vein contact, which is commonly associated with fine-grained pyrite and arsenopyrite (Fig. 4.15A). In Stage 2, quartz forms as elongated shape that is dominant texture and subhedral to euhedral of coarse- to fine-grained crystals (0.05 mm to 0.8 mm in length) which is generally associated with gold and sulfide minerals (Fig. 4.15B). Quartz in Stage 3 is subhedral to euhedral of coarse- to medium-grained crystals (0.2 mm to 0.5 mm in length) that are associated with chlorite and calcite (Figs. 4.15C and D).

Calcite is relatively abundant in Stage 3 in comparison to Stage 2. In Stage 2, calcite occurs in minor amounts in association with quartz, gold and sulfide minerals such as pyrite, sphalerite, galena and chalcopyrite (Fig. 4.15B). It commonly forms as approximately 0.1 to 0.3 mm in diameter and tends to occur at center of veins or open space filling fractures (Fig. 4.15B). Calcite is the most abundant in Stage 3 and tends to occur in center of the vein, after the comb-quartz. Here, it associates with quartz and chlorite (Figs. 4.15C, D and 8A, B).

Chlorite is particularly abundant in Stage 3 veins/veinlets. Numerous chlorites form as tabular aggregated or layers-rich crystals. However, this vein stage does not contain any gold and sulfide minerals (Figs. 4.16A and B). In Stage 3, chlorite forms as minor fine- to medium-grained (0.05 mm to 0.4 mm in length) crystals associated with quartz and calcite (Figs. 4.16A and B). Chlorite usually occur border of veins and is occasionally present at the center of veins (Figs. 4.16A and B).

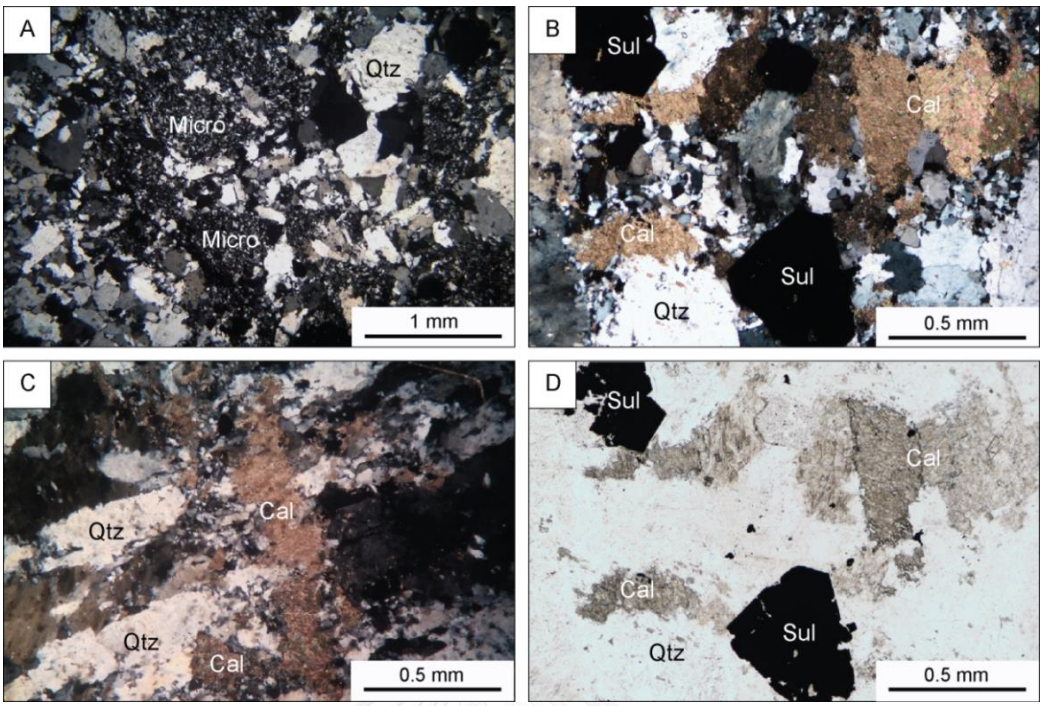

Fig. 4. 15 Characteristic features of quartz in different Stages **A.** Quartz in Stage 1 forms as microcrystalline quartz that associated with fine-grained of pyrite and arsenopyrite, Sample No. TS4, Nam Pan ore lens. **B.** Quartz in Stage 2 occurs as elongated shape, euhedral to euhedral granular quartz which closely intergrowth with sulfide minerals (pyrite) and calcite (CPL), Sample No. HKE057_26.7, Houay Keh ore lens. **C.** Quartz shows elongated shape in Stage 3 generally associated with calcite and chlorite, which is located in rim and central vein, Sample No. HKE090_289, Houay Keh ore lens. **D.** Quartz in Stage 2 associates closely intergrowth with sulfide minerals (pyrite) and calcite (PPL), Sample No. HKE057_26.7, Houay Keh ore lens. Abbreviation: Qtz = quartz, Cal = calcite, Chl = chlorite, Sul = sulfides.

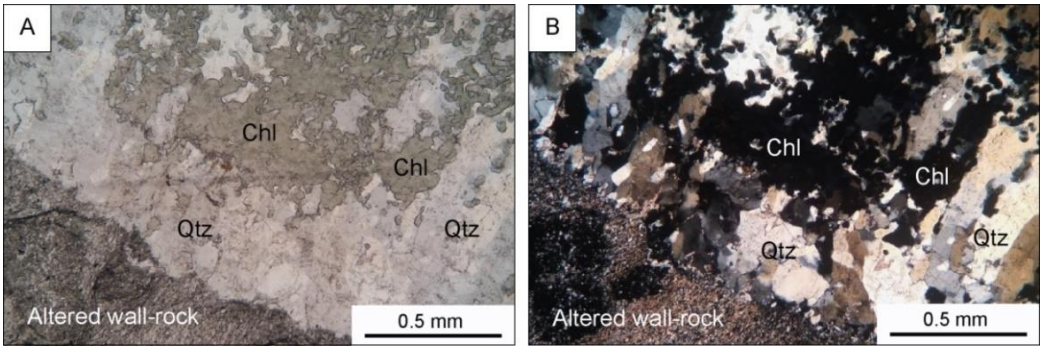

Fig. 4. 16 Characteristic features of chlorite in Stage 3 **A.** Chlorite closely intergrowth with in quartz and calcite (PPL), Sample No. HKE090_289, Houay Keh ore lens. **B.** Chlorite nearly associates with in quartz, which occurs as coarse-grained (XPL), Sample No. HKE090_289, Houay Keh ore lens. Abbreviation: Qtz = quartz, Chl = Chlorite, Cal = calcite.

4.5 Wall Rock Alteration

4.5.1 Introduction

The formation of veins and associated hydrothermal alteration occurs in response to the physical – chemical change in the ore fluids while it approaches to shallow levels together with cooling and/or boiling of ore fluid due to interaction with nearby wall - rocks (White and Hedenquist, 1995). The hydrothermal alteration and distribution can be useful indicator of high-grade ore zones in epithermal ore deposits (White and Hedenquist, 1995) and others similar hydrothermal deposits. Study the hydrothermal alteration system that related to mineralization can lead to a better understanding of ore fluid and wall rock interactions which is expected to be the factors controlling ore deposition.

4.5.2 Methodology

A total of 15 diamond drill core samples (Appendix C) were selected based on cross-sections A-A' and B-B' from Nam Pan and Houay Keh ore lenses. Samples were collected from proximal to distal to the veins. The study is mainly focused on stage 2 mineralization as it is directly associated with gold mineralization and due most pervasive and extensive in comparison to others mineralization stages. Diamond drill core and hand specimen samples have been collected for petrographic investigation and XRD analyzes. In this study, petrographic investigation has been undertaken using modern ore microscope and confirms by quantitative X-ray Diffraction Analyses (XRD) using instrument Model D8 Advance: Bruker AXS, Germany (Appendix D: XRD instrument) and Diffract Plus software of the Bruker Analytical X-ray System (XRD Commander).

4.5.3 Khamkeut Saen Oudom hydrothermal alteration

Two main alteration assemblages are recognized at Khamkeut Saen Oudom based on distinctive alteration mineral assemblages present (1) Quartz - sericite - chlorite - calcite alteration and (2) Chlorite - sericite - calcite alteration. Alteration minerals identified include quartz, sericite, chlorite and calcite. Quartz (including cryptocrystalline quartz) - sericite - chlorite - calcite alteration occurs closely

mineralization vein zone which is less numerous alterations mineral, narrow distribution. Chlorite - sericite - calcite alteration occurs distant from mineralization vein zone. The second alteration zone contains abundance of chlorite.

The alteration in KSO deposit is generally less altered rocks and similar with Kalgoorlie in western Australia. Fluid chemistry in Kalgoorlie deposit consists of chlorite, muscovite, sericite, dolomite and calcite calculations undertaken using the computer software thermocalc in the model system Na_2O–CaO–K_2O–FeO–MgO–Al_2O_3–SiO_2–H_2O–CO_2 show that mineral assemblages of the alteration halo are consistent with equilibrium of the protoliths with a fluid of composition $X_{CO2} = CO_2/(CO_2 + H_2O)$ = 0.1 to 0.25 (less acid) for temperatures of 315 to 320 °C (White et al., 2003). The KSO deposit has mineral assemblages consisting of cryptocrystalline quartz, sericite, chlorite and calcite which similar with Kalgoorlie in western Australia.

4.5.3.1 Quartz - sericite - chlorite - calcite alteration

This alteration assemblage is characterized by the present of cryptocrystalline quartz, sericite, chlorite and sericite. Cryptocrystalline quartz predominantly replaced siltstone and fine-grained sandstone wall-rock particularly in matrix. The extension of this alteration in the wall-rock depends on size of veins and type of rocks. The alteration of this type is confined to very narrow zone, about 0.5 to 1 cm from mineralized vein. Figure 4.17 presents hand specimen and photomicrograph of this alteration type in which mineral assemblages (cryptocrystalline quartz, sericite, illite, minor chlorite and calcite.

4.5.3.2 Chlorite - sericite - calcite alteration

The chlorite - sericite - calcite alteration assemblage/type is widely distribution. Chlorite - sericite - calcite assemblage (Fig. 4.18) characterizes this type of alteration. In drill core, the rocks that have undergone chlorite - sericite - calcite alteration are apparently. Under microscope, it consists of very tiny crystal of chlorite, sericite and minor calcite. Figure 4.13B in under microscope is found the minority of sericite, illite and carbonate (calcite) while chlorite is found more numerous.

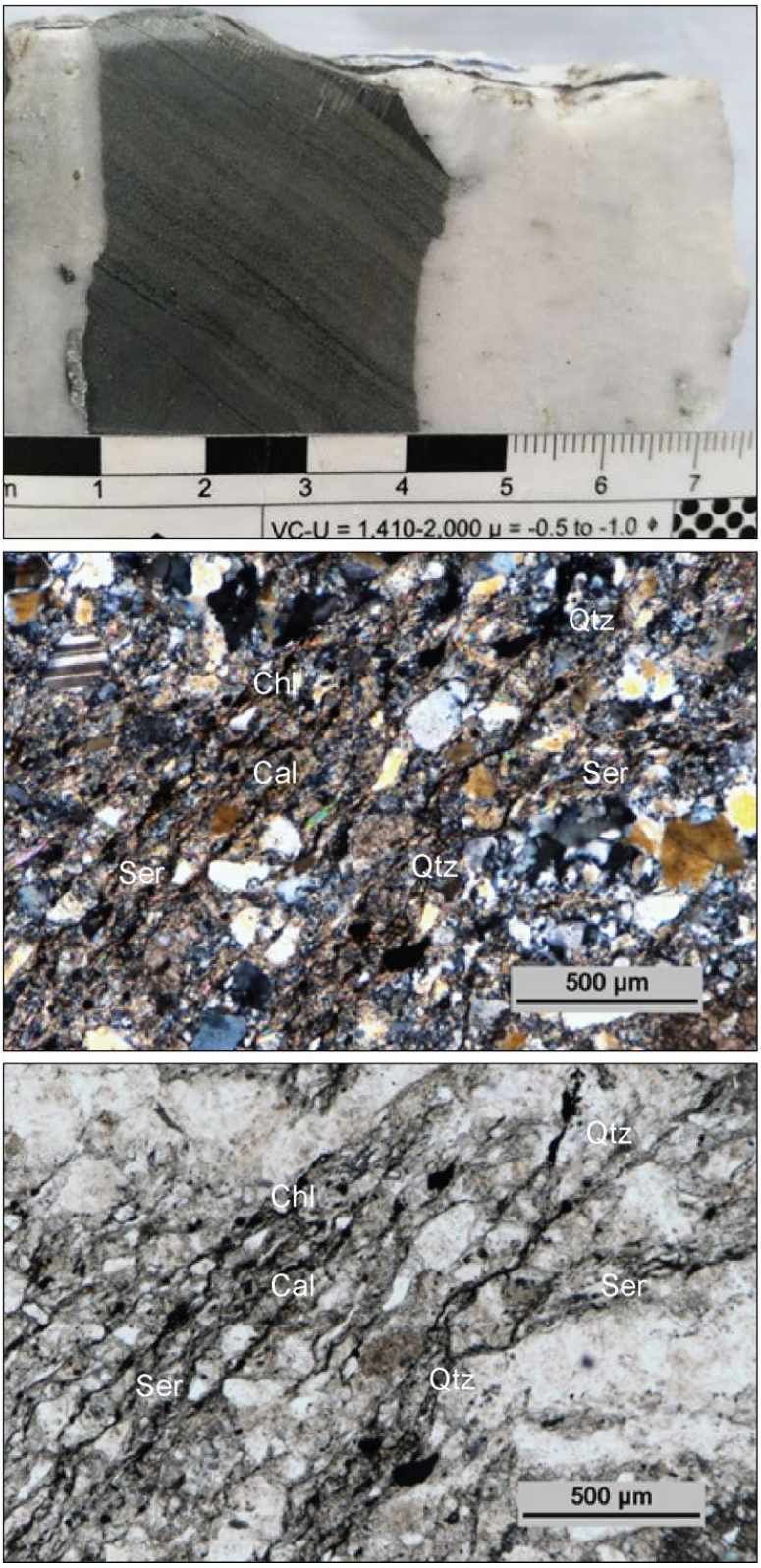

Fig. 4. 17 Characteristic features of alteration at Khamkeut Saen Oudom deposit (quartz - calcite - sericite - chlorite alteration showing calcite, sericite and minor chlorite) Sample No. HKS-02, Houay Keh ore lens.

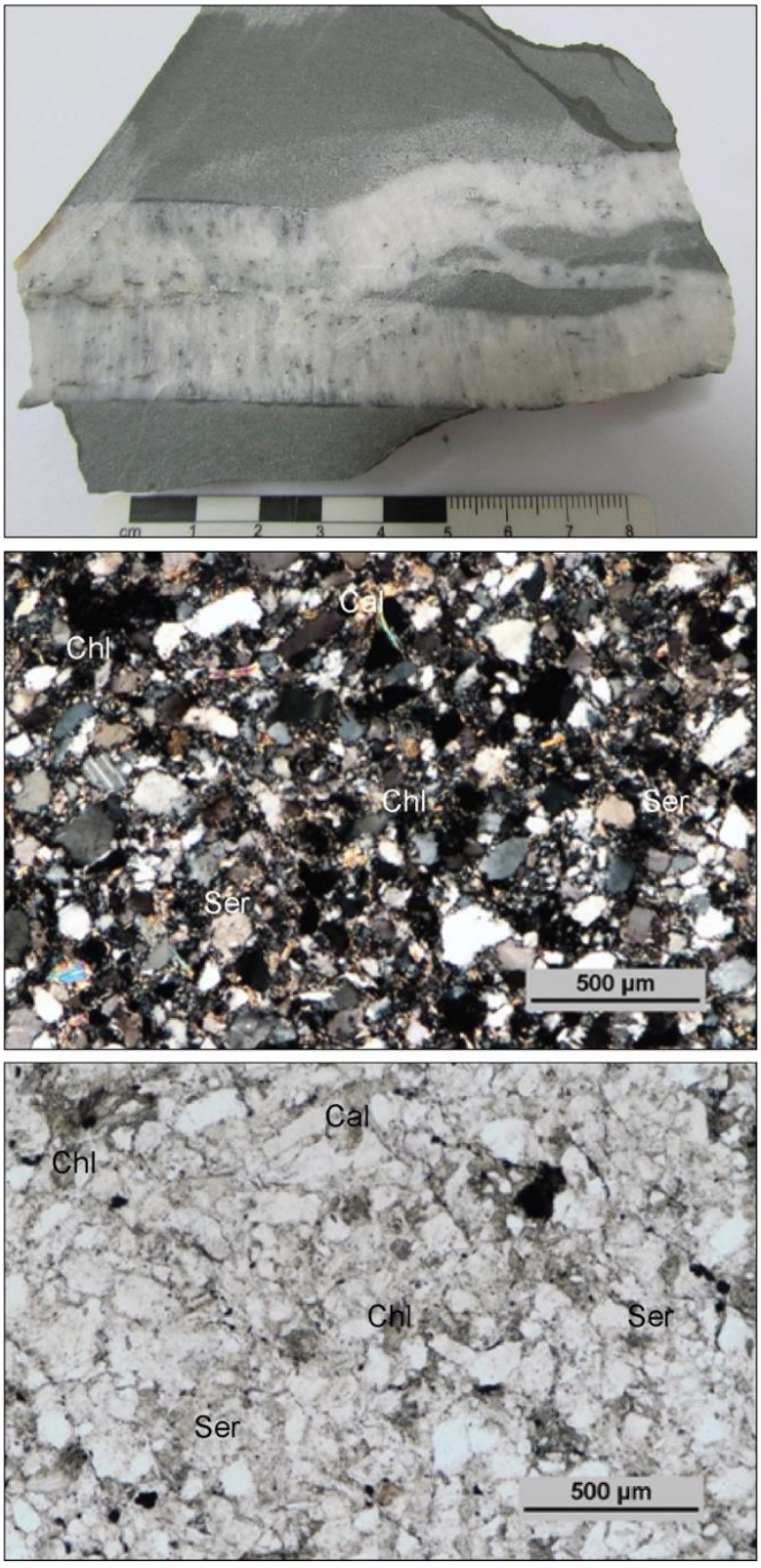

Fig. 4. 18 Characteristic features of alteration at Khamkeut Saen Oudom deposit (chlorite – sericite - carbonate (calcite) alteration showing chlorite and minor sericite and calcite) NPW715_120, Nam Pan ore lens.

CHAPTER V

MINERAL CHEMISTRY

5.1 Introduction

This chapter describes geochemistry of sphalerite chemistry (FeS content) and gold fineness. As describes earlier in Chapter 4, only stage 2 mineralization that contains suitable sphalerite and gold crystals for analyzes (e.g. EPMA). Samples from Nam Pan and Houay Keh ore lenses have been selected this analyzes. This aims to compare FeS content in sphalerite and gold fineness from both ore lenses laterally and vertically. Based on ore petrographic investigation given in chapter 4, sphalerite and gold crystals were selected for analyzes. Total of forty-six gold crystals from Houay Keh and Nam Pan were analyzed. Sphalerite and gold bearing minerals crystals were selected EPMA analysis and details provided in Appendix E.

5.2 Gold fineness

The analyzes then calculated using a formula of (Au/ (Au + Ag) provided by Marsden (2006) to obtain gold fineness. The results and their calculated gold fineness of gold bearing minerals from Houay Keh and Nam Pan are given in Table 5.1 and 5.2.

Au: Ag ratio of gold bearing minerals from Nam pan ore lens ranging from 2:1 to 3:1 with some analyzes contain bismuth mostly less than 1% and no significant amount of copper has been detected. In contrast, the analyses of gold bearing minerals from Houay Keh have Au: Ag 4:1 to 5:1. In which haft of analyzes has little bismuth.

Levitan (2008) suggests that the gold bearing mineral that has gold fineness ranging from 700 to 890 is classified as native gold whereas; that gold fineness ranging from 300 to 700 is classified as electrum. The analyzes from Nam Pan ore lens obtain from this study reveals that the fineness ranging 637.7 to 715.6 suggesting

they are electrum (Table 5.1). In contrast, the values of fineness from Houay Keh ore lens fall in between 827.1 to 866.1 suggesting they are native gold (Table 5.2).

The gold fineness data from Nam Pan and Houay Keh ore lenses are shown in histogram (Fig. 5.1A). The plot reveals from Nam Pan has slightly broader gold fineness in comparison with HK ore lenses. Plot of gold fineness from Nam Pan ore lens with grain size reveals moderate correlation, whereas no correlation for data from HK.

Yilgarn, West Australia (Duuring et al., 2000), Hillgrove, New Southwest Australia (Ashley and Craw, 2004) and one part of Bohemian massif (Zacharias and Hübst, 2012) are high metamorphic rocks have higher values than KSO. Yuryang (Pak et al., 2005) and one part of bohemian massif (Zacharias and Hübst, 2012) are low grade metamorphic rock which have similar range to KSO (Fig. 5.1). The value of gold fineness of the KSO deposit corresponds to orogenic deposit which low grade metamorphic rock.

Table 5. 1 EPMA analyzes of gold in Vein 2 (Stage 2) of the Nam Pan ore lens.

Nam Pan						
Ag	Au	Bi	Fe	Te	Cu	Fineness
26.45	60.06	0.70	0.07	0.22	< DL	694
25.49	59.21	0.57	0.09	0.09	< DL	699
26.17	59.07	0.69	0.03	0.01	0.03	693
26.54	60.27	0.70	< DL	0.11	0.05	694
27.97	56.51	0.69	0.01	0.17	< DL	669
28.94	57.27	0.69	0.10	0.07	< DL	664
29.18	57.13	0.54	< DL	0.14	0.04	662
29.18	57.20	0.74	0.13	0.18	0.03	662
23.79	59.87	0.79	0.67	0.16	< DL	716
28.62	57.90	0.63	0.04	0.15	< DL	669
28.49	59.00	0.76	< DL	0.02	< DL	674
29.56	57.83	0.90	0.11	0.11	0.01	662
29.37	57.56	0.54	0.03	0.17	0.01	662
29.96	56.17	0.75	0.12	0.08	0.03	652
29.67	53.66	0.59	0.50	0.14	< DL	644
29.65	57.05	0.53	0.33	0.19	0.01	658
26.04	48.00	0.69	5.29	0.18	< DL	648
29.19	57.41	0.67	0.07	0.25	0.01	663
29.03	58.00	0.83	0.09	0.14	0.01	666
28.88	57.20	0.76	0.06	0.13	< DL	665
25.91	57.71	0.62	0.21	0.09	0.01	690
31.73	55.85	0.55	0.03	0.23	< DL	638
31.56	55.83	0.57	< DL	0.21	0.01	639

Table 5. 2 EPMA analyze of gold in Vein 2 (Stage 2) from Houay Keh ore lens.

Houay Keh						
Ag	Au	Bi	Fe	Te	Cu	Fineness
15.12	85.37	0.73	< DL	0.04	0.01	850
14.70	85.33	0.71	< DL	0.02	< DL	853
14.54	85.57	0.86	0.01	0.08	0.01	855
14.32	82.81	0.81	0.02	0.10	< DL	853
15.17	83.46	0.75	0.01	0.10	0.01	846
13.47	87.13	0.75	< DL	< DL	0.03	866
14.88	83.93	0.86	< DL	< DL	< DL	849
15.30	84.41	< DL	< DL	0.06	< DL	847
14.83	84.91	0.01	< DL	0.07	0.01	851
14.39	84.36	< DL	< DL	0.06	0.01	854
13.56	85.62	0.10	0.01	0.02	0.02	863
14.85	86.22	< DL	< DL	0.16	< DL	853
15.32	85.11	0.05	0.04	0.03	< DL	848
14.19	84.12	0.05	< DL	0.06	< DL	856
16.98	81.20	< DL	0.01	0.03	0.02	827
15.62	80.21	< DL	< DL	0.05	0.03	837
15.39	82.54	< DL	< DL	0.05	< DL	843
16.21	82.34	0.04	< DL	0.07	0.01	835
16.44	82.94	< DL	< DL	0.09	< DL	835
16.03	82.89	< DL	< DL	0.11	< DL	838
14.43	85.91	< DL	0.02	0.04	0.01	856
14.40	83.41	< DL	0.01	0.06	< DL	853
14.48	82.79	0.06	< DL	0.02	0.04	851

* <DL = under detection limit

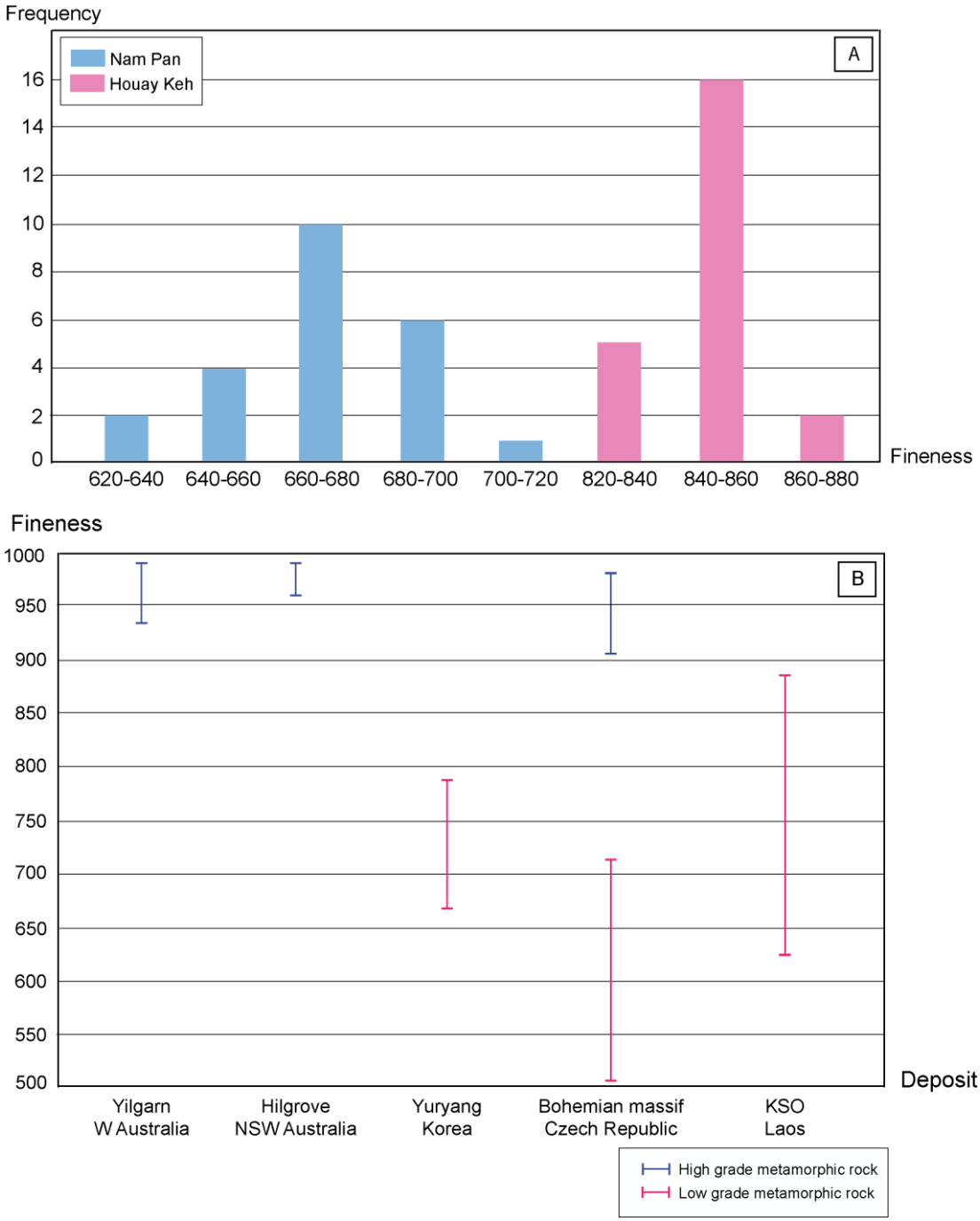

Fig. 5. 1 A. Histogram of gold fineness values from gold bearing Stage 2 veins of the Nam Pan and Houay Keh ore lenses suggests that the majority values of Nam Pan and Houay Keh are electrum and native gold respectively, **B.** Plot of Gold fineness in KSO compared with other deposits in terms of Orogenic gold deposit.

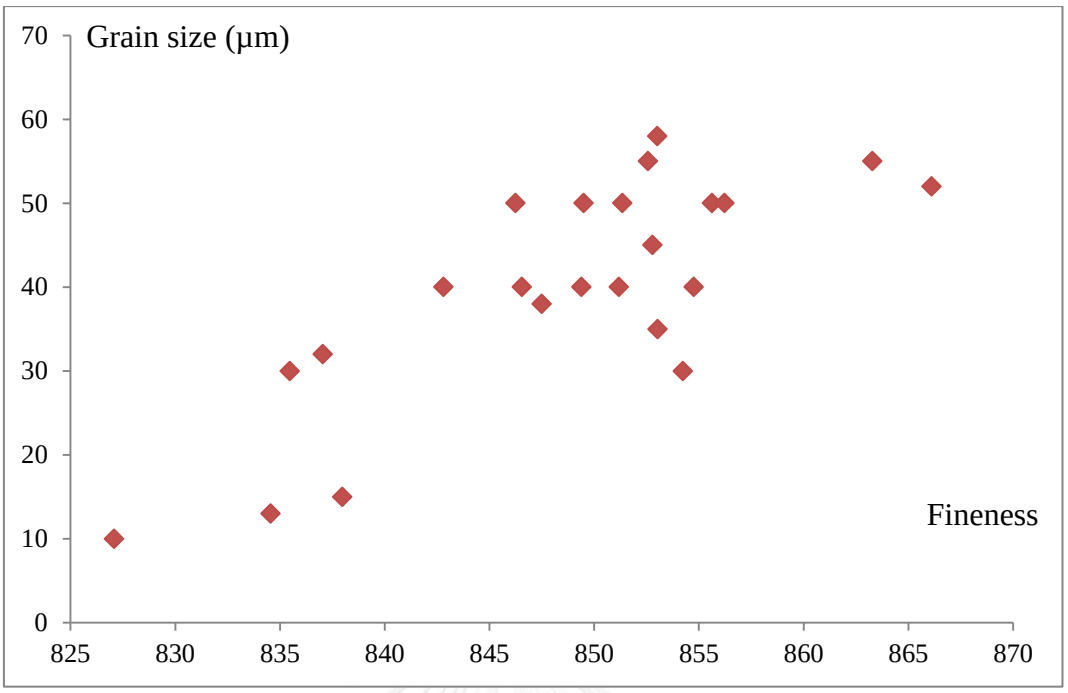

Fig. 5. 2 Histogram of gold fineness values are compared with grain size (µm) in the Nam Pan ore lens.

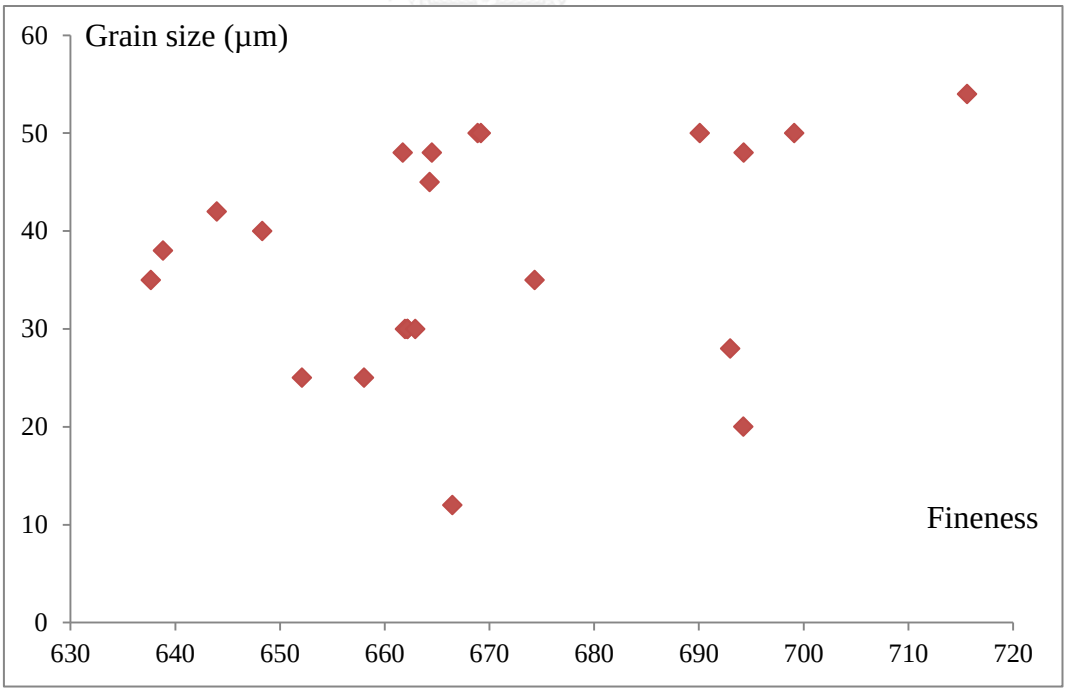

Fig. 5. 3 Histogram of gold fineness values are compared with grain size (µm) in the Houay Keh ore lens.

5.3 Sphalerite chemistry

The FeS content of sphalerite can be an indicator of the physio-chemical conditions of ore forming fluids in the hydrothermal system. Most of the case studies have been conducted on VHMS deposits (Hannington and Scott, 1989; Khin Zaw et al., 1996). However, there are some studies of FeS content of sphalerite in epithermal deposits to determine the ore-forming fluid characters (Gemmell et al., 1988). It has also been reported that the FeS content of sphalerite can be used as a geothermometry for metamorphosed sulfide deposits (Khin Zaw, 1991; Khin Zaw et al., 1996).

A total of twenty-three large grained from five samples of Khamkeut Saen Oudom sphalerite has been analyzed to determine FeS content. In this study, the FeS contents of sphalerite in the Nam Pan and Houay Keh ore lens are analyzed and focused on the relationships with the gold and silver grade in hand specimen of diamond drill cores which each depth such as low to high depth to understand the gold and silver mineralization.

The measured chemical composition of sphalerite from the Khamkeut Saen Oudom deposit is listed in the Appendix B. The calculated FeS mole % values are present in Table 5.3 and shown in Figure 5.4. The composition of sphalerite at Nam Pan ore lens has a range from 5.00 to 8.05 FeS mole %, whereas sphalerite at Houay Keh ore lens has a range from 8.49 to 16.08 FeS mole % (Table 5.3). The correlations between the FeS mole % of sphalerite with gold and silver assay results of each drill core sample at Nam Pan and Houay Keh are shown in Figures. 5.4 and 5.5. A moderate correlation between FeS mole % and gold grade was found (slope = 0.85), but no correlation with silver grade.

Barton and Toulmin (1966); Scott and Barnes (1971) introduced the significant of the FeS content of sphalerite together with pyrite, galena and pyrrhotite as a potential geothermometry and geobarometer in formula P(kbar) = 26.18 – 1.903(mole percent FeS) + 0.0309(mole percent FeS)^2. The study of FeS mole % of sphalerite in KSO deposit has FeS average of two pits such as 6.53 and 12.29 mole % respectively which estimated from FeS mole percent function of temperature and confining pressure (Lusk and Ford, 1978) of having lowest temperature approximately 450 ˚C and 320 ˚C respectively and calculated of pressure approximately 15.08 and 7.17 kbar.

Table 5. 3 Summary of microprobe analysis of average FeS mole% composition in sphalerite with gold and silver grade of diamond drill core samples from the NP and HK deposits.

Pit	Depth	No. of grain (spot)	FeS mole%	Au (g/t)	Ag (g/t)	Assigned stage
Houay Keh						
HK	80	10	8.49	0.26	0.01	Stage 2
HK	152	10	11.75	0.40	0.01	Stage 2
HK	172	10	13.90	0.36	0.01	Stage 2
HK	267	10	16.08	0.47	0.01	Stage 2
Nam Pan						
NP	153	10	5.00	0.25	0.01	Stage 2
NP	282	10	8.05	0.37	0.01	Stage 2

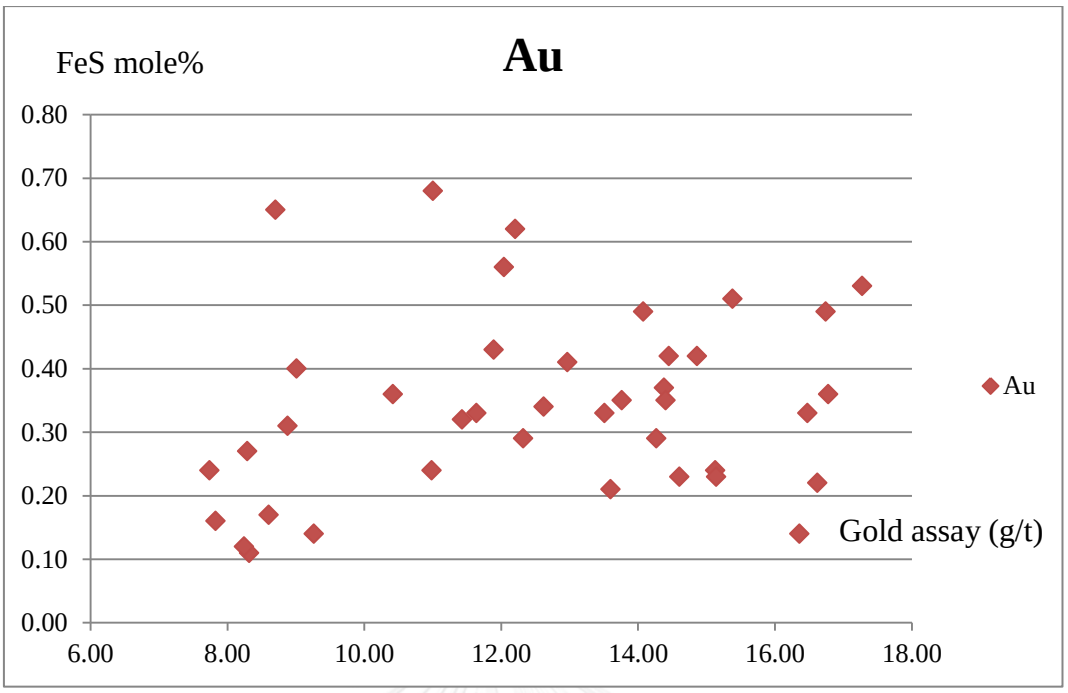

Fig. 5. 4 Plot of FeS mole % in sphalerite and gold assay (g/t) of the sample from Houay Keh deposits, Laos PDR.

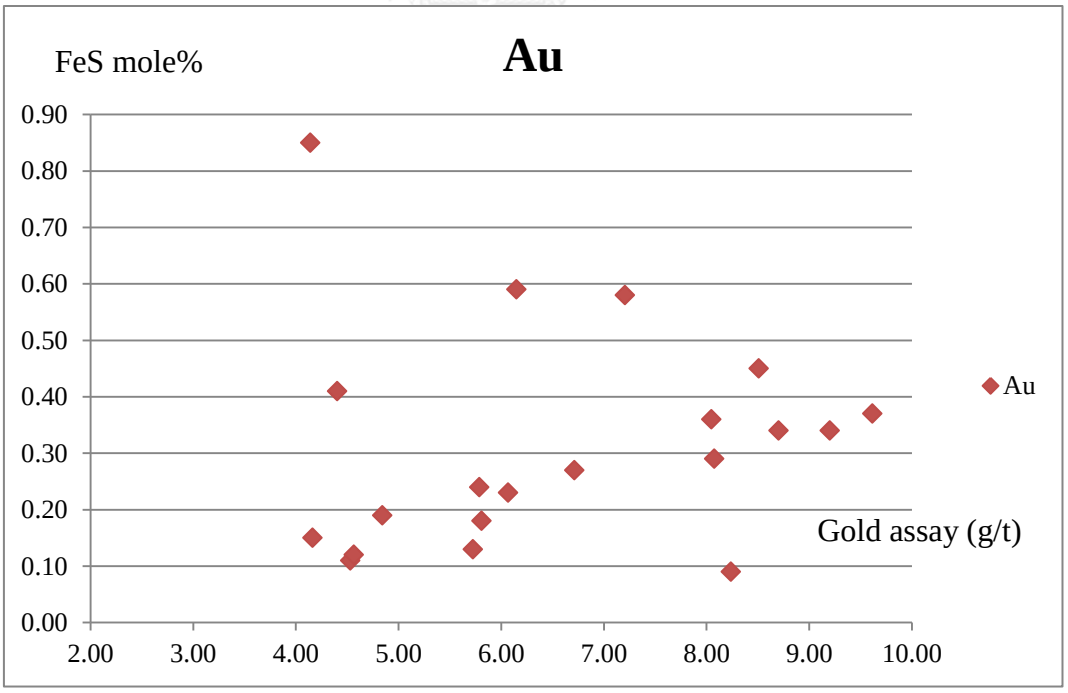

Fig. 5. 5 Plot of FeS mole % in sphalerite and gold assay (g/t) of the sample from Nam pan deposits, Laos PDR.

Compositional variation of sphalerite

Gemmell et al. (1988) study sphalerite at Santo Nino Ag-Pb-Zn epithermal deposit, Mexico suggested that the positive correlates between the FeS content and colour of sphalerite such as darker sphalerite has higher FeS content. The Nam Pan and Houay Keh have value approximately 5.00 to 8.05 and 8.49 to 16.08 mole % of FeS content in sphalerite respectively. FeS mole% in sphalerite of KSO compared with other deposits styles of deposits reveals as follow:

FeS mole % in sphalerite of other deposits; for example, Pongkor in Indonesia (Warmada et al., 2003) has value 0.1 to 2.0 mole %, Central Khamchatka in Russia (Andreeva et al., 2013) has value around 0.0 to 3.0 mole %, Tongyoung in Korea (Yoo et al., 2010) has 6.2 to 13.8 mole %, Cheongyang in Korea (Yoo et al., 2006) has 5.9 to 8.3 mole %, Yuryang deposit in Korea (Pak et al., 2005) has 11.0 to 17.6 mole %, Olary block in South Australia (Bierlein et al., 1995) has 3.8 to 18.7 mole %.

Pongkor, Indonesia (Warmada et al., 2003) and Central Khamchatka, Russia (Andreeva et al., 2013) are low sulfidation epithermal deposit have lower values than KSO. Tongyoung (Yoo et al., 2010) and Cheongyang (Yoo et al., 2006) are mesothermal deposits have similar range to KSO. Orogenic gold deposit from Olary block in South Australia (Bierlein et al., 1995) and Yuryang deposit in Korea (Pak et al., 2005) also shown similar to KSO (Fig. 5.6). The value of FeS mole% of the KSO deposit corresponds to mesothermal and orogenic deposits.

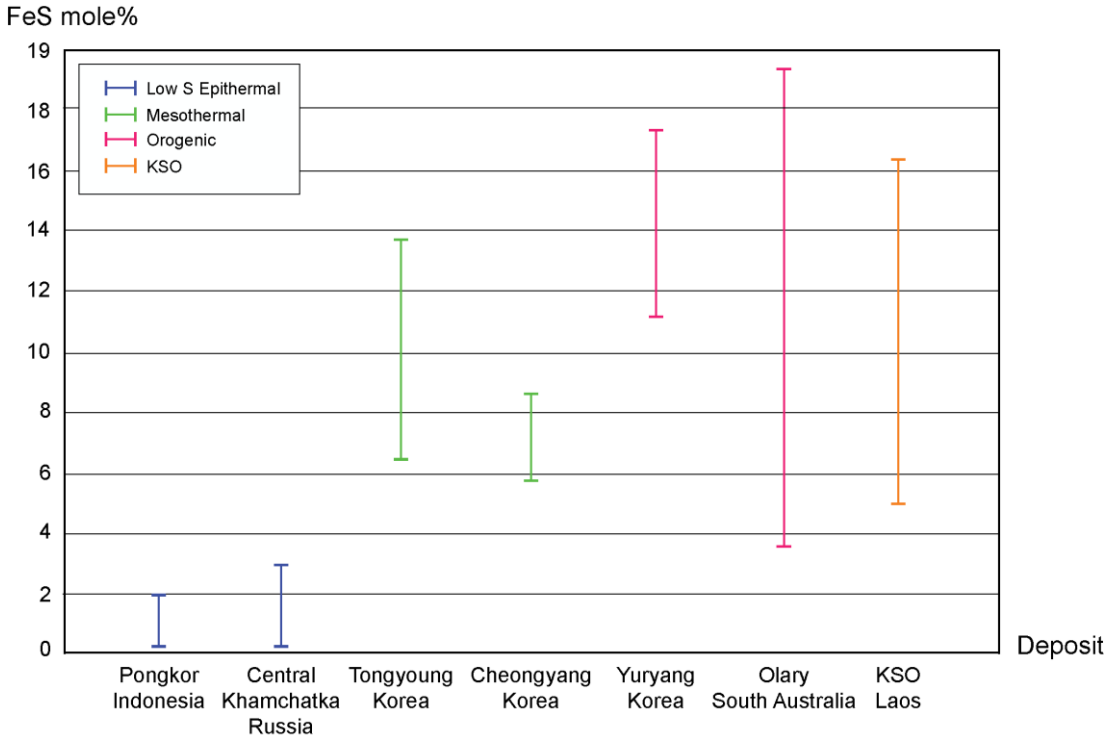

Fig. 5. 6 Plot of FeS mole % in sphalerite in KSO compared with other deposits in terms of Low S Epithermal, Mesothermal and Orogenic gold deposit.

CHAPTER VI

DISCUSSION AND CONCLUSIONS

6.1 Discussion

Prior to the development of east-west major fault at KSO, sediments of Nam Houay Formation were regionally metamorphosed into metasandstone and metasiltstone of low grade greenschist facies by at least one episode of tectonism as recognized by S_1 foliation. This metamorphism may play important role in the enrichment metal particularly gold (see later section).

Before major shearing, at least one episode of fracturing occurs in the study area. Those open fractures were infilled by quartz-sulfides veins and veinlets. These veins and veinlets may contribute to silicification in host metasandstone and metasiltstone.

The major shearing in the KSO area has a similar strike to regional-scale northwest-trending fault zones. That widely developed in northwest-southeast fold belt. However, the timing of the shearing/faulting is not known.

Subsequent to the shearing probably related to a change in tectonic regime from compression to extension, the older KSO shear zone was open up and provided an excellent channel way for various stages of later mineralization. Moderate temperature hydrothermal solutions of metamorphic origin, which were heated by S-type granitic intrusions located about 1 km to the east of the study area, were responsible for KSO mineralization.

One of the key characteristics of orogenic gold deposit is hosted in metamorphic rocks (e.g. Selinsing orogenic gold-antimony deposit in Peninsular Malaysia; Makoundi et al. (2014), although many of them occur in older rocks such as Archean rock and of higher metamorphic grades ranging from upper amphibolite to granulite facies. However, several gold deposits have similar characters to typical orogenic gold deposits are reported particularly in southeast Asia (e.g. Selinsing

orogenic gold-antimony deposit in Peninsular Malaysia; Makoundi et al. (2014). KSO gold deposit is also hosted in low-grade metamorphic rocks consisting of metasandstone and metasiltstone similar to Selinsing orogenic gold-antimony deposit in Peninsular Malaysia (Makoundi et al., 2014). Chae Sorn antimony-gold deposit in northern Thailand is another example in which antimony-gold bearing quartz veins hosted in metasedimentary rocks (e.g. meta-phyllite; Salam (1992). Second similarity to orogenic gold deposit of KSO deposit is geometry and nature of gold bearing quartz veins which tends to form as massive (absent of colloform, crustiform banding) and partly controlled by deformation (i.e. infilling fractures/faults), although at KSO deformation is less developed in comparison to typical orogenic gold deposits. Massive gold bearing quartz veins are similar to the orogenic gold type (Goldfarb et al., 2001; Groves et al., 1998; Groves et al., 2003). Furthermore, the main mineralization at KSO deposit forms as single major ore zone at Nam Pan-west and splays to three small discrete veins at Houay Keh ore lens. This pattern of ore zone is similar to various fault controlled deposits including orogenic gold deposits (e.g. SW Yukon and Interior in British Columbia, Yilgarn craton in western Australia, Otago, South Island in New Zealand). The distinctive sheeted veins identified at Houay Keh ore lens in the east of KSO deposit could be similar to the pattern observed in the intrusion-related gold deposits (Hart et al., 2000). However, the absent of intrusions in adjacent area and no clear metal zonation found at KSO make the intrusion-related deposit style less likely. In addition, gold fineness study at Nam Pan and Houay Keh ore lenses reveals distinctive in which gold occurs at Nam Pan as electrum whereas at Houay Keh it occurs as native gold. The native gold characteristic is consistent with orogenic gold deposit rather than epithermal or intrusion related gold deposits. Considering the hydrothermal alterations at KSO deposit, it reveals that this deposit has less pervasive and extensive alteration mainly characterized by (1) quartz - sericite - chlorite - calcite and (2) chlorite - sericite - calcite mineral assemblages, which is similar to orogenic gold deposit such as those in Reefton goldfield, South Island in New Zealand and Yilgarn block in Western Australia (Christie and Brathwaite, 2003; Eilu and Groves, 2001).

6.2 Conclusions

1. KSO deposit is hosted in meta-sedimentary rocks including metasandstone and metasiltstone and minor phyllite of Nam Houay Formation. The host sedimentary sequence is moderately folded.

2. Gold bearing quartz veins are characterized as massive (absent of colloform and crustiform banding, a typical texture of epithermal gold deposits) and partly controlled by lithology and faults.

3. The main mineralization at KSO deposit forms as single major ore zone at Nam Pan-west and splays to three small discrete veins at Houay Keh ore lens. Ore zone is characterized by distinctive sheeted veins at Houay Keh ore lens in the east of KSO deposit but as massive single zone at Nam Pan ore lens.

4. At least three mineralization stages have been identified, namely, Stage 1 Quartz - arsenopyrite – pyrite; Stage 2 Quartz ± calcite - sulfides (arsenopyrite - pyrite - sphalerite - chalcopyrite – galena - pyrrhotite) - gold; Stage 3 Quartz - chlorite - calcite. Stage 2 is gold bearing stage and responsible for gold resources at KSO deposit.

5. Stage 2 is main gold mineralization which consists of pyrite, arsenopyrite, galena, sphalerite, chalcopyrite, and pyrrhotite

6. Gold occurs as free grains associated with quartz and sulfide minerals such as pyrite, arsenopyrite, sphalerite and galena. In addition, it also forms as inclusions in sulfide minerals particularly arsenopyrite.

7. At Nam Pan, mineral assemblage is typically characterized by pyrite, arsenopyrite and minor base metal whereas, at Houay Keh more base metal rich assemblage.

8. At KSO deposit, hydrothermal alterations are less developed or are less pervasive and intensive and mainly confine to veins peripheral reveals that this deposit has less pervasive and extensive alteration mainly characterized by (1) quartz - sericite - chlorite - calcite and (2) chlorite - sericite - calcite mineral assemblages which can imply fluid at KSO deposit is likely low temperature approximately 315 to 320 °C.

9. Gold fineness study reveals distinctive gold fineness between Nam Pan ore lens and Houay Keh ore lens in which Nam Pan is characterized by electrum whereas at Houay Keh as native gold.

10. Dark-color sphalerite occurs at Nam Pan and has value about 5.00 to 8.05 mole % of FeS content. In contrast, at Houay Keh ore lens has 8.49 to 16.08 mole % of FeS content**.** The value of FeS mole% of the KSO deposit corresponds to mesothermal and orogenic deposits.

11. Tectonic model: The KSO gold deposit occurs in Truong Son Fold Belt in during Triassic age. Early Triassic (250 Ma) occurs granite along Truong Son Fold Belt which give significant minerals such as gold and copper and deposited in Late Triassic (200 Ma).

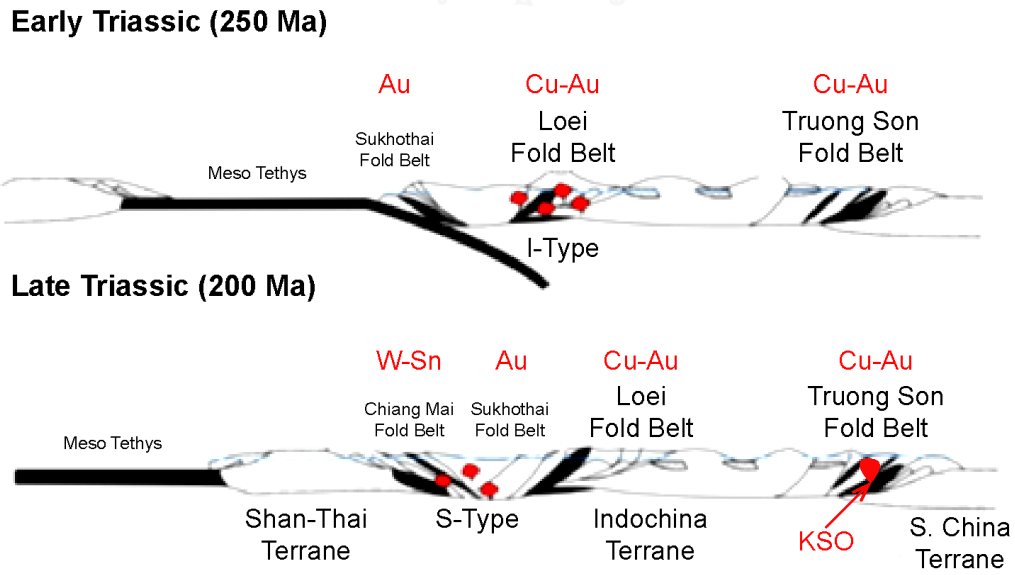

Fig. 6. 1 Tectonic model of KSO gold deposit in Truong Son Fold Belt

12. Model of KSO deposit A) Sedimentation and formation of fine grained clastic sequence B) Low grade metamorphism and C) Faulting and formation of gold.

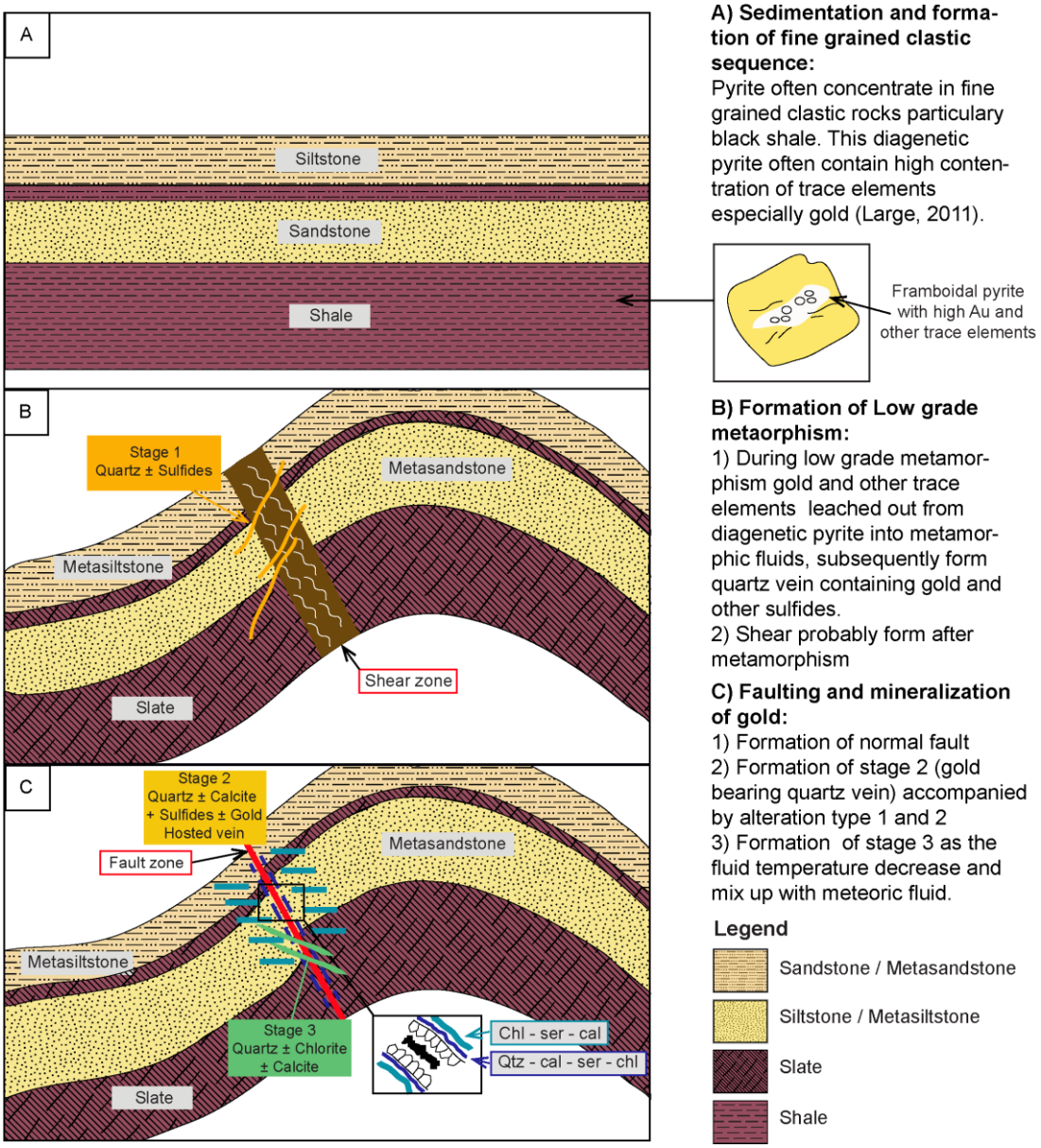

Fig. 6. 2 Geological model of KSO gold deposit

Andreeva, E. D., Matsueda, H., Okrugin, V. M., Takahashi, R., and Ono, S., 2013, Au–Ag–Te Mineralization of the Low-Sulfidation Epithermal Aginskoe Deposit, Central Kamchatka, Russia: Resource Geology, v. 63, no. 4, p. 337-349.

Ashley, P., and Craw, D., 2004, Structural controls on hydrothermal alteration and gold–antimony mineralisation in the Hillgrove area, NSW, Australia: Mineralium Deposita, v. 39, no. 2, p. 223-239.

Backhouse, D., 2004, Geological Setting, Alteration and Nature of Mineralization at the Phu Kham Copper–Gold Deposit, Laos PDR: Unpublished BSc (Hons) thesis) University of Tasmania, Hobart (75 pp.).

Banks, M., Murfitt, R., Quynh, N., and Hai, L., Gold exploration of the Phuoc Son–Tam Ky Suture, central Vietnam—a case study, *in* Proceedings Proceedings of PacRim Congress2004, p. 95-104.

Barton Jr, P., and Bethke, P. M., 1987, Chalcopyrite disease in sphalerite: pathology and epidemiology: American Mineralogist, v. 72, no. 5-6, p. 451-467.

Barton, P. B., and Toulmin, P., 1966, Phase relations involving sphalerite in the Fe-Zn-S system: Economic Geology, v. 61, no. 5, p. 815-849.

Bierlein, F., Ashley, P., and Plimer, I., 1995, Sulphide mineralisation in the Olary Block, South Australia: Mineralium Deposita, v. 30, no. 6, p. 424-438.

Bunopas, S., and Vella, P., Tectonic and geologic evolution of Thailand, *in* Proceedings Proceedings of a workshop on stratigraphic correlation of Thailand and Malaysia1983, Volume 1, p. 307-322.

Christie, A. B., and Brathwaite, R. L., 2003, Hydrothermal alteration in metasedimentary rock-hosted orogenic gold deposits, Reefton goldfield, South Island, New Zealand: Mineralium deposita, v. 38, no. 1, p. 87-107.

Cromie, P., Smith, S., and Zaw, K., 2006, New insights through LA-ICP-MS and sulphur isotope investigations into the occurrence of gold in the Sepon gold deposits, Laos, ASEG Extended Abstracts 2006, Australian Society of Exploration Geophysicists (ASEG), p. 1-3.

Cromie, P., Zaw, K., and Ryan, C., Geological setting, gold-ore paragenesis and trace element geochemistry of the gold and copper deposits in the Sepon mineral district, *in* Proceedings Lao PDR. 13th Quadrennial International Association on Genesis of Ore Deposits (IAGOD) Symposium2010, p. 6-9.

Crossing, J., 2004, Geology of the Chatree District, Thailand: Unpublished technical report, Kingsgate Limited, p. 81.

Cumming, G., James, R., Salam, A., Zaw, K., Meffre, S., Lunwongsa, W., and Nuanla-Ong, S., Geology and Mineralisation of the Chatree Epithermal Gold-Silver Deposit, Petchabun Province, Central Thailand, *in* Proceedings PACRIM 2008, The Pacific Rim: Mineral Endowment, Discoveries & Exploration Frontiers2008, p. 409-416.

De Little, J., 2005, Geological setting, nature of mineralisation, and fluid characteristics of the Wang Yai prospects, central Thailand: University of Tasmania.

Dedenczuk, D., 1998, Epithermal Gold mineralization Khao Sai, Central Thailand: Unpublished B. Science (Hons) Thesis, Hobart, University of Tasmania, p. 1-50.

Diemar, M., and Diemar, V., Geology of the Chatree epithermal gold deposit, Thailand, *in* Proceedings Proceedings of the PACRIM'99 International Congress, Bali1999, p. 11-13.

Duuring, P., Hagemann, S., and Groves, D., 2000, Structural setting, hydrothermal alteration, and gold mineralisation at the Archaean syenite-hosted Jupiter deposit, Yilgarn Craton, Western Australia: Mineralium Deposita, v. 35, no. 5, p. 402-421.

Eilu, P., and Groves, D., 2001, Primary alteration and geochemical dispersion haloes of Archaean orogenic gold deposits in the Yilgarn Craton: the pre-weathering scenario: Geochemistry: Exploration, Environment, Analysis, v. 1, no. 3, p. 183-200.

Fontaine, H., and Workman, D., Review of the geology and mineral resources of Kampuchea, Laos and Vietnam, *in* Proceedings Third Regional Conference on Geology and Mineral Resources of Southeast Asia, Bangkok, Thailand1978, p. 541-603.

Fromaget, J., 1927, Etudes géologiques sur le nord de l'Indo-Chine centrale: Bulletin du service géologique de l'Indo-Chinen.

Gemmell, J. B., Simmons, S. F., and Zantop, H., 1988, The Santo Nino silver-lead-zinc vein, Fresnillo District, Zacatecas, Mexico; Part I, Structure, vein stratigraphy, and mineralogy: Economic Geology, v. 83, no. 8, p. 1597-1618.

Goldfarb, R., Groves, D., and Gardoll, S., 2001, Orogenic gold and geologic time: a global synthesis: Ore geology reviews, v. 18, no. 1, p. 1-75.

Groves, D. I., Goldfarb, R. J., Gebre-Mariam, M., Hagemann, S., and Robert, F., 1998, Orogenic gold deposits: a proposed classification in the context of their crustal distribution and relationship to other gold deposit types: Ore geology reviews, v. 13, no. 1, p. 7-27.

Groves, D. I., Goldfarb, R. J., Robert, F., and Hart, C. J., 2003, Gold deposits in metamorphic belts: overview of current understanding, outstanding problems, future research, and exploration significance: Economic geology, v. 98, no. 1, p. 1-29.

Hannington, M. D., and Scott, S. D., 1989, Sulfidation equilibria as guides to gold mineralization in volcanogenic massive sulfides; evidence from sulfide mineralogy and the composition of sphalerite: Economic Geology, v. 84, no. 7, p. 1978-1995.

Hart, C. J., Baker, T., and Burke, M., 2000, New exploration concepts for country-rock-hosted, intrusion-related gold systems: Tintina gold belt in Yukon: The Tintina gold belt: concepts, exploration and discoveries. British Columbia and Yukon Chamber of Mines, Special, v. 2, p. 145-172.

Hoa, T. T., Anh, T. T., Phuong, N. T., Dung, P. T., Anh, T. V., Izokh, A. E., Borisenko, A. S., Lan, C., Chung, S., and Lo, C., 2008, Permo-Triassic intermediate–felsic magmatism of the Truong Son belt, eastern margin of Indochina: Comptes Rendus Geoscience, v. 340, no. 2, p. 112-126.

Hutchison, C. S., 1989, Geological evolution of South-east Asia, Clarendon Press Oxford.

Intasopa, S., Dunn, T., and Lambert, R. S., 1995, Geochemistry of Cenozoic basaltic and silicic magmas in the central portion of the Loei–Phetchabun volcanic

belt, Lop Buri, Thailand: Canadian Journal of Earth Sciences, v. 32, no. 4, p. 393-409.

Kamvong, T., and Zaw, K., 2009, The origin and evolution of skarn-forming fluids from the Phu Lon deposit, northern Loei Fold Belt, Thailand: evidence from fluid inclusion and sulfur isotope studies: Journal of Asian Earth Sciences, v. 34, no. 5, p. 624-633.

Kamvong, T., Zaw, K., and Harris, A., 2006, Geology and geochemistry of the Phu Lon copper-gold skarn deposit at the northern Loei Fold Belt, Northeast Thailand: ASEG Extended Abstracts, v. 2006, no. 1, p. 1-9.

Kamvong, T., Zaw, K., Meffre, S., Maas, R., Stein, H., and Lai, C.-K., 2014, Adakites in the Truong Son and Loei fold belts, Thailand and Laos: genesis and implications for geodynamics and metallogeny: Gondwana Research, v. 26, no. 1, p. 165-184.

Khin Zaw, 1991, The effect of Devonian metamorphism and metasomatism on the mineralogy and geochemistry of the Cambrian VMS deposits in the Rosebery-Hercules district, western Tasmania: University of Tasmania.

Khin Zaw, Burrett, C., Berry, R., and Bruce, E., 1999, Geological and metallogenic relations of mineral deposits in SE Asia, Geologic, tectonic and metallogenic relations of mineral deposits in SE Asia.

Khin Zaw, Gemmell, J., Large, R., Mernagh, T., and Ryan, C., 1996, Evolution and source of ore fluids in the stringer system, Hellyer VHMS deposit, Tasmania, Australia: evidence from fluid inclusion microthermometry and geochemistry: Ore Geology Reviews, v. 10, no. 3-6, p. 251-278.

Khin Zaw, Meffre, S., Kamvong, T., Salam, A., Manaka, T., and Khositanont, S., 2007a, Metallogenic relations and deposit-scale studies: Final Report, Geochronology, metallogenesis and deposit styles of Loei Foldbelt in Thailand and Laos PDR, ARC Linkage Project.

Khin Zaw, Meffre, S., Lai, C.-K., Burrett, C., Santosh, M., Graham, I., Manaka, T., Salam, A., Kamvong, T., and Cromie, P., 2014, Tectonics and metallogeny of mainland Southeast Asia—a review and contribution: Gondwana Research, v. 26, no. 1, p. 5-30.

Khin Zaw, Rodmanee, T., Khositanont, S., Thanasuthipitak, T., and Ruamkid, S., Geology and genesis of Phu Thap Fah gold skarn deposit, northeastern Thailand: implications for reduced gold skarn formation and mineral exploration, *in* Proceedings Proceedings of GEOTHAI'07 International Conference on Geology of Thailand, Bangkok, Thailand2007b, p. 93-95.

Khositanont, S., 2008, Gold and iron-gold mineralisation in the Sukhothai and Loei-Phetchabun Fold Belts, v. Unpublish PhD thesis, Chiang Mai University, Thaialnd, p. 170.

Kromkhun, K., 2005, Geological setting, mineralogy, alteration, and nature of ore fluid of the H zone, the Chatree deposit, Thailand: University of Tasmania.

Lee, Y., Zaw, K., Meffre, S., and Halpin, J., 2010, Geological setting and mineralisation characteristics of the Bong Mieu gold mine, central Vietnam.

Lepvrier, C., Maluski, H., Van Tich, V., Leyreloup, A., Thi, P. T., and Van Vuong, N., 2004, The early Triassic Indosinian orogeny in Vietnam (Truong Son Belt and Kontum Massif); implications for the geodynamic evolution of Indochina: Tectonophysics, v. 393, no. 1, p. 87-118.

Lepvrier, C., Maluski, H., Van Vuong, N., Roques, D., Axente, V., and Rangin, C., 1997, Indosinian NW-trending shear zones within the Truong Son belt (Vietnam) 40 Ar□ 39 Ar Triassic ages and Cretaceous to Cenozoic overprints: Tectonophysics, v. 283, no. 1, p. 105-127.

Lepvrier, C., Van Vuong, N., Maluski, H., Thi, P. T., and Van Vu, T., 2008, Indosinian tectonics in Vietnam: Comptes Rendus Geoscience, v. 340, no. 2, p. 94-111.

Levitan, G., 2008, Gold deposits of the CIS.

Lusk, J., and Ford, C., 1978, Experimental extension of the sphalerite geobarometer to 10 kbar: American Mineralogist, v. 63, no. 5-6, p. 516-519.

Makoundi, C., Zaw, K., Large, R. R., Meffre, S., Lai, C.-K., and Hoe, T. G., 2014, Geology, geochemistry and metallogenesis of the Selinsing gold deposit, central Malaysia: Gondwana Research, v. 26, no. 1, p. 241-261.

Manaka, T., 2008, Geological setting and mineralisation characteristics of the Long Chieng Track and Ban Houayxai deposits, Lao PDR: University of Tasmania.

Manaka, T., Dinh, S. Q., Zaw, K., Meffre, S., Halpin, J., Tran, H., Hai, L., and Hung, N., Geology and mineralisation of the Phuoc Son gold deposits, central Vietnam, *in* Proceedings 13th Quadrennial Symposium of the International Association on the Genesis of Ore Deposits (IOGAD)2010, p. -.

Manaka, T., Zaw, K., Meffre, S., Vasconcelos, P. M., and Golding, S. D., 2014, The Ban Houayxai epithermal Au–Ag deposit in the Northern Lao PDR: Mineralization related to the Early Permian arc magmatism of the Truong Son Fold Belt: Gondwana Research, v. 26, no. 1, p. 185-197.

Manini, A., Aquino, J., Gregory, C., and Aneka, S., 2001, Discovery of the Sepon district gold and copper deposits, Laos, NewGenGold 2001, Perth, 2001, p. 93-108.

Marsden, J. H., lain, 2006, The Chemistry of Gold Extraction, Society for mining, Metallurgy, and Exploration, Inc.

Meinert, L. D., Dipple, G. M., and Nicolescu, S., 2005, World skarn deposits: Economic Geology, v. 100, no. 4, p. 299-336.

Metcalfe, I., 1995, Gondwana dispersion and Asian accretion: An overview: Gondwana dispersion and Asian accretion, Final Results Volume for IGCP Project, v. 321.

Metcalfe, I., 2006, Palaeozoic and Mesozoic tectonic evolution and palaeogeography of East Asian crustal fragments: the Korean Peninsula in context: Gondwana Research, v. 9, no. 1, p. 24-46.

Muller, C. J., 1999, Geochemistry, fluid characteristics and evolution of the French Mine gold skarn system: Unpub. B.Sc. (Hons) thesis, University of Tasmania.

Nakano, N., Osanai, Y., Minh, N. T., Miyamoto, T., Hayasaka, Y., and Owada, M., 2008, Discovery of high-pressure granulite-facies metamorphism in northern Vietnam: constraints on the Permo-Triassic Indochinese continental collision tectonics: Comptes Rendus Geoscience, v. 340, no. 2, p. 127-138.

Nam, T. N., Sano, Y., Terada, K., Toriumi, M., and Van Quynh, P., 2001, First SHRIMP U–Pb zircon dating of granulites from the Kontum massif (Vietnam) and tectonothermal implications: Journal of Asian Earth Sciences, v. 19, no. 1, p. 77-84.

Olberg, D., and Manini, T., The Sepon gold deposits, Laos: Exploration, geology, and comparison to Carlin-type gold deposits in the Great Basin Stuart Smith* Chief Exploration Geologist, Oxiana Ltd., PO Box 960, Parkes, NSW Australia 2870, *in* Proceedings Symposium 2005: Window to the World: Symposium Proceedings2005, Volume 2, Geological Society of Nevada, p. 899.

Osanai, Y., Nakano, N., Owada, M., Nam, T. N., Toyoshima, T., Tsunogae, T., and Pham, B., 2004, Permo-Triassic ultrahigh-temperature metamorphism in the Kontum massif, central Vietnam: Journal of Mineralogical and Petrological Sciences, v. 99, no. 4, p. 225-241.

Paipana, S., 2014, Geological and Mineralisation Characteristics of Bo Thong Antimony-Gold Deposit, Chonburi Province, Eastern Thailand.

Pak, S. J., Choi, S.-G., Oh, C. W., Kim, S. W., and Wee, S.-M., Genetic environment of the Yuryang Te-bearing Au deposit: Batholith-type orogenic Au mineralization in Korea, *in* Proceedings Mineral Deposit Research: Meeting the Global Challenge2005, Springer, p. 1029-1031.

Quynh, N. N., Murfitt, R., Sirinawin, T., and Shywolup, W., The Bong Mieu gold project, Phuoc Son–Tam Ky Suture, central Vietnam, *in* Proceedings Proceedings of PacRim2004, Volume 2004, p. 347-358.

Rodmanee, T., 2000, Genetic model of Phu Thab Fah gold deposit Ban Huai Phuk Amphoe Wang Saphung Changwat Loei: Chiang Mai: Graduate School, Chiang Mai University, 2000.

Salam, A., 1992, Geological, mineralogical and fluid inclusion studies of Antimony-Gold mineralization at Tambon Chae Sorn, King Amphoe Muang Pan, Changwat Lampang.

Salam, A., Zaw, K., Meffre, S., Golding, S., McPhie, J., Suphanathi, S., and James, R., Mineralisation and oxygen isotope zonation of Chatree epithermal gold-silver deposit, Phetchabun province, central Thailand, *in* Proceedings PACRIM 2008, The Pacific Rim: Mineral Endowment, Discoveries & Exploration Frontiers2008, p. 123-132.

Salam, A., Zaw, K., Meffre, S., James, R., and Stein, H., Geological setting, alteration, mineralization and geochronology of Chatree epithermal gold–silver deposit, Phetchabun Province, central Thailand, *in* Proceedings Proceedings of Ores and Orogenesis Symposium2007, p. 24-30.

Salam, A., Zaw, K., Meffre, S., McPhie, J., and Lai, C.-K., 2014, Geochemistry and geochronology of the Chatree epithermal gold–silver deposit: Implications for the tectonic setting of the Loei Fold Belt, central Thailand: Gondwana Research, v. 26, no. 1, p. 198-217.

Salam, A., Zaw, K., Meffre, S., McPhie, J., and Lai, C., 2013, Geochemistry and geochronology of epithermal Au-hosted Chatree volcanic sequence: implication for tectonic setting of the Loei Fold Belt in central Thailand: Gondwana Research, v. 8.

Sanematsu, K., Moriyama, T., Sotouky, L., and Watanabe, Y., 2011, Mobility of Rare Earth Elements in Basalt-Derived Laterite at the Bolaven Plateau, Southern Laos: Resource geology, v. 61, no. 2, p. 140-158.

Scott, S., and Barnes, H., 1971, Sphalerite geothermometry and geobarometry: Economic Geology, v. 66, no. 4, p. 653-669.

Singharajwarapan, S., 1994, Deformation and metamorphism of the Sukhothai Fold Belt, northern Thailand: University of Tasmania.

Sitthithaworn, E., Albino, G., and Fyfe, W., 1993, Copper-gold porphyry and skarn mineralization at Phu Lon, Northern Thailand: Transactions of the institution of minning and metallurgy section B-applied earth science, v. 102, p. B181-B191.

Smith, P. F. L., Stokes, R. B., Bristow, C., and Carter, A., 1996, Mid-Cretaceous inversion in the northern Khorat Plateau of Lao PDR and Thailand: Geological Society, London, Special Publications, v. 106, no. 1, p. 233-247.

Smith, S., Olberg, D., and Manini, T., The Sepon gold deposits, Laos: exploration, geology and comparison to Carlin-type gold deposits in the Great Basin, *in* Proceedings Steininger RC, Vikre P G. Window to the world. Symposium proceedings2005, Volume 2.

Sone, M., and Metcalfe, I., 2008, Parallel Tethyan sutures in mainland Southeast Asia: new insights for Palaeo-Tethys closure and implications for the Indosinian orogeny: Comptes Rendus Geoscience, v. 340, no. 2, p. 166-179.

Srichan, W., Crawford, A., and Berry, R., Geochemistry and geochronology of the Lampang area igneous rocks, northern Thailand, *in* Proceedings Proceedings of the International Symposium on Geoscience Resources and Environments of Asian Terranes (GREAT 2008), 4th IGCP2008, Volume 516.

SRK, 2011, KSO Gold Mine & Exploration Concession, Initial Site Visit: Observations and Recommendations.

Stokes, R. B., Smith, P. F. L., and Soumphonphakdy, K., 1996, Timing of the Shan-Thai-Indochina collision: new evidence from the Pak Lay Foldbelt of the Lao PDR: Geological Society, London, Special Publications, v. 106, no. 1, p. 225-232.

Tate, N. M., Discovery, geology and mineralisation of the Phu Kham copper-gold deposit Lao People's Democratic Republic, *in* Proceedings Mineral Deposit Research: Meeting the Global Challenge2005, Springer, p. 1077-1080.

Thassanapak, H., Udchachon, M., and Burrett, C., 2012, Devonian radiolarians and tentaculitids from central Laos: Journal of Asian Earth Sciences, v. 60, p. 104-113.

Vilaihongs, M., and Areesiri, S., Geology of lignite deposit and tectonic evolutions in Hong Sa Tertiary basin, Khwaeng Sayaburi, northern Laos PDR, *in* Proceedings The International Conference on Stratigraphy and Tectonic Evolution of Southeast Asia and the South Pacific, Bangkok, Thailand1997, p. 613-639.

Warmada, I. W., Lehmann, B., and Simandjuntak, M., 2003, Polymetallic sulfides and sulfosalts of the Pongkor epithermal gold–silver deposit, West Java, Indonesia: The Canadian Mineralogist, v. 41, no. 1, p. 185-200.

White, N. C., and Hedenquist, J. W., 1995, Epithermal gold deposits: styles, characteristics and exploration: SEG newsletter, v. 23, no. 1, p. 9-13.

White, R., Powell, R., and Phillips, G., 2003, A mineral equilibria study of the hydrothermal alteration in mafic greenschist facies rocks at Kalgoorlie, Western Australia: Journal of Metamorphic Geology, v. 21, no. 5, p. 455-468.

Workman, D., 1975, Tectonic evolution of Indochina.

Yoo, B. C., Lee, H. K., and White, N. C., 2006, Gold-bearing mesothermal veins from the Gubong mine, Cheongyang gold district, Republic of Korea: fluid inclusion and stable isotope studies: Economic Geology, v. 101, no. 4, p. 883-901.

Yoo, B. C., Lee, H. K., and White, N. C., 2010, Mineralogical, fluid inclusion, and stable isotope constraints on mechanisms of ore deposition at the Samgwang mine (Republic of Korea)—a mesothermal, vein-hosted gold–silver deposit: Mineralium Deposita, v. 45, no. 2, p. 161-187.

Zacharias, J., and Hübst, Z., 2012, Structural evolution of the Roudný gold deposit, Bohemian Massif: a combination of paleostress analysis and review of historical documents: Journal of GEOsciences, v. 57, no. 2, p. 87.

APPENDIX A

Sample catalogue

No.	Sample No.	Depth	Description
1	NPE128	225.2	Quartz sulfide banded veins, white band consist of quartz and disseminated sulfide, dark band is argillaceous rich band and disseminated sulfide, gold associated with dark band.
2	NPE128	227	Moderate to strong silicified siltstone, mineralization consist at least 3 mineralization zone such as Quartz – carbonate – sulfide ± gold vein (2-5mm wide) and cross cut by quartz veinlets and again cut by quartz-carbonate veinlets.
3	NPE128	240	Weakly silicified grey laminated mudstone, cubic pyrite cross cut by less than 0.5 mm wide quartz-carbonate veinlets.
4	NPE128	243.6	Big euhedral arsenopyrite in wall rock which is slightly black mudstone (carbonaceous mudstone), mudstone contain euhedral arsenopyrite less than 1mm wide parallel to core axis.
5	NPE128	246	Multiple brecciated strong silicified clast, mineralization quartz-carbonate main mineralization quartz sulfide with minor carbonate, main mineralization cross cut by less quartz veinlet apparently quartz breccia.
6	NPE128	250.3	Quartz with lath shape mineral vein cross cut by sulfide rich veinlets.
7	NPE128	255.3	Strongly silicified interbedded siltstone and mudstone, mineralization consist at least 2 Stage such as sulfide rich breccia and quartz-carbonate-sulfide rich breccia arsenopyrite.
8	HKE085	266.7	Strongly silicified shale breccia of quartz sulfide vein.
9	HKE085	266.9	Strongly silicified shale breccia of quartz sulfide vein and cross cut by quartz-carbonate-sulfide vein around 3mm to 1.2 cm.
10	HKE085	271.3	Large quartz-carbonate-sulfide vein cross cut by chlorite veinlets.
11	HKE085	296.7	Laminated siltstone and shale cross cut by quartz-chlorite-carbonate about 8 mm to 1.4 cm.
12	HKE085	299.5	Mix clasts of vein breccia of Stage 1 and Stage 2.
13	HKE057	26.7	Very fine sandstone/siltstone, moderate silicified

			siltstone, containing less than 2 mm wide quartz-carbonate-chlorite-sulfide vein, dominant chlorite vein.
14	HKE057	37.5	Siltstone cross cut by multi quartz-carbonate-sulfide sheeted vein.
15	HKE057	40.2	Strongly silicified siltstone containing at least 2 Stages such as sulfide rich and quartz-carbonate-sulfide rich.
16	HKE057	44.6	Massive quartz vein, overprint by chlorite rich.
17	HKE057	47.8	Strongly silicified siltstone, mineralization occur quartz-carbonate-sulfide vein few cm wide vein overprint later quartz-carbonate chlorite.
18	HKE057	55.4	Quartz - carbonate vein cross cut by chlorite vein.
19	HKE057	85.4	Deformed laminated mudstone, silicified mudstone and argillaceous mudstone, breccia vein younger than shear style.
20	HKE057	90.8	Quartz is broken up into sectional that occur after the shear vein up. The characteristics of the alternating of silicified mudstone and argillaceous mudstone, layer contain quartz-sulfide follow shear cleavage, quartz broken by shear.
21	HKE057	106.8	Cataclastic phelonite is similar to phyllite which occur Cataclastic process in shear zone area.
22	HKE057	117.5	Breccia vein occur after siltstone.
23	HKE057	122.1	Hydrothermal breccia clast mainly siliceous mudstone contain abundant small pyrite matrix of quartz with minor sulfide pyrite strongly.
24	HKE057	130.6	Cataclastic rock (old vein is characteristics of the alternating and calcite vein cut to later which in 0.02 mm wide)
25	HKE057	133.8	Shear zone occurs after Stage 1 and Stage 2.
26	HKE057	152.2	Hydrothermal breccia vein
27	HKE057	165.4	Stage 1 (quartz – arsenopyrite - pyrite) vein cross cut by Stage 2 (quartz – pyrite – arsenopyrite - base metals - calcite) vein in siltstone.
28	HKE057	175.2	Laminated siltstone
29	NPW715	120	Late Stage cross cut in sulfide rich rock (shale).
30	NPW715	155	Multiple clasts of vein breccia contain of Stage 2 such as sandstone siltstone and shale (Silicified alteration in clast and it is very pale in clast)

APPENDIX B

Sphalerite geochemical data

Appendix B. Microprobe analyzed of sphalerite chemical composition (wt. %) at the Nam Pan deposit, Lao PDR. Number in red color with blanket = under detection limit.

Sample No.	Zn	Cu	Fe	Mn	S	Ag	Cd	Se	Te	Au	Total	FeS mole%
HK_80_A	57.92	0.02	4.98	0.00	36.01	0.03	0.39	0.00	0.00	0.65	100.00	8.70
HK_80_B	60.13	0.01	4.92	0.01	35.63	0.01	0.33	0.02	0.00	0.11	101.17	8.32
HK_80_C	58.53	0.07	4.97	0.03	35.98	0.03	0.22	0.00	0.00	0.17	100.00	8.60
HK_80_D	58.76	0.03	5.25	0.01	35.26	0.01	0.21	0.08	0.01	0.40	100.02	9.01
HK_80_E	58.97	0.00	5.43	0.00	36.12	0.00	0.43	0.05	0.01	0.14	101.15	9.26
HK_80_F	59.47	0.02	4.82	0.00	35.29	0.01	0.23	0.04	0.00	0.12	100.00	8.24
HK_80_G	68.05	0.13	5.15	0.01	36.21	0.00	0.41	0.00	0.00	0.24	110.20	7.74
HK_80_H	59.51	0.02	5.23	0.01	34.12	0.02	0.36	0.01	0.01	0.31	99.60	8.88
HK_80_I	59.51	0.01	4.56	0.00	35.43	0.01	0.32	0.00	0.00	0.16	100.00	7.83
HK_80_J	58.26	0.00	4.75	0.02	36.22	0.03	0.45	0.00	0.00	0.27	100.00	8.29
HK_152_A	56.78	0.00	7.12	0.01	35.19	0.00	0.25	0.03	0.00	0.62	100.00	12.20
HK_152_B	57.20	0.17	6.38	0.01	35.27	0.00	0.27	0.02	0.00	0.68	100.00	11.00
HK_152_C	61.07	0.02	7.11	0.00	34.45	0.01	0.22	0.01	0.00	0.32	103.21	11.43
HK_152_D	56.93	0.13	7.03	0.00	34.95	0.02	0.35	0.03	0.00	0.56	100.00	12.04
HK_152_E	57.85	0.00	6.44	0.02	35.13	0.01	0.33	0.00	0.01	0.24	100.03	10.98
HK_152_F	56.46	0.03	6.71	0.01	36.15	0.00	0.29	0.02	0.00	0.33	100.00	11.64
HK_152_G	57.75	0.01	7.32	0.00	34.28	0.03	0.31	0.00	0.01	0.29	100.00	12.32
HK_152_H	56.99	0.06	6.94	0.01	35.43	0.02	0.32	0.03	0.00	0.43	100.23	11.89
HK_152_I	57.00	0.11	5.98	0.04	36.24	0.01	0.25	0.01	0.00	0.36	100.00	10.42
HK_152_J	55.79	0.07	7.92	0.01	35.52	0.00	0.43	0.00	0.02	0.21	99.97	13.60
HK_172_A	55.84	0.03	8.46	0.02	35.14	0.01	0.18	0.05	0.00	0.37	100.10	14.38
HK_172_B	55.50	0.23	8.20	0.05	35.21	0.00	0.32	0.00	0.00	0.49	100.00	14.07
HK_172_C	56.33	0.12	8.11	0.01	34.62	0.02	0.12	0.03	0.01	0.35	99.72	13.76
HK_172_D	55.33	0.00	8.43	0.00	35.25	0.01	0.34	0.00	0.01	0.42	99.79	14.45
HK_172_E	56.41	0.13	7.95	0.01	34.89	0.01	0.25	0.02	0.00	0.33	100.00	13.51
HK_172_F	55.43	0.21	8.32	0.01	35.36	0.00	0.32	0.04	0.02	0.29	100.00	14.26
HK_172_G	66.54	0.00	8.67	0.00	36.23	0.00	0.35	0.00	0.01	0.34	112.14	12.62
HK_172_H	56.24	0.05	7.56	0.02	35.26	0.01	0.41	0.03	0.01	0.41	100.00	12.97
HK_172_I	56.07	0.19	8.51	0.03	34.59	0.03	0.22	0.01	0.00	0.35	100.00	14.40
HK_172_J	54.83	0.11	8.46	0.01	35.64	0.00	0.41	0.00	0.00	0.23	99.69	14.61
HK_267_A	53.23	0.01	9.68	0.03	35.79	0.00	0.86	0.04	0.00	0.36	100.00	16.78
HK_267_B	52.95	0.01	9.52	0.01	36.53	0.01	0.73	0.02	0.00	0.22	100.00	16.62
HK_267_C	53.19	0.00	10.02	0.07	35.47	0.00	0.71	0.01	0.01	0.53	100.01	17.27
HK_267_D	54.21	0.01	8.89	0.05	35.64	0.01	0.65	0.03	0.00	0.51	100.00	15.38
HK_267_E	53.39	0.02	9.42	0.04	36.32	0.02	0.62	0.01	0.02	0.14	100.00	16.36
HK_267_F	54.23	0.07	9.65	0.00	34.67	0.00	0.48	0.00	0.00	0.33	99.43	16.48
HK_267_G	64.21	0.19	10.11	0.01	35.42	0.01	0.59	0.03	0.01	0.42	111.00	14.86
HK_267_H	55.54	0.05	8.93	0.03	34.74	0.01	0.45	0.01	0.00	0.24	100.00	15.13
HK_267_I	53.53	0.13	9.71	0.02	35.68	0.00	0.42	0.00	0.02	0.49	100.00	16.74
HK_267_J	55.54	0.00	8.94	0.01	34.35	0.00	0.51	0.02	0.01	0.23	99.61	15.14

Sample No.	Zn	Cu	Fe	Mn	S	Ag	Cd	Se	Te	Au	Total	FeS mole%
NP_153_A	61.68	0.04	2.64	0.00	35.12	0.02	0.38	0.01	0.00	0.11	100.00	4.53
NP_153_B	60.06	0.01	3.29	0.00	36.20	0.01	0.27	0.03	0.00	0.13	100.00	5.72
NP_153_C	60.72	0.02	2.38	0.01	36.34	0.02	0.29	0.04	0.03	0.15	100.00	4.16
NP_153_D	58.86	0.03	2.54	0.02	36.90	0.00	0.35	0.09	0.09	0.12	99.00	4.57
NP_153_E	60.40	0.10	3.52	0.03	35.45	0.03	0.26	0.00	0.00	0.23	100.02	6.07
NP_153_F	61.58	0.02	2.40	0.05	34.68	0.01	0.40	0.01	0.00	0.85	100.00	4.14
NP_153_G	65.22	0.03	2.71	0.00	35.23	0.00	0.37	0.02	0.02	0.41	104.01	4.40
NP_153_H	60.46	0.01	3.35	0.01	34.14	0.00	0.42	0.00	0.01	0.24	98.64	5.79
NP_153_I	60.55	0.00	2.78	0.03	36.01	0.01	0.39	0.04	0.00	0.19	100.00	4.84
NP_153_J	59.13	0.03	3.29	0.03	36.96	0.00	0.38	0.00	0.00	0.18	100.00	5.81
NP_282_A	59.89	0.00	4.85	0.03	35.54	0.02	0.26	0.01	0.04	0.09	100.73	8.24
NP_282_B	59.31	0.02	3.85	0.05	36.07	0.00	0.39	0.00	0.04	0.27	100.00	6.71
NP_282_C	59.24	0.19	4.15	0.01	35.52	0.02	0.27	0.02	0.00	0.58	100.00	7.21
NP_282_D	59.66	0.03	5.13	0.04	34.54	0.01	0.22	0.00	0.01	0.34	99.98	8.70
NP_282_E	62.09	0.01	4.92	0.01	35.36	0.00	0.41	0.03	0.00	0.29	103.12	8.07
NP_282_F	58.66	0.02	5.63	0.00	34.93	0.01	0.34	0.02	0.02	0.37	100.00	9.62
NP_282_G	58.51	0.04	4.91	0.02	35.71	0.00	0.36	0.00	0.00	0.45	100.00	8.51
NP_282_H	62.78	0.01	3.71	0.01	34.42	0.02	0.45	0.00	0.01	0.59	102.00	6.15
NP_282_I	57.75	0.05	4.56	0.03	36.23	0.03	0.42	0.01	0.03	0.36	99.47	8.05
NP_282_J	59.40	0.13	5.43	0.00	34.35	0.00	0.35	0.00	0.00	0.34	100.00	9.20

APPENDIX C
XRD results

Mineral Phases Identified in the Samples as a Group:

1) **Quartz**
2) **Illite**
3) **Muscovite**
4) **Chlorite**
5) **Calcite**
6) **Oligoclase**
7) **Albite**
8) **Phlogopite**
9) **Montmorillonite**
10) **Epidote**
11) **Talc**

Comments on Results:

To allow comparison, all phases identified in the samples as a group have been included in all refinements. Because of this, some minerals will be recorded as present at low levels (background or noise contributions), when they may be absent, results less than 0.3 wt. % should be considered as not detected.

Phase	057_37.5	057_175.15	085_296.7	128_240	057_47.8	713_153.1	057_133.8	074-193.6	080-115.4	080-123	080-123.6	HKW1	HKW2
Quartz	84.55	72.98	76.08	69.29	85.58	74.29	81.26	35.05	59.68	50.55	43.02	64.77	41.77
Illite	0.73	0.00	0.00	0.00	0.00	0.00	0.00	5.64	0.00	6.23	0.00	0.00	10.08
Muscovite	2.65	8.24	10.30	16.18	9.51	14.40	4.03	15.95	7.31	7.27	6.30	20.27	14.12
Chlorite	1.89	8.64	8.88	7.85	3.16	9.18	4.47	14.21	12.64	17.07	7.69	2.97	25.98
Calcite	2.08	3.29	0.00	0.00	0.00	0.00	0.00	17.22	2.31	0.00	20.22	4.06	0.00
Oligoclase	6.14	0.28	0.00	3.87	0.91	0.00	0.00	0.00	3.20	0.00	6.95	4.80	0.00
Albite	1.96	0.00	0.00	0.00	0.84	1.56	1.40	0.00	4.61	12.93	0.00	2.62	5.06
Phlogopite	0.00	1.82	1.70	0.00	0.00	0.21	4.48	0.00	5.32	2.30	10.01	0.00	3.00
Montmorillonite	0.00	4.74	3.04	0.00	0.00	0.36	4.36	5.54	4.93	3.65	0.00	0.00	0.00
Epidote	0.00	0.00	0.00	2.80	0.00	0.00	0.00	6.39	0.00	0.00	0.00	0.00	0.00
Talc	0.00	0.00	0.00	0.00	0.00	0.00	0.00	0.00	0.00	0.00	5.81	0.00	0.00

KSO samples for XRD (squared parts were analyzed)

HKE080/115.40m

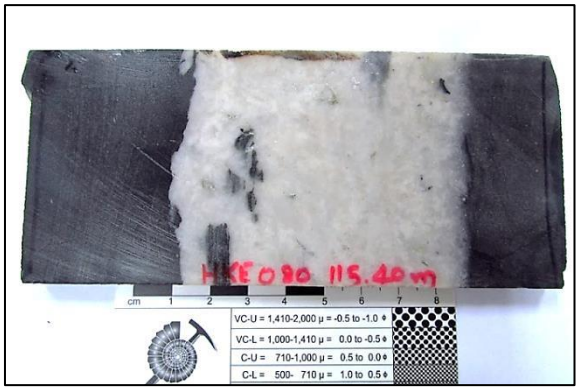

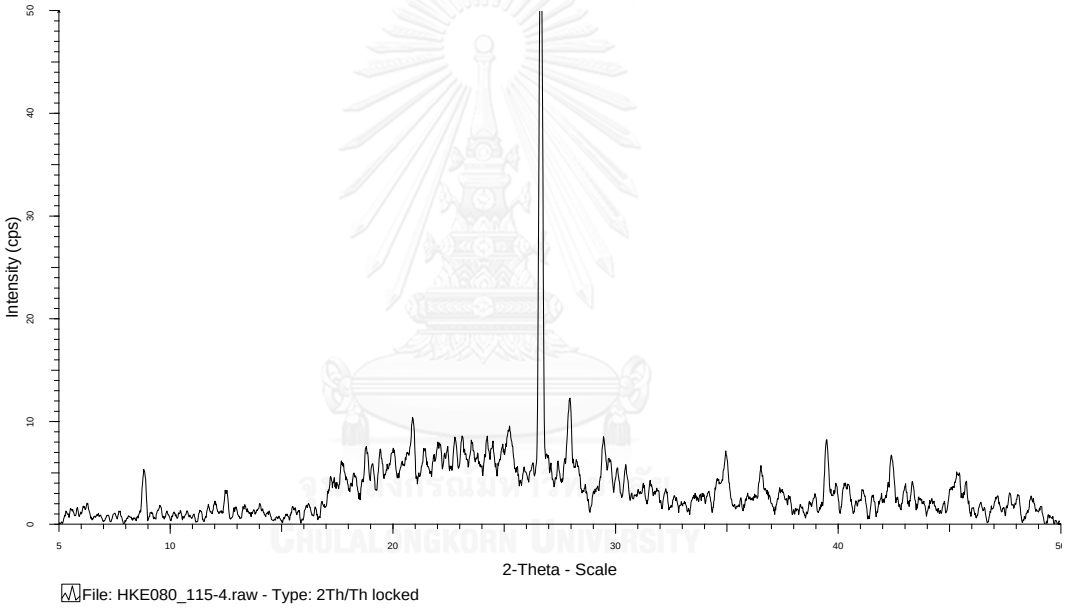

Left Angle	Right Angle	Net Height	Raw Area	Net Area		
2-Theta °	2-Theta °	Cps	Cps x 2-Theta °	Cps x 2-Theta °		
26.48	26.82	49.7	11.94	9.378	70.68	**Quartz**
27.76	28.08	6.24	3.041	1.149	8.66	**Muscovite**
24.68	25.52	4.36	6.04	1.986	14.97	**Chlorite**
29.26	29.62	4.14	2.267	0.755	5.69	**Sericite**
				13.268	100.00	

HKE080/123m

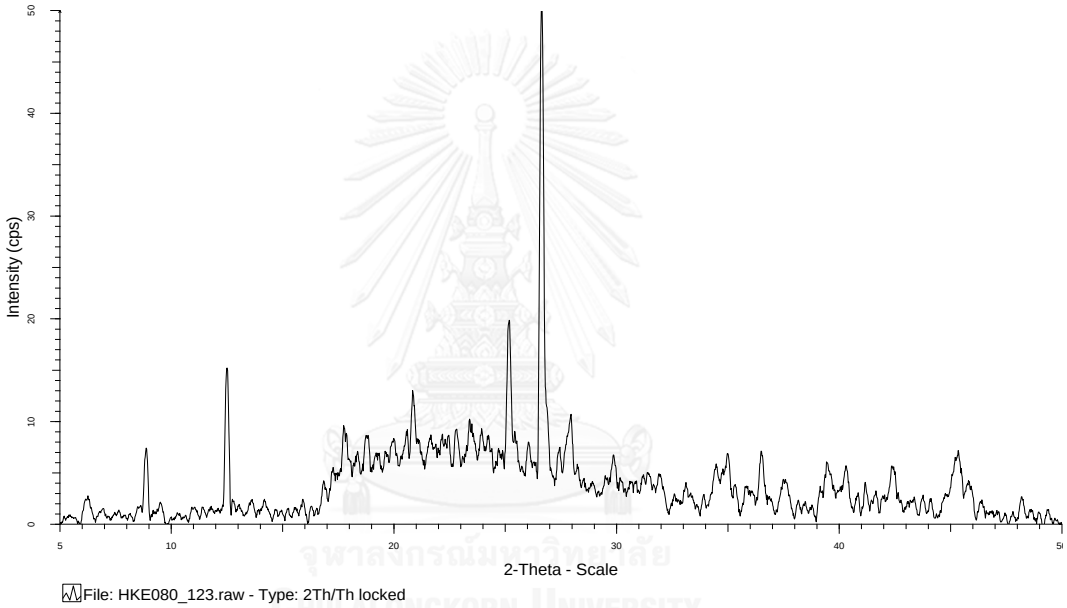

Left Angle	Right Angle	Net Height	Raw Area	Net Area		
2-Theta °	2-Theta °	Cps	Cps x 2-Theta °	Cps x 2-Theta °		
26.48	26.8	48.7	10.67	7.5	59.57	**Quartz**
27.6	28.12	6.57	4.194	1.886	14.98	**Muscovite**
34.86	35.16	3.75	1.705	0.608	4.83	**Iilite**
25	25.3	15.3	4.547	2.259	17.94	**Chlorite**
21.42	21.76	2.95	2.596	0.337	2.68	**Sericite**
				12.59	100.00	

HKE074/193.6m

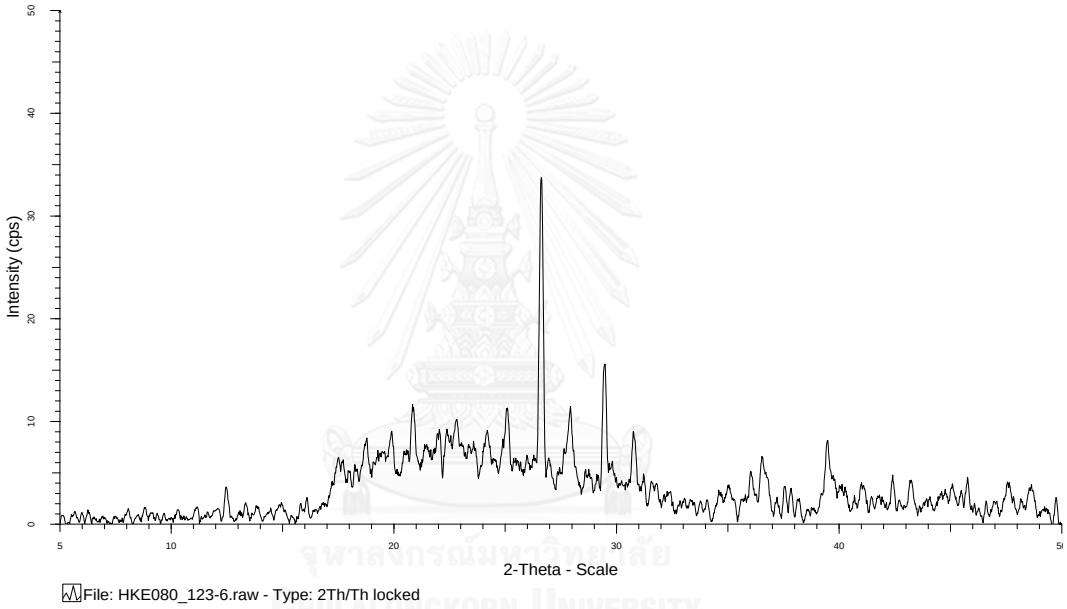

Left Angle	Right Angle	Net Height	Raw Area	Net Area		
2-Theta °	2-Theta °	Cps	Cps x 2-Theta °	Cps x 2-Theta °		
26.48	26.86	30.6	8.555	6.052	44.25	**Quartz**
27.74	28.16	12.9	4.569	2.679	19.59	**Muscovite**
22.58	23.4	3.85	6.033	1.996	14.59	**Iilite**
29.32	29.7	15.1	4.416	2.951	21.57	**Chlorite**
				13.678	100.00	

HKW1

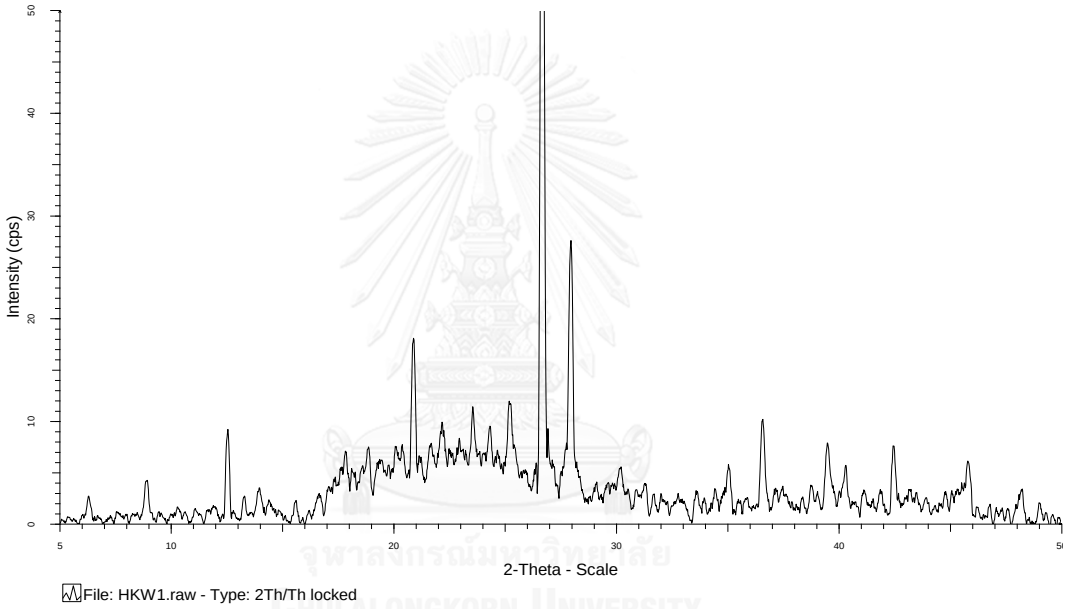

Left Angle	Right Angle	Net Height	Raw Area	Net Area		
2-Theta °	2-Theta °	Cps	Cps x 2-Theta °	Cps x 2-Theta °		
26.5	26.84	82.6	18.6	15.31	76.14	**Quartz**
27.78	28.1	20.3	6.178	3.84	19.10	**Muscovite**
25.04	25.36	4.97	3.153	0.959	4.77	**Chlorite**
				20.109	100.00	

HKW2

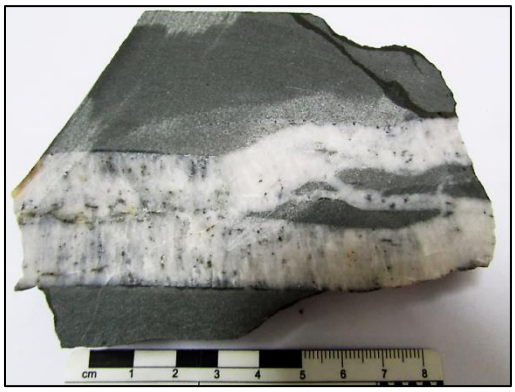

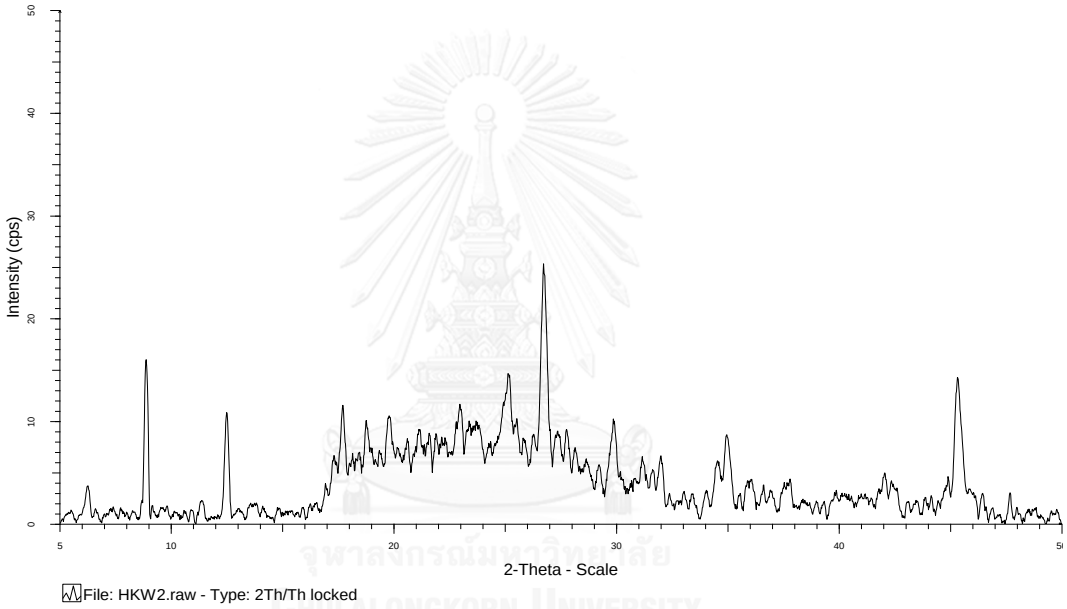

Left Angle	Right Angle	Net Height	Raw Area	Net Area		
2-Theta °	2-Theta °	Cps	Cps x 2-Theta °	Cps x 2-Theta °		
26.44	27.12	18.2	10.2	5.917	42.01	**Quartz**
29.46	30.1	6.23	4.316	2.037	14.46	**Muscovite**
8.56	9.06	15.5	3.418	3.194	22.68	**Iilite**
12.24	12.7	10	2.546	2.222	15.78	**Chlorite**
19.6	19.92	3.5	2.959	0.715	5.08	**Sericite**
				14.085	100.00	

HKE057_37.5 (T1)

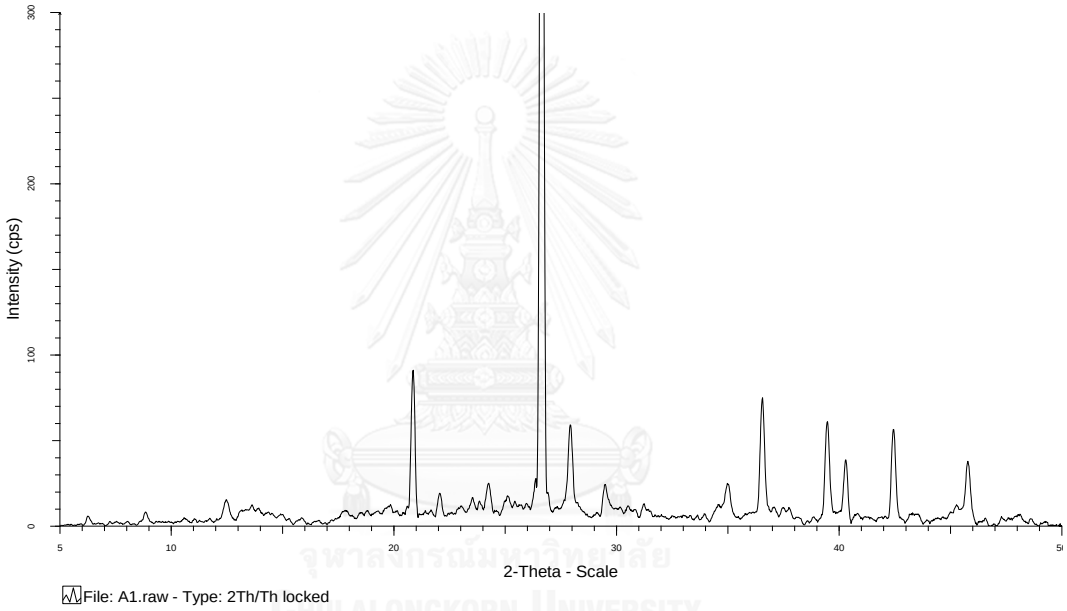

Left Angle	Right Angle	Net Height	Raw Area	Net Area		
2-Theta °	2-Theta °	Cps	Cps x 2-Theta °	Cps x 2-Theta °		
26.4	26.88	624	135.6	126.6	86.79	**Quartz**
12.1	12.9	12	5.059	3.897	2.67	**Chlorite**
29.24	29.82	14.7	7.563	3.8	2.61	**Calcite**
27.54	28.24	44.2	18.51	11.58	7.94	**Muscovite**
				145.877	100.00	

HKE057_175.15 (T2)

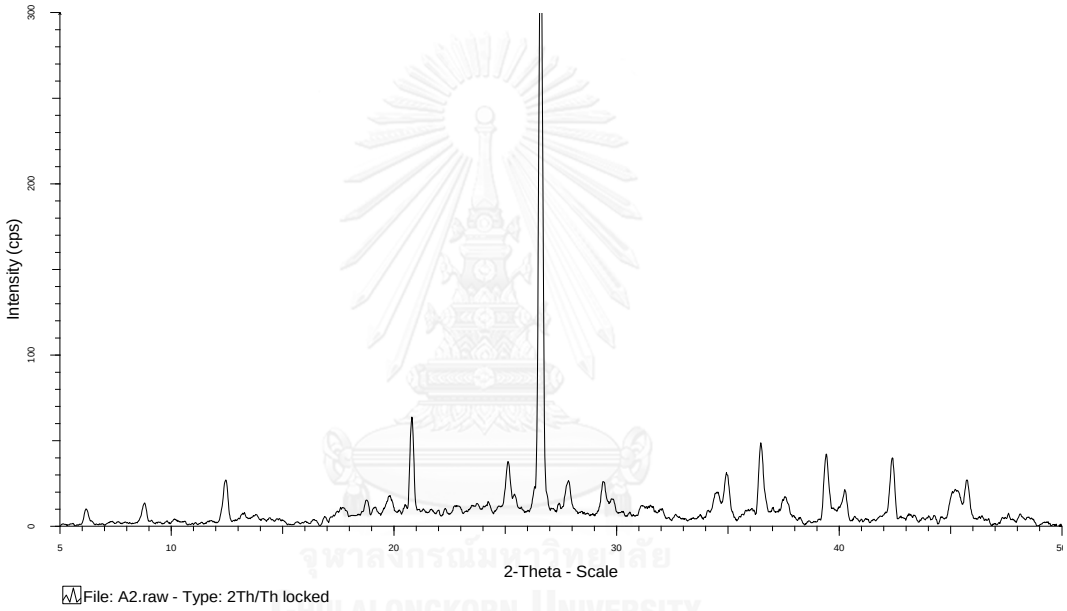

Left Angle	Right Angle	Net Height	Raw Area	Net Area		
2-Theta °	2-Theta °	Cps	Cps x 2-Theta °	Cps x 2-Theta °		
26.2	26.94	340	83.94	75.33	78.34	**Quartz**
41.98	42.66	34.5	10.44	8.51	8.85	**Muscovite**
24.52	25.58	27.7	17.12	8.915	9.27	**Chlorite**
29.1	29.68	15.2	8.371	3.4	3.54	**Calcite**
				96.155	100.00	

HKE085_296.7 (T3)

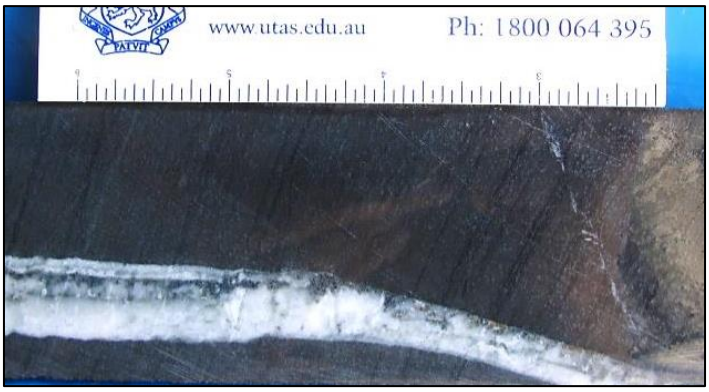

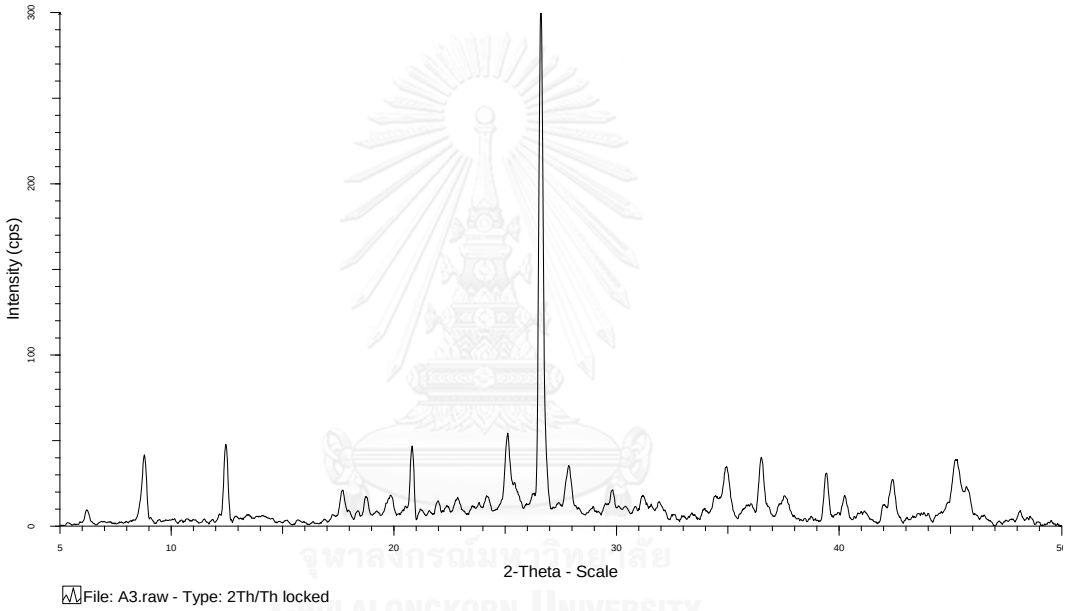

Left Angle	Right Angle	Net Height	Raw Area	Net Area		
2-Theta °	2-Theta °	Cps	Cps x 2-Theta °	Cps x 2-Theta °		
26.36	27.02	287	76.68	67.98	78.95	**Quartz**
12.24	12.66	42.6	10.27	8.922	10.36	**Chlorite**
8.42	9	36.8	10.95	9.205	10.69	**Muscovite**
				86.107	100.00	

NPE128_240 (T4)

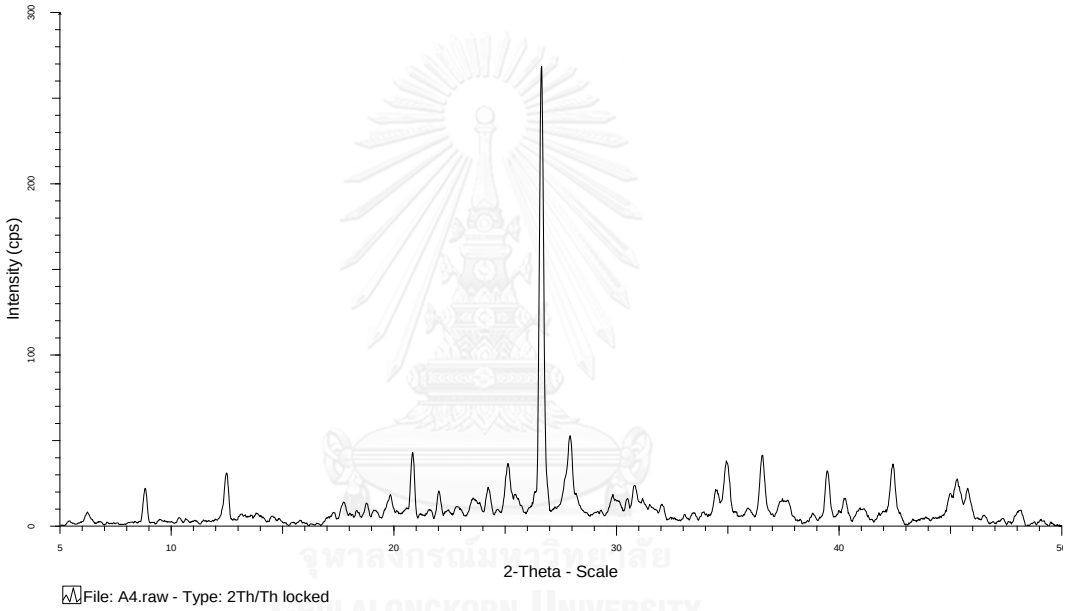

Left Angle	Right Angle	Net Height	Raw Area	Net Area		
2-Theta °	2-Theta °	Cps	Cps x 2-Theta °	Cps x 2-Theta °		
26.4	27	252	64.75	57.03	74.25	**Quartz**
27.4	28.32	40.1	22.98	13.32	17.34	**Muscovite**
24.84	25.38	24.7	11.63	6.459	8.41	**Chlorite**
				76.809	100.00	

HKE057_47.8 (T5)

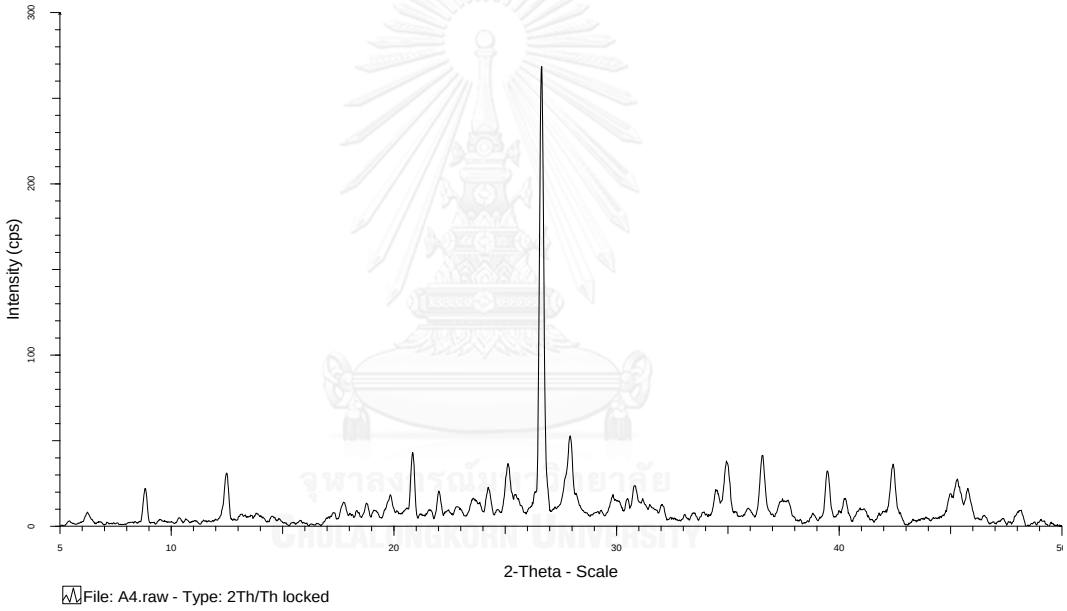

Left Angle	Right Angle	Net Height	Raw Area	Net Area		
2-Theta °	2-Theta °	Cps	Cps x 2-Theta °	Cps x 2-Theta °		
26.24	26.88	618	147.3	136.9	87.10	**Quartz**
27.42	28.36	48.6	21.07	15.22	9.68	**Muscovite**
24.84	25.52	15.2	10.53	5.049	3.21	**Chlorite**
				157.169	100.00	

NPW713_153.1 (T13)

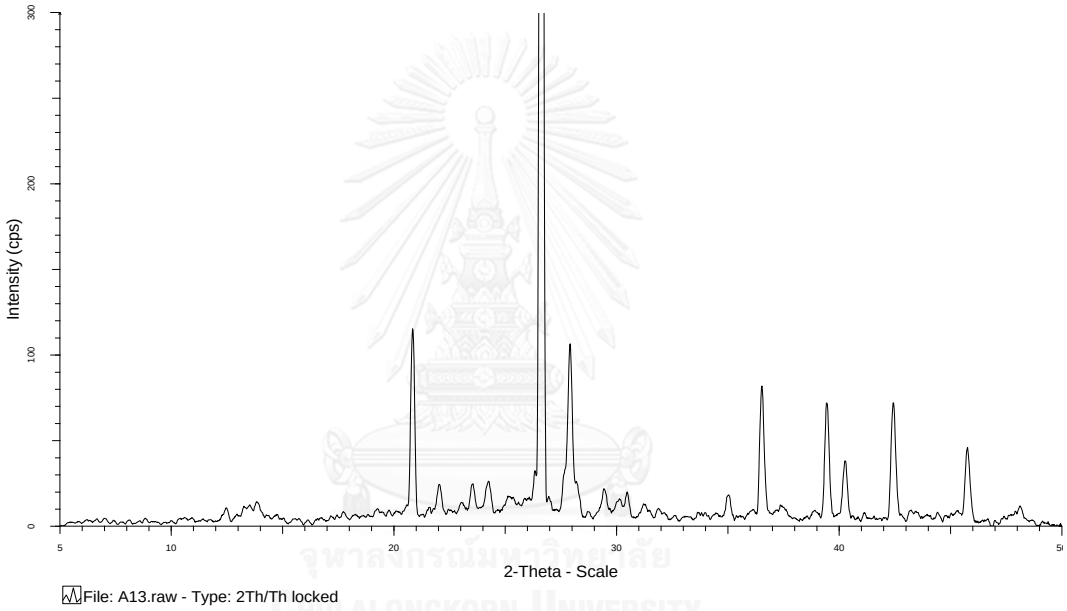

Left Angle	Right Angle	Net Height	Raw Area	Net Area		
2-Theta °	2-Theta °	Cps	Cps x 2-Theta °	Cps x 2-Theta °		
26.42	26.86	769	165.4	156.4	77.10	**Quartz**
27.52	28.46	95.9	37.32	30.32	14.95	**Muscovite**
36.32	36.8	72.2	19.59	16.14	7.96	**Chlorite**
				202.86	100.00	

HKE057_133.8 (T17)

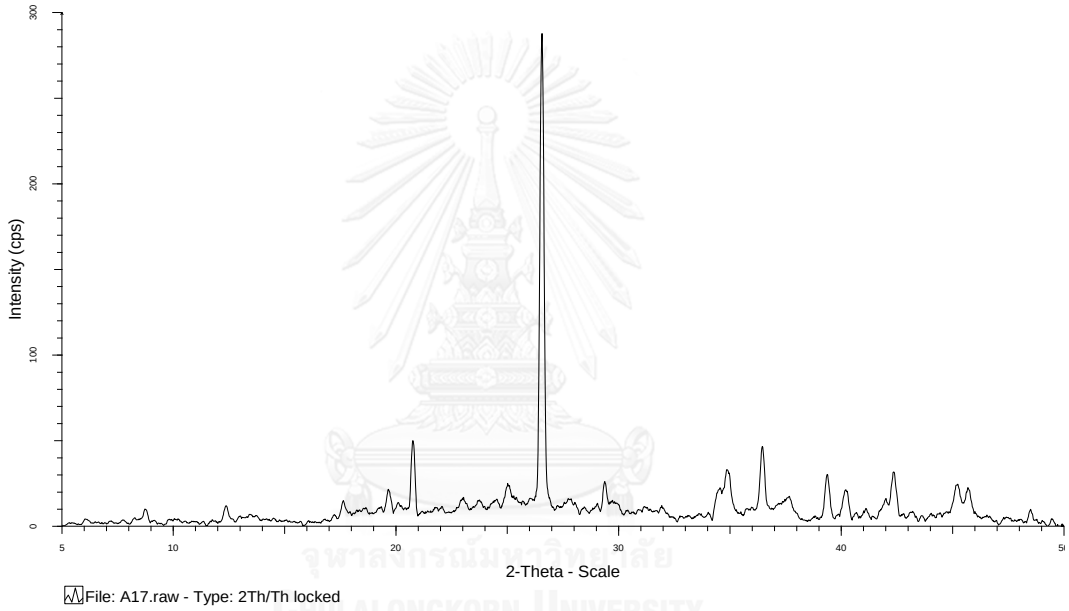

Left Angle	Right Angle	Net Height	Raw Area	Net Area		
2-Theta °	2-Theta °	Cps	Cps x 2-Theta °	Cps x 2-Theta °		
26.28	26.88	271	68.2	59.18	90.53	**Quartz**
29.18	29.58	15.4	6.323	2.937	4.49	**Muscovite**
24.72	25.32	11.9	9.99	3.252	4.97	**Chlorite**
				65.369	100.00	

APPENDIX D
XRD Instrument

Analytical Instrument	X-Ray Diffractometer (XRD) Model D8 Advance: Bruker AXS, Germany
Target/Wavelength	Cu / 1.5406
Voltage/Current	40 kV / 30 mA
Conditions	2 theta 5-50 degree, Increment 0.02 degree, Scan speed 1 sec per step
Program used	Diffrac Plus software of the Bruker Analytical X-ray System (XRD Commander)
Interpreted using	Eva Program which Search-match routine based on the sample's Powder Diffraction File (PDF) and compared with the JCPDS's reference PDF database.

APPENDIX E
EPMA Instrument

Analytical Instrument	Electron Probe Micro Analyzer (EPMA) JXA-8100
Accelerating Voltage	15.0 kV
Current	2.50, E-8
Magnification	40
Probe Diameter	0
Probe Scan	Off

APPENDIX F

EPMA analysis of the sulfide minerals

EPMA analysis and Photomicrograph of the sulfide minerals in Figure 4.7, 4.8 and 4.9 which associated with gold and other unidentified minerals.

S	As	Cu	Ag	Au	Hg	In	Fe	Cd	Zn	Bi	Pd	Mn	Total	Minerals
55.76	0.23	0.01	0.01	0.00	0.00	0.01	43.89	0.02	0.06	0.01	0.00	0.00	100	Pyrite
56.90	0.03	0.08	0.00	0.20	0.00	0.01	42.72	0.00	0.00	0.01	0.02	0.03	100	Pyrite
56.60	0.24	0.00	0.01	0.22	0.01	0.00	42.84	0.01	0.00	0.06	0.00	0.02	100	Pyrite
55.93	0.06	0.06	0.01	0.00	0.00	0.00	43.95	0.00	0.00	0.00	0.00	0.00	100	Pyrite
56.64	0.00	0.02	0.00	0.00	0.00	0.02	43.32	0.00	0.01	0.00	0.00	0.00	100	Pyrite
54.88	0.91	0.03	0.01	0.00	0.01	0.00	44.11	0.00	0.04	0.02	0.00	0.00	100	Pyrite
Hg	Se	Au	Ag	Bi	Sb	Cu	Pd	Pt	Fe	Te	Total			Minerals
9.19	0.02	75.48	14.37	0.74	0.00	0.01	0.00	0.00	0.02	0.00	99.83			Gold
0.32	0.02	82.53	16.39	0.82	0.00	0.01	0.00	0.00	0.07	0.06	100.22			Gold
8.27	0.03	75.79	14.89	0.69	0.00	0.00	0.00	0.00	0.00	0.00	99.67			Gold
8.58	0.00	75.56	14.66	0.81	0.00	0.01	0.00	0.00	0.08	0.00	99.70			Gold
9.49	0.00	75.94	13.64	0.73	0.08	0.00	0.00	0.00	0.00	0.00	99.88			Gold
8.98	0.04	76.70	13.39	0.73	0.00	0.03	0.00	0.00	0.00	0.02	99.89			Gold
8.90	0.00	75.14	14.78	0.82	0.00	0.00	0.00	0.00	0.02	0.01	99.66			Gold
8.25	0.02	75.76	14.50	0.64	0.00	0.00	0.00	0.00	0.03	0.02	99.21			Gold
8.25	0.00	76.37	14.18	0.65	0.00	0.06	0.00	0.00	0.04	0.01	99.56			Gold
9.44	0.00	75.00	14.66	0.78	0.00	0.03	0.00	0.00	0.18	0.01	100.10			Gold
7.20	0.00	68.58	13.51	0.55	0.00	0.30	0.00	0.00	7.53	0.00	97.68			Gold
8.44	0.01	74.08	14.64	0.00	0.00	0.00	0.00	0.00	0.15	0.04	97.35			Gold
9.28	0.00	74.13	14.62	0.68	0.00	0.00	0.00	0.00	0.03	0.00	98.73			Gold
10.16	0.04	74.52	14.40	0.84	0.00	0.00	0.00	0.00	0.01	0.01	99.98			Gold
9.75	0.00	75.33	14.90	0.86	0.00	0.00	0.00	0.00	0.01	0.03	100.87			Gold
9.78	0.02	75.43	13.77	0.71	0.00	0.00	0.00	0.00	0.01	0.03	99.74			Gold
9.32	0.00	75.92	13.71	0.73	0.00	0.03	0.00	0.00	0.00	0.00	99.72			Gold
9.09	0.00	77.64	12.16	0.86	0.00	0.05	0.00	0.00	0.00	0.00	99.79			Gold
9.82	0.01	77.04	12.12	0.77	0.00	0.06	0.00	0.00	0.00	0.00	99.82			Gold
9.48	0.01	76.50	12.92	0.79	0.00	0.01	0.00	0.00	0.00	0.00	99.70			Gold
10.16	0.00	74.78	14.23	0.80	0.00	0.03	0.00	0.00	0.05	0.01	100.04			Gold
9.62	0.02	76.65	12.73	0.79	0.00	0.11	0.00	0.00	0.00	0.00	99.91			Gold
9.19	0.00	76.27	13.51	0.78	0.00	0.02	0.00	0.00	0.03	0.01	99.81			Gold
9.58	0.01	77.16	12.23	0.69	0.00	0.05	0.00	0.00	0.00	0.05	99.77			Gold
9.38	0.00	77.10	12.53	0.75	0.00	0.00	0.00	0.00	0.00	0.04	99.80			Gold
8.45	0.02	77.29	13.01	0.72	0.00	0.00	0.00	0.00	0.01	0.00	99.50			Gold
8.63	0.00	69.11	22.94	0.66	0.00	0.02	0.00	0.00	0.07	0.02	101.44			Gold
8.21	0.00	76.68	15.00	0.62	0.00	0.05	0.00	0.00	0.00	0.00	100.57			Gold

Fe	Mn	S	As	Zn	Cu	Bi	Cd	Ni	Total		Minerals
46.25	0.00	34.22	0.00	0.35	0.00	0.00	0.02	0.00	80.86		Pyrrhotite
46.92	0.06	35.51	0.03	0.37	0.01	0.00	0.03	0.00	82.92		Pyrrhotite
48.35	0.01	34.46	0.00	0.26	0.00	0.11	0.00	0.00	83.19		Pyrrhotite
46.87	0.00	34.84	0.00	0.08	0.00	0.20	0.00	0.00	82.00		Pyrrhotite
47.58	0.03	34.40	0.00	0.33	0.00	0.10	0.00	0.05	82.49		Pyrrhotite
47.38	0.06	34.96	0.00	0.65	0.00	0.04	0.01	0.05	83.14		Pyrrhotite
46.39	0.03	35.30	0.00	0.57	0.00	0.21	0.00	0.01	82.51		Pyrrhotite
48.52	0.00	0.00	0.00	0.00	0.00	0.04	0.02	0.04	83.78		Pyrrhotite
47.31	0.00	35.61	0.03	0.52	0.02	0.02	0.00	0.00	83.48		Pyrrhotite
46.99	0.00	35.01	0.01	0.51	0.00	0.00	0.00	0.00	82.52		Pyrrhotite
47.58	0.02	34.69	0.01	1.38	0.06	0.06	0.00	0.02	83.77		Pyrrhotite
46.18	0.01	35.70	0.03	1.19	0.02	0.02	0.00	0.00	83.16		Pyrrhotite
46.50	0.00	33.39	0.03	0.00	0.00	0.00	0.00	0.00	79.93		Pyrrhotite
48.42	0.00	33.90	0.00	0.03	0.00	0.00	0.00	0.01	82.37		Pyrrhotite
48.98	0.00	32.91	0.02	0.00	0.03	0.03	0.00	0.03	81.99		Pyrrhotite
47.44	0.00	34.09	0.00	0.00	0.02	0.02	0.00	0.05	81.71		Pyrrhotite
47.59	0.03	31.95	0.04	0.11	0.03	0.03	0.00	0.00	79.89		Pyrrhotite
S	Se	Au	Ag	Zn	Te	Cd	Cu	Fe	Mn	Total	Minerals
24.39	0.04	0.48	0.00	52.93	0.00	0.29	0.02	1.38	0.00	79.53	Sphalerite
28.84	0.09	0.00	0.00	59.01	0.09	0.35	0.03	2.54	0.00	90.94	Sphalerite
29.76	0.00	0.00	0.00	54.58	0.04	0.39	0.02	8.85	0.05	93.69	Sphalerite
29.90	0.00	0.19	0.00	55.60	0.00	0.39	0.00	7.78	0.03	93.88	Sphalerite
28.49	0.00	0.00	0.00	55.31	0.00	0.38	0.03	7.29	0.03	91.52	Sphalerite
29.49	0.00	0.05	0.00	55.55	0.00	0.39	0.02	7.98	0.00	93.47	Sphalerite
30.70	0.01	1.25	0.00	53.19	0.00	0.40	0.02	10.40	0.05	96.01	Sphalerite
29.47	0.02	0.08	0.00	56.79	0.00	0.27	0.19	7.15	0.00	93.96	Sphalerite
29.52	0.00	0.17	0.00	60.56	0.00	0.22	0.07	2.97	0.03	93.53	Sphalerite
28.89	0.00	0.68	0.00	57.22	0.00	0.27	0.17	6.38	0.01	93.62	Sphalerite
29.42	0.00	0.00	0.00	61.47	0.00	0.21	0.00	3.12	0.01	94.23	Sphalerite
29.36	0.00	0.00	0.00	61.25	0.01	0.21	0.03	3.25	0.01	94.11	Sphalerite
29.34	0.00	0.49	0.00	60.50	0.00	0.32	0.23	3.20	0.05	94.14	Sphalerite
30.04	0.05	0.37	0.01	35.21	0.00	0.18	14.66	14.46	0.02	95.00	Sphalerite
30.02	0.03	0.56	0.00	60.77	0.00	0.35	0.31	3.03	0.00	95.06	Sphalerite
MgO	CaO	FeO	MnO	Total							Minerals
3.83	40.93	4.50	2.95	52.22							Calcite
0.41	50.62	0.77	2.53	54.31							Calcite
0.60	49.36	1.09	2.99	54.04							Calcite
0.99	47.39	1.54	3.36	53.27							Calcite
0.59	49.40	1.10	2.72	53.81							Calcite
0.18	49.94	0.36	2.42	52.90							Calcite
0.12	51.18	0.26	2.39	53.95							Calcite
0.18	50.69	0.37	3.22	54.46							Calcite
0.24	49.75	0.48	3.40	53.87							Calcite

REFERENCES

APPENDIX

VITA

Miss Kamonluk Tanutkit was born in Nonthaburi, Thailand on 5th March 1992. She completed high school from Benjamarachutit, Ratchaburi in 2010. After finished the high school, she got the Scholarship from Development and Promotion of Science and Technology talents (DPST) and she was studying at Department of Geoscience, Faculty of Science, and Mahidol University. She graduated her Bachelor's Degree (B.Sc.) in geology in 2014 focused on Stability of Limestone mine. And start her Master's Degree Program in Geology at Chulalongkorn University. Her research has been focused on Geology, Mineralization and Alteration of Orogenic gold deposit, The Khamkeut Saen Oudom (KSO) Gold mine, Lao PDR and published in Bulletin of Earth Sciences of Thailand (BEST), International Journal of Earth Sciences.